UNIVERSITY OF FOGGIA

Department of the Sciences of Agriculture, Food and Environment

THE USE OF EDIBLE INSECTS IN CONVENTIONAL AND INNOVATIVE FOODS

Applications in extruded and 3D printed snacks

Candidate:

Domenico Azzollini

Tutor:

Prof. Carla Severini

Thesis committee

Supervisor
Prof. dr. Carla Severini
Professor of Food Processing
University of Foggia, Foggia, IT

Coordinator
Prof. dr. Giancarlo Colelli
Professor of Postharvest Technology of horticultural crops
University of Foggia, Foggia, IT

Other members
Prof. Dr. Marzia Albenzio, University of Foggia, Italy
Prof. Riccardo Massantini, University of Tuscia, Italy
Dr. Carla Di Mattia, University of Teramo, Italy

UNIVERSITY OF FOGGIA

Department of the Sciences of Agriculture, Food and Environment

Doctoral Thesis in
Management of Innovation in the Agricultural and Food Systems of the
Mediterranean Region
– XXIX cycle –

THE USE OF EDIBLE INSECTS IN CONVENTIONAL AND INNOVATIVE FOODS

Applications in extruded and 3D printed snacks

Candidate:

Domenico Azzollini

Tutor:

Prof. Carla Severini

"I hear and I forget. I see and I remember. I do and I understand."

Confucius

TABLE OF CONTENTS

Chapter *1*

Introduction

1.1   The need for alternative proteins

Growing wealth and urbanization are the major determinants for changes in food demand, which occur from vegetable to animal-based diet with ready to eat foods. Between 1950 and 2000 the world's population moved from 2.7 to 6.7 billion people. At the same time, the global meat production increased fivefold, from 45 to 233 billion kilos per year (FAO, 2012). Furthermore, there is a wide agreement that from 2012 to 2050, the demand for food of animal origin is projected to increase by 70% to cope with the demand of additional 2 billion people (Pelletier & Tyedmers, 2010). More specifically, per capita meat consumption is expected to remain high but steady in high-income countries but to grow steadily in rapidly growing countries, including North Africa, India, China, and Brazil. Thanks to their amino acid balance, animal based proteins are considered of high quality and accounts for almost 40% of humanity's total protein intake (Van der Spiegel et al., 2013). However, animal proteins are produced inefficiently. Depending on the animal species and various conditions, 2 to 15 kg plant material is needed to produce 1 kg of animal products; and 40% to 50% of the global grain harvest is used for feed production (Van der Spiegel et al., 2013). Nonetheless, conventional livestock meat production accounts for about 70% of all agricultural land, and it is responsible for about 15% of the total emission of greenhouse gases (Foley et al., 2011). Furthermore, expansion of agricultural acreage by land clearing is a major source of greenhouse gases emissions, and a large contributor to global warming (Oonincx & de Boer, 2012). Therefore, ensuring food protein security by sustainable food production systems persuades the search for alternative protein sources.

In this prospect, a mitigation measure is a shift towards protein from lower impact animal species. Beside conventional proteins (*e.g.* fish, milk and legumes) and novel protein sources (*e.g.* microalgae, seaweed, duckweed and rapeseed), the use of insects as food is receiving an ample attention and it is expecting that the developments will be fast.

1.2   Insects as a source of food

Entomophagy is the habit of eating insects as food. This practice dates to human origins, when through their calorific and nutritional properties, insects have contributed to the development of early *Hominids* (McGrew, 2014). In modern times, insects play a significant but variable role in diets of many contemporary human populations and constitute a vital source of nutritious food for many (Raubenheimer & Rothman, 2011). Entomophagy is traditionally practiced by over 2 billion people (van Huis, 2013). About 2000 insect species have recently been reported as consumed by humans, mostly in tropical and sub-tropical zones (Figure 1.1) (Jongema, 2012). The global centre of human entomophagy is the Americas, where about 679 species are reported as eaten across 23 countries. About 524 species of insects are eaten in Africa, 349 species are consumed in Asia, 154 species in the Pacific region, and 41 insect species in Europe (Raubenheimer & Rothman, 2011).

Figure 1.1. Number of insect species consumed as food by humans at global scale
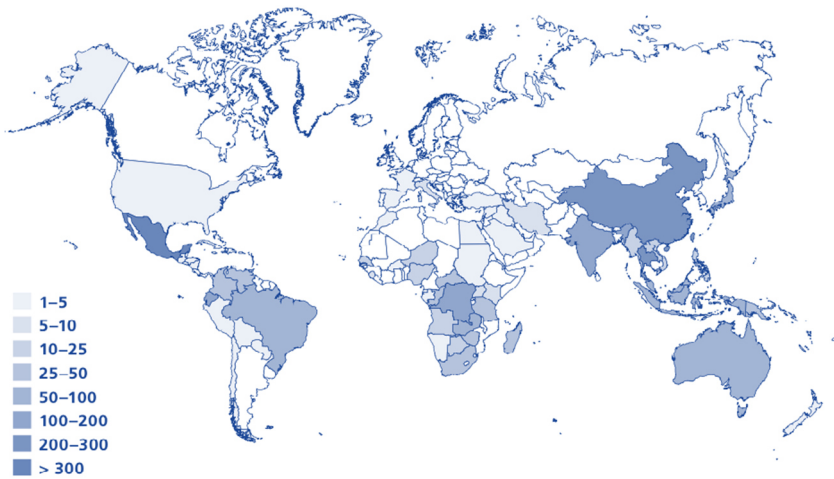
Source: Centre of Geo Information, Wageningen University, based on data compiled by (Jongema, 2012). *All rights granted.*

Wherever humans eat insects as part of their diet, they mainly harvest them from the wild. Yet, further to nutritional aspects, collection, sale and consumption practices also generates additional source of household income to several rural populations. Depending on their order, insects are normally eaten as larvae, pupae, eggs or at adult stage (Table 1.1).

Table 1.1. Commonly eaten insect species (Jongema, 2012).

Order	English name	Most abundant stage of consumption	N. of species consumed
Coleoptera	beetles	adults and larval	590
Lepidoptera	butterflies and moths	larval (caterpillar)	340
Hymenoptera	bees, wasps and ants	larval and pupal, egg	270
Orthoptera	grasshoppers, locusts and crickets	adult	250
Hemiptera	cicadas, true bugs, leafhoppers	adult	190
Isoptera	termites	adult	57
Others (Odonata, Diptera etc.)	dragonflies, flies etc.		200

Providing definitive figures on the nutritional quality of insects is difficult due to the large number of species being consumed. In fact, the nutrient composition of insects spans a broad range of protein, fat and carbohydrate concentrations, allowing them to fall within the Acceptable Macronutrient Distribution Range (AMDR), and are by this definition balanced with respect to human macronutrient requirements. Potentially, thanks to their wide macronutrient variations, insects could serve as equivalents not only of meat, fish and egg, but also of a range of other foods including some shellfish, nuts, pulses, vegetables and even fruits (Raubenheimer et al., 2014). For instance, the concentration of carbohydrate may range from 0.7% in larvae of palm beetle (*Rhynchophorus phoenicis*) to 81% in honey ant (*Myrmecocystus melliger*), while lipids span from 9.7% in grasshoppers (*Sphenarium histrio*) up to 90% in moths (*Phassus triangularis*). Insects are highly valued as a source of protein, with amino acid compositions that are generally balanced for humans. Recently, in parts of central Africa, more than 50% of animal protein eaten was derived from insects, and this figure might reach 64% in parts of the Democratic Republic of Congo (Raubenheimer & Rothman, 2011).

1.3   Insects as a sustainable production of animal proteins

Where insects are a substantial source of nutrients, they are mainly harvested from the wild, leading to phenomena of overharvesting. Management of practices through introduction of mass-rearing facilities of insects for human consumption are essential to guarantee sufficient production of animal proteins, introduction of insects in the Western world and avoid long-term environmental threatening practices. Candidate insects are selected based on the acquaintance of industrial rearing, productivity, nutritional benefits, and marketability (Birgit a. Rumpold & Schlüter, 2013). Thanks to their extensive knowledge and widespread availability, species like Yellow mealworms (*Tenebrio molitor*), lesser mealworms (*Alphitobius diaperinus*), giant mealworms (*Zophobas atratus*), house crickets (*Acheta domesticus*), migratory locust (*Locusta migratoria*), wax moths (*Galleria mellonella*) and silk worms (*Bombyx mori*) are in the spotlight as being the global most promoted insects for mass rearing. Insect farming holds promise for sustainable production of animal proteins. Several benefits of cultivating insects for food consumption have recently been reported. Concisely, Table 1.2 provides a comparison of the most important environmental indexes between Yellow mealworm rearing and conventional animal breeding required to obtain 1 kg of edible protein.

Table 1.2. Comparison of the environmental impact of Yellow mealworms (*T. molitor*) with other animal products.

Index (1/kg of edible proteins)	Species and derivatives			
	Mealworms	Pig meat	Chicken meat	Bovine meat
Global warming potential (kg CO_2 equivalent)*	14	21-54	18-37	77-217
Land use (m²/year)*	18	46-63	41-51	142-254
Water footprint (L)**	23000	57000	34000	112000

Source Oonincx & de Boer, (2012)*; Miglietta et al., (2015)**.

Cultivating Yellow mealworms for protein has lower environmental impact than other animals, due to less global warming potential, land use and water requirement. Several aspects characterize insects as environmental friendly. Firstly, compared to other animals, insects are poikilothermic (coldblooded) and therefore expense no calorie to maintain thermal homeostasis. This characteristic, together with an efficient digestive system increases their feed conversion efficiency (the amount of feed required to produce 1 kg increase in live animal biomass), placing insects in an advantageous position. According to Oonincx et al. (2010), producing 1 kg of edible Yellow mealworms requires 2.2 kg of feed,

while increasing chicken, pork and cattle of 1 kg requires respectively about 2.5, 5 and 10 kg (Smil, 2002). However, if the edible part is considered, the amount of feed required per kg of meat increases. This is not the case for Yellow mealworms, which are considered entirely edible. In addition, the high feed conversion efficiency and the possibility of rearing insects in vertical settlements results in a lower land use, both for feed growth and farming land. Therefore, compared to other animal protein sources, insects rearing has a much lower environmental impact (Oonincx & de Boer, 2012).

1.4   The Yellow mealworms (*Tenebrio molitor*)

Insects (from Latin insectum) are a class of invertebrates within the arthropod phylum. From the anatomic point of view, insects possess an articulated chitinous external skeleton (exoskeleton), a three-part body (head, thorax and abdomen), three pairs of jointed legs, compound eyes and one pair of antennae. Among more than 20 orders, Coleoptera comprise the largest order of insects, with over a quarter of a million described species. Yellow mealworm (*T. molitor*) is part this order and it is among the most promising insect species for food production. Its potential is given by factors like larval size, safety, reproducible and survival potential and nutritional benefit. The species has four distinct life stages, which are egg, larva, pupa and adult, illustrated in Figure 1.2, and the larvae are considered edible. Yellow mealworms can easily be reared in large-scale industrialised systems and feed on cereals or by-products of the food industry (van Broekhoven et al., 2015). As such, they can convert materials which are not edible by humans into human food. In addition, having a short life cycle (6 - 8 months), Yellow mealworms are considered fast growing organisms, a characteristic that allow the design of a farm system that can respond to changes in demand. During the larval stage, Yellow mealworms eat to store energy for transformation in pupal and adult stage, reaching a length of 2.5 cm. The larva grows in an exoskeleton for body support and protection, which colour changes from white to brown over time and moulting. The nutritional composition of larvae may vary depending on larval developmental stage, rearing conditions and substrate of growth.
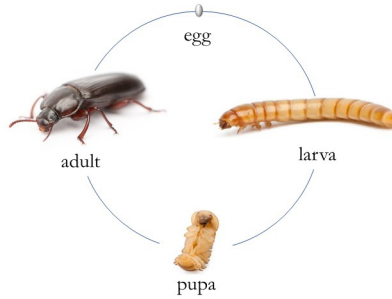
On average, Yellow mealworm larvae contain about solids 41g ±15 per 100 grams of edible matter (Payne et al., 2016). Solids in mealworms consists of 44-69% crude protein, 23-27% lipid and a significant amount of fibre, vitamins and minerals (Veldkamp et al., 2012). Proteins from Yellow mealworm larvae contain all the essential amino acids in quantities that are necessary for humans and are therefore considered of high quality (Yi et al., 2013). Fresh larvae contain up to 71% moisture (Nowak et al., 2014), they can be classified as perishable food. Methods of preservation of larvae of Yellow mealworms reported in literature focus on microbial decontamination through both thermal treatments in hot water baths and hot-air drying (Klunder et al., 2012; Rumpold et al., 2014), and non-thermal treatments, including direct and indirect plasma, and high hydrostatic pressure (Rumpold et al., 2014). Drying and grinding are two processes largely applied to larvae to avoid storage problems and obtain a manageable form that would improve their marketability. This may be achieved by means of several methods, including hot air, sun drying, freeze-drying, osmotic dehydration, etc. Researches involving the drying of insects in literature are exiguous and often involve a first heating step of blanching to reduce the microbial count and avoid enzymatic reactions. This thesis investigated the dehydration kinetic of Yellow mealworm larvae and their changes in quality under different operative conditions when technologically processed.

1.5 Cultural perception of edible insects in Western societies

Deliberate human entomophagy is not a commonplace in temperate zones. With honeybees, silkworms and some others being the exceptions, a few general observations may justify such a different attitude. Primarily, in ancient times, populations of European countries and Fertile Crescent domesticated mammals to respond to several needs. In addition to meat (animal-based proteins), heavy animals provided milk, leather, wool, warmth and any sort of traction. In turn, those "new" concepts of farming system resulted

in a shift in lifestyle, so insects failed to become a staple food (DeFoliart, 1999). Secondly, because agriculture originated and dominated in these regions, insects threatened food production and therefore they were viewed as crop-damaging pests. It is conceivable that these historical reasons, together with Western urbanization that left people out of realities of the natural world, might have drawn those preconceptions of a reluctance towards insects as a whole. In fact, in parts of the world where the consumption of insects in not traditional, such as Europe and North America, consumer negative perception is identified as a significant barrier to their widespread adoption (Deroy et al., 2015; Looy et al., 2014; Shelomi, 2015; Tan et al., 2015). Most humans in developed countries regard the consumption of insects with some revulsion, and for them, insects would hardly meet Western imaginary standards of ideal food. To overcome the disgust of Western consumers, researches have focused on rational promotion through ethical and nutritional arguments (De Boer et al., 2013), identification of psychological individual traits (Schösler, de Boer, & Boersema, 2012; Tan, van den Berg, & Stieger, 2016a; Verbeke, 2015), sensory appeal and appropriateness of developed food product (Caparros Megido et al., 2014; Tan et al., 2015). By comparing visible whole insects with chocolate-coated insects and insect-based protein in pizza, Schösler and Boersema (2012) showed that consumers' acceptability increases by decreasing the degree of visibility of the whole insect. Recently, Tan et al., (2016) confirmed this aspect but warned about the role food carriers can play, arguing that since familiarity arises sensory expectations, the combination of insects with a carrier perceived as inappropriate may result in low consumption intentions. Not surprisingly, researches are being performed on the quality of dry forms of insects and their extracts (Bußler et al., 2016; Yi et al., 2013; Zhao et al., 2016) to implement this trend. Therefore, alongside socially aware marketing campaigns, advances in processing practices and the design appropriate insect products with no sensory expectations is a critical factor. To this end, processing of edible insects into more palatable forms in conventional and innovative food products is essential to trigger their consumption. In this thesis, extrusion-cooking and 3D printing were chosen respectively as conventional and novel processing technologies.

1.6   Extrusion cooking

Snacks are part of the dietary habits of a great portion of the population. Among different types of snacks, expanded ready-to-eat snack foods and breakfast cereals are predominantly made by extrusion-cooking technology. Globally, extruded snack market is projected to reach 31 billion of dollars by 2019 (marketsandmarkets, 2014). Extrusion-cooking is a thermal/mechanical process that combines several unit operations, from mixing to

kneading, shearing and shaping of dry granulated starchy food materials which melt and expand into a low density, crisp foam (Guy, 2001). Compared to traditional batch processing, continuous extrusion is an environmentally friendly process characterized by lower energy requirements and zero waste production. From a mechanical point of view an extruder consists of one (single) or two (twin)-screws, which conveys starchy raw materials through a heated barrel. By means of thermal and shearing forces respectively driven by the heated barrel and screw rotation, the food is heated to its melting point and forced to pass through a die under high pressure. After the melt leaves the die, it expands and cools in consequence of rapid evaporation of water, solidifying into a honeycomb-shaped structure. Expansion and texture of snacks are important characteristics of final product and depend on the composition of raw materials and processing conditions. Microscopically, puffed snacks from cereals consist of a homogeneous network of gelatinized starch, which is the dominant polymer and plays a major role in expansion. Other compounds such as proteins, lipids and fibre, also known as fillers, are dispersed in the starch network and their role is to improve the flexibility of the melt inside the extruder (Moscicki, 2011). The presence of fillers in quantity above 15% by weight influences the rheological properties of the melt, reducing the swelling of the starch and impacting the final shape of an extruded product. Proteins have an effect on expansion through their ability to bind water and create network through covalent interactions. Fibres introduce discontinuity of the starch matrix by disrupting the air bubbles, while lipids have a twofold role. Their presence in limited amount (0.5-1%) facilitates transport by acting as lubricating agent, while higher concentrations reduce the melt viscosity causing a loss in shear forces that favour starch gelatinization and its expansion (Ilo, Schoenlechner, & Berghofe, 2000). Similarly, processing parameters such as screw speed, barrel temperature, screw configuration influence the quality of the final product. Since extruded products are predominantly made from high-starch raw materials such as maize, wheat, rice, potato, tapioca flours, these types of snacks tend to be high in carbohydrates and low in protein (Singh et al., 2007). Attempts to improve the protein content of extruded snacks with other protein sources such as whey, soy bean flour and caseins have been limited due to the adverse effects on the final properties of the products (Li et al., 2005; Onwulata et al., 2001a; Onwulata et al., 2001b). An increasing demand of healthy snack foods makes it worth to explore the potential of edible insects to improve their quality. Major quality aspects, such as microstructure, texture, nutritional value are important characteristics that drive consumption and affect acceptability of snacks, and no researches are reported regarding the use of insect in extruded products.

1.7 3D food printing

3D Printing is the popular term for what is formally known as additive manufacturing. Originally, the term described technologies which created physical prototypes from a digital design, but now it refers to technologies used for many more purposes. The basic principle of 3D printing is that a model, generated using a three-dimensional Computer-Aided Design (CAD) system, can be fabricated by adding material in layers and each layer is a thin cross-section of the CAD (Figure 1.3).

Figure 1.3. Schematic representation of steps from design to final 3D printed component.

CAD File   Numerical Slicing   Layer Processing   Layer by layer Manufacture   Final Component
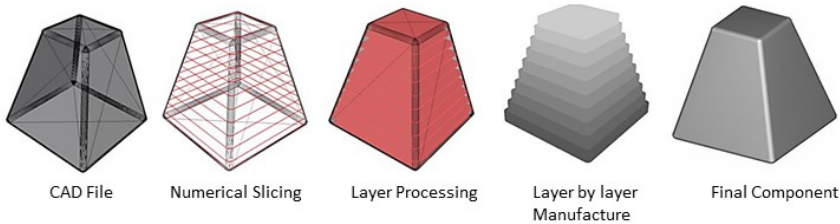
The several technologies, which belong to 3D printing, differ mainly for materials to be used, how layers are created and how they are bonded to each other. The American Society for Testing and Materials (ASTM) group "ASTM F42 – Additive Manufacturing", classified the range of Additive Manufacturing processes into 7 categories, as in Table 1.3 (ASTM., 2015). According to Wohlers (2015), additive manufacturing is currently a $2.2 billion trade with sales of products and services projected to exceed $6 billion by 2017, with a variable uptake across industries. Notable areas of success include the medical industries, aerospace, electronics and automotive (Pinkerton, 2016). Other promising industries where additive manufacturing is being used are armaments, jewellery, house manufacturing, sports, textile, general manufacturing and surgical devices (Gausemeier, Echterhoff, & Wall, 2011). Besides, food is also regarded as an area with large potential for industrial and home applications of 3D printing (Lipton et al., 2015; Pallottino et al., 2016; Sun et al., 2015; Wegrzyn et al., 2012). Among numerous applications, additive food manufacturing is becoming popular thanks to the possibility to design foods with customized shapes, appealing forms and new textures (Yang et al., 2015). Furthermore, the ability of additive manufacturing to produce items in small batches allows for customization of foods with specific nutritional values (Lipton et al., 2015; Severini & Derossi, 2016). Currently, powder bed fusion, binder jetting and material extrusion, are the main types of processes currently studied in food-related printing. For instance, the Dutch Organization for Applied Science (TNO) applied SLS to chocolate powders to build solids 3D objects with complex geometries (Gray, 2010), while Southerland et al., (2011) fabricated sugar treats with

customizes shapes employing the binder jetting technology. Thanks to its low cost and ease of use, the selective deposition (material extrusion technology) has become the most widely studied technology in additive food manufacturing. With this technology, a soft-material formulated of edible ingredients is loaded into a cylinder and extruded in consecutive layers through a nozzle by force of a piston (Godoi et al., 2016). Aregawi et al. (2015) applied the selective deposition system to print cookies with a honeycomb structure, while Lipton et al. (2010) printed a cube with a deconstructed meat paste with the aid of transglutaminase enzyme. Severini et al. (2016) obtained snacks with different texture by printing a wheat dough with designed values of porosity. The European PERFORMANCE project employed the same technology to design 3D printed meals with proper consistency for older people who have difficulties with swallowing (Fp7, 2016). An example of 3D printing technology applied to edible insects is represented by Soares & Forkes (2014), who printed larvae of Yellow mealworms (*T. molitor*) in combination with fondant to produce icing for top cakes' decoration. 3D printing can therefore be considered an important tool at disposal of edible insect industries (Payne et al., 2016) to design appropriate insect products with appealing shapes and good nutritional quality, yet without arising sensory expectations.

Table 1.3. Additive manufacturing process categories as classified by (ASTM., 2015).

Process type	Description	Related technologies
Powder bed fusion	Thermal energy selectively fuses regions of a powder bed	Electron beam melting (EBM), selective laser sintering (SLS), selective heat sintering (SHS), and direct metal laser sintering (DMLS)
Directed energy deposition	Focused thermal energy is used to fuse materials by melting as the material is being deposited	Laser metal deposition (LMD)
Material extrusion	Material is selectively dispensed through a nozzle or orifice	Fused deposition modelling (FDM)
Vat photopolymerization	Liquid photopolymer in a vat is selectively cured by light-activated or UV polymerization	Stereolithography (SLA), digital light processing (DLP)
Binder jetting	A liquid bonding agent is selectively deposited to join powder materials, and then product is baked in an oven for final curing.	Power bed and inkjet heat (PHIH), plaster-based 3D printing (PP)
Material jetting	Droplets of build material are selectively deposited	Multijet modelling (MJM))
Sheet lamination	Sheets of material are bonded to form an object	Laminated object manufacturing (LOM), ultrasonic consolidation (UC)

1.8 Aim and outline of the research

The objective of this research is to build knowledge for supporting the introduction of insects in Western diet. The incorporation of insects invisibly in snack foods obtained by conventional and innovative food technologies has been identified as major opportunity for their acceptability, leading to the following outline of this thesis.

Chapter 2 reports the first step towards understanding how pre-treatments affect technological and nutritional attributes of larvae of Yellow mealworms. More specifically, the effects of blanching and dehydration on nutritional attributes colour and sorption isotherms were studied. This chapter delivers essential knowledge for obtaining a dry and stable insect powder necessary for any industrial application.

In view of an immediate industrial use of insects, in **Chapter 3,** the potential of Yellow mealworms as valuable source of protein in extruded snacks was investigated. In this chapter, it was hypothesised that processing variables and formulation vary major quality attributes of end products, including microstructure, texture and nutritional characteristics. Furthermore, mechanical properties and in vitro digestibility of snacks were linked with microstructure, opening horizons in designing innovative food microstructures with tailored characteristics.

Chapter 4 addresses the feasibility of using the 3D printing technology to develop a computer controlled cereal-based food with innovative shapes. The combined effect of printing variables and internal shape design was investigated by analysing the printing performance, microstructure and mechanical properties of a wheat-based snack.

As a preliminary study, the 4th chapter provided the background for **Chapter 5**, where 3D printing was adopted to obtain a snack enriched with larvae of Yellow mealworms. In this study, the effects of formulation and processing conditions on microstructure, nutritional profile and quality attributes of snacks were investigated.

The final chapter (**Chapter 6**) presents a synthesis and a critical discussion of the main findings, together with conclusions and implications of the knowledge acquired in this thesis.

— Understanding the drying kinetic and hygroscopic behaviour of larvae of Yellow mealworm *(Tenebrio molitor)* and the effects on their quality —

Chapter 2

Abstract

The use of insects for preparing high nutritional value foods is emerging. The dehydration kinetic of Yellow mealworm larvae and its hygroscopic behaviour were described also analysing the changes in quality attributes. Blanching was performed before air drying at 50, 60 and 70°C while sorption isotherms were studied after air drying and freeze-drying. The Page model described the dehydration kinetic at 50, 60 and 70°C with a coefficient of determination of 0.993. Moisture diffusion coefficients between 4.85×10^{-11} and 1.62×10^{-10} m²/s were estimated and their temperature dependence was described by the Arrhenius equation, estimating an Ea of 52.1 kJ mol^{-1}. The GAB model well fitted experimental data, showing isotherms of type II and estimating a monolayer value of 0.05 gH$_2$O/g d.m.. Blanching significantly modified the adsorption isotherms, increased the moisture of fresh larvae without affecting their proximate composition. Rehydration after lyophilisation produced higher colour degradation probably due to the increase of enzymatic activity.

2.1 Introduction

The world in 2050, foreseen as more crowded, urbanised and wealthier, is also projected to need more than twice of today's meat-based products (FAO, 2013). Currently, livestock products (beef, poultry, pork and other products) provide one-third of humanity's protein intake (Van der Spiegel et al., 2013). On the other hand, though, livestock production is among the most environmentally detrimental of all anthropogenic activities and is therefore unsuitable to meet future sustainable requirements (Abbasi et al., 2015). Entomophagy, the consumption of edible insects, is receiving a remarkable worldwide attention as an alternative source of high quality proteins (Nowak et al., 2014). Compared to conventional livestock, insects have a higher feed conversion efficiency, require less land to grow and emit lower greenhouse gases (Oonincx et al. 2010). Depending on several factors, including the species and its developmental stage, insects are not only rich in proteins, but also in fats, vitamins and minerals (Rumpold & Schlüter, 2013). Entomophagy is mostly practiced in tropical countries including Asia, Latina America and Africa, where insects are eaten raw, sun dried, boiled or fried (FAO, 2013). Whereas, where entomophagy is not traditionally practiced, like in Western societies, consumers consider insects as pests and do not easily accept this dietary behaviour (Yen, 2009). In an effort to address the acceptance and rejection factors of insects, Tan et al. (2015) recently highlighted that the willingness to try insects improves with the reduction of their visibility and incorporation into familiar food items. Similar results were obtained by Verbeke (2014). Under this consideration, obtaining powder from insects, that can be used to formulate complex foods, could be of great interest for food industry.

Larvae of *Tenebrio molitor* (*T. molitor*), often referred to as Yellow mealworms, are among the most promising insect species for food production. They have a life cycle between 280 and 630 days depending on environmental conditions, can easily be reared in large-scale industrialised systems and feed on cereals or by-products of the food industry (Ramos-Elorduy and González, 2002; van Broekhoven et al., 2015). Depending on their developmental stage and substrate of growth, Yellow mealworms may contain 44-69% of crude protein, 23-27% crude fat (dry weight) and a significant amount of minerals, including magnesium, zinc, iron, copper and manganese (Veldkamp et al., 2012). Methods of preservation of Yellow mealworm larvae reported in the literature focus on microbial decontamination through both thermal treatments in hot water baths and hot-air drying (Klunder et al., 2012; Rumpold et al., 2014) and non-thermal treatments, including direct and indirect plasma, and high hydrostatic pressure (Rumpold et al., 2014). The removal of

water content by dehydration is a traditional method of food preservation largely applied to fruit, vegetables and meat products. This may be achieved by means of several methods, including hot air, sun drying, freeze-drying, osmotic dehydration, etc. During dehydration the reduction of moisture content and water activity are related to each other by the desorption isotherm which are of great importance for the understanding of the state of water in food. In fact, at certain level of water activity (a_w), the rate of deterioration reactions and microbial spoilage are minimized and the shelf life is extended. In countries where insects are traditionally eaten, they undergo a drying process to extend their shelf life and this is mainly done by sun drying. Nonetheless, this practice is still concentrated at household level (FAO, 2013). Few researches involving the drying of insects can be found in the literature. Aguilar-Miranda et al. (2002) dried Yellow mealworms at 60, 70 and 100°C after a 3 min blanching in a boiling water bath and found that larvae dried at temperatures higher than 60°C appeared darker. Klunder et al. (2012) reported that Yellow mealworms were microbiologically stable at room temperature after being blanched in distilled water for 5 min and dried in a hot oven for 24 hours at 55°C. Siemianowska et al. (2013) dried Yellow mealworms in an hot-air oven 60°C after 3 min of blanching in a water bath, while Kinyuru (2009) dried termites employing a solar drier until a moisture content below 10% was reached. Ramos-Elorduy et al. (2002) dried mealworm larvae at 50°C before being fed for broiler chickens. Experience on drying of insects for feed purposes exist as given by the company Agriprotein from South Africa which employs a fluidised bed dryer to dry black soldier fly larvae (*Hermetia illucens*), or HaoCheng Mealworms Inc. in China that dries Yellow mealworms for feed through microwave drying technology. Under these considerations, understanding the behaviour of Yellow mealworms during drying and its effect on quality attributes would be essential for future development and industrial applications. To date, no systematic drying trials have been performed and data regarding some quality properties of Yellow mealworms are missing.

The aim of this Chapter was to describe the dehydration kinetic and sorption isotherm of Yellow mealworm larvae and their changes in quality under different operative conditions. More specifically, the effects of blanching on nutritional attributes and dehydration on colour and sorption isotherms were studied.

2.2 Materials and methods

2.2.1 Mealworm larvae

Live Yellow mealworm larvae were purchased from a local pet-store in Molfetta, Italy. After purchase, larvae were sieved to remove the residual maize grits and faeces, starved for 24 h in order to empty their gut and sieved again. Larvae were then frozen at -18°C until the experiments. Frozen larvae are hereafter referred to as fresh.

2.2.2 Blanching treatment

A blanching step was applied to mealworm larvae before drying in order to prevent blackening reactions to occur. In fact, although harmless to consumers, newly formed brown pigments during melanosis affect the sensory characteristics, reducing the quality of the end product (Gonçalves & de Oliveira, 2016). To support this choice, the colour of unblanched air-dried larvae have been discussed further in the manuscript. Approximately 100 g of larvae were thawed at 25°C until reached 5°C before being blanched in 1 L of boiling distilled water for 3 min. A water:product mass ratio of 10:1 was used to limit the drop of water temperature. Blanched samples were drained on a perforated stainless tray for 2 min (35x40 cm, 1 mm holes diameter) and excess water from the bottom tray was removed with the aid of absorbent paper. Since changes in moisture content of foods modify the relative contents of other components, in order to avoid any dilution or concentration effect, proximate composition has been reported on dry basis.

2.2.3 Drying process

Air-drying (AD). Blanched larvae were uniformly distributed as a thin layer on the same tray used for draining and placed in a forced-air oven (model Venti-Line 115, VWR International BVBA, Leuven, Belgium) at 50, 60 and 70 °C. During drying, ten different sampling times were chosen to ensure the last sample reached the equilibrium moisture content. At each time, three different samples of larvae (ca. 2g) were randomly selected and their moisture content determined. The drying experiments at the base of the kinetic modelling were carried out in triplicates. To obtain samples for adsorption isotherms and colour determination, further drying processes were repeated in duplicate until constant weight was reached.

Freeze drying. Fresh (FFD) and blanched (BFD) larvae were frozen at -50°C and freeze dried at -55°C with a pressure of 0.2 mbar for 96 hours using a ScanVac CoolSafe™ 55 freeze drier (LaboGene ApS, Lynge, Denmark). Freeze drying experiments were carried out in duplicate.

2.2.4   Characterisation of Yellow mealworm larvae

Blanched larvae were gently blotted with tissue paper with the aim of removing adhering water on the surface of samples. Fresh and blanched larvae were subjected to moisture analysis (105°C until constant weight). In order to investigate the effects of blanching treatment on larvae chemical composition, both freeze dried samples (fresh and blanched) grinded with a blade grinder (Moulinex model A591, Ecully, France) for 30 seconds and analysed for their protein, lipid and ash content. The AOAC methods (1995) were used for protein and ash, using a nitrogen to protein conversion factor of 6.25. The analysis proteins done through the measurement of nitrogen implies an overestimation of the real protein content due to nitrogen in chitin. However, given the low amount of nitrogen in chitin, a measure of the crude protein provides a reasonable estimate of the true protein (Finke, 2007). A modified Bligh and Dyer method (1959) was used to determine the lipid content. 2 g of samples were suspended with 12.5 ml chloroform, 25 ml methanol and 10 ml distilled water (1:2:0.4, v/v). After stirring for 60 min, 10 ml of water and 10 ml of chloroform were added, stirred for 5 min and filtered through a Wathman® filter paper n.1 (Whatman; GE Healthcare Life whatSciences, Little Chalfont, UK) under suction. The filtrate was then allowed to separate for 5 min, the lower phase was collected and chloroform evaporated using a rotary evaporator (Laborotar-4000 Efficient, Heidolph, Schwabach, Germany) at 35°Cunder vacuum. Each analysis was carried out in duplicate.

2.2.5   Mathematical modelling of drying curves

Several semi-theoretical thin layer drying models derived both from Newton's law of cooling and Fick's second law of diffusion are available in literature (Erbay and Icier, 2010). In this Chapter, experimental moisture ratio changes as a function of time were fitted to three exponential models (Table 2.2) using nonlinear regression. The determination of appropriate model was evaluated as explained in the statistical analysis section.

The moisture ratio (MR) of samples obtained during drying at different temperatures has been calculated using the following equation:

$$MR = \frac{M_t - M_e}{M_0 - M_e} \qquad \text{(Eq.1)}$$

where MR is the moisture ratio (dimensionless), M_t, M_0 and M_e are moisture contents of samples at time t, t_0 and equilibrium (g H_2O/ g dry matter). Following, the drying rate (DR) of mealworm larvae has been calculated using the equation 2

$$DR = \frac{dM_t}{dt} = \frac{M_t - M_{t+\Delta t}}{\Delta t} \qquad \text{(Eq.2)}$$

Where $M_{t+\Delta t}$ is moisture content at the time $t + \Delta t$ and Δt is the time interval considered (min).

2.2.6 Prediction of effective moisture diffusivity and activation energy

In choosing the most suitable Fickian solution to estimate the effective moisture diffusivity, the geometry plays an important role. In this Chapter, the diameter and the length of 50 fresh larvae was measured using a digital calliper of 0.01 mm last count and the average values were obtained as 2.61 mm and 27.33, respectively. Given that the length to the radius ratio of larvae was greater than 20, the geometry of an infinite cylinder was considered (Incropera and DeWitt, 1996). Therefore, the Fick's second law of diffusion solved for an infinite cylinder by (Cranck, 1975) was used to estimate the coefficient of diffusion of Yellow mealworms under different drying temperatures (Equation 3).

$$Mr = \frac{Mt - Me}{Mo - Me} = \sum_{n=1}^{\infty} \frac{4}{\lambda_n^2} \exp\left(-\frac{\lambda_n^2 \cdot D_{eff} \cdot t}{r^2}\right) \qquad \text{(Eq.3)}$$

where, λ_n are the roots of Bessel function of order zero $J_0 = 0$, D_{eff} is the effective moisture diffusivity (m^2/s), t is the experimental drying time (s) and r is the radius of larvae (mm). For sufficient long drying time, using only the first term in the series gives a good estimate of the solution (Sharma and Prasad 2004).

Therefore, for n=1 and λ_n=2.405, the Equation 3 can be solved numerically for Fourier number as shown in Equation 4.1 and 4.2

$$F_0 = -0.173 \cdot \ln(Mr) - 0.0637 \qquad \text{(Eq.4.1)}$$

$$D_{eff} = \frac{(F_0)}{\left(\frac{t}{r^2}\right)} \qquad \text{(Eq.4.2)}$$

The positive values of Fourier numbers obtained by Equation 4.1, their corresponding drying times (s) and the average value of radius (mm) were substituted in equation (Equation 4.2) to estimate the effective moisture diffusivity (D_{eff}) (m²/s). The average D_{eff} was determined by summing all the positive values of D_{eff}. The same method was employed by Jain and Pathare (2007) to estimate the effective moisture diffusion of prawns. The dependence of diffusivity on temperature was evaluated by the Arrhenius equation (Equation 5) through nonlinear regression analysis

$$D_{eff} = D_0 \cdot e^{\left(-\frac{E_a}{R \cdot T}\right)} \qquad \text{(Eq.5)}$$

Where E_a represents the activation energy (kJ/mol), D_0 is the pre-exponential factor (m²/s), R is the universal gas constant (8.314 J/ mol K) and T is the absolute temperature (K).

2.2.7 Determination and modelling of sorption isotherms

Moisture sorption isotherms were obtained at 25°C for grounded freeze dried (fresh and blanched) and air-dried larvae (50, 60 and 70°C) following the dynamic equilibrium method developed by de Souza (2013). In detail, samples were first dehydrated in a vacuum desiccator containing silica gel for 24 hours, then weighed (1 g ± 0.0001 g) in plastic sample cups appropriate for the hygrometer and successively transferred to a desiccator with water. Triplicate samples obtained for two drying experiments (six samples for each drying condition) were taken at increasing times and weighed. The difference in weight was used to determine the moisture content. Afterwards, the a_w of the samples was measured with a hygrometer with an accuracy of ± 0.003 at 25°C (AquaLab 4TE, Decagon Devices Inc., WA – USA) calibrated with standard salt solutions (Decagon, Devices Inc., USA). Once the value of a_w was measured, samples were returned to the desiccator to continue the humidification process until constant weight. Approximately two days were necessary to obtain each isotherm.

Experimental data of moisture content and a_w were fitted with the Guggenheim-Anderson-de Boer (GAB) equation (Equation 6), as recommended by the European COST 90 project (Spiess and Wolf, 1983).

$$m = \frac{m_0 \cdot C \cdot k \cdot a_w}{[(1 - k \cdot a_w) \cdot (1 + (C-1) \cdot k \cdot a_w)]} \qquad \text{(Eq.6)}$$

Where m is moisture content (g H_2O/g dry matter); m_0 is the monolayer moisture content (g H_2O/g dry matter); a_w is the water activity; k and C are constant parameters. As reported in statistical section, GAB parameters were estimated by nonlinear regression analysis.

2.2.8   Colour measurement

Colour measurement of grounded freeze dried (fresh and blanched) air-dried larvae was determined by a Minolta Chroma meter CR-400 (Minolta Co., Osaka, Japan) calibrated against a standard white plate. The colour is reported in terms of L*, a* and b* values. Six measurements were performed on duplicate samples and the mean values were used.

2.2.9   Statistical analyses

Nonlinear regression analysis was employed to estimate kinetic parameters of drying equations. The regression was performed using the Levenberg-Marquardt curve fitting algorithm. Different statistical criterions were used to evaluate the fitting quality of each mathematical model, including the coefficient of determination (r^2), reduced chi square (χ^2) and root mean square errors (RMSE). The lowest χ^2 and RMSE and the highest r^2 indicate a high fit quality of the model. Fit quality of Arrhenius and GAB models was evaluated by the mean of r^2.

Differences among sorption isotherms obtained from different treatments and drying conditions were evaluated using the global curve fitting approach reported in Motulsky and Christopoulos (2003). In detail, data sets were fitted to GAB equations, both as a single data set (null hypothesis) and two distinct data sets (alternative hypothesis). The Fisher critical value was determined using the following equation (Equation 7):

$$F = \frac{\frac{SS\,shared - SS\,unshared}{df\,shared - df\,unshared}}{\frac{SS\,unshared}{df\,unshared}} \qquad\qquad (Eq.7)$$

where SS and df are respectively the sums-of-squares and degrees of freedom of shared (null hypothesis) and unshared (alternative hypothesis) fitting data sets. Probability values (p-value) of Fisher distribution were determined based on obtained F-values, numerator and denominator degrees of freedom.

Analysis of variance (ANOVA) was carried out on proximate composition, effective moisture diffusivity obtained at different drying conditions, GAB parameters and on colour of dried samples. The Fisher's Least Significant Difference (LSD) with significance level of α=0.05 and a confidence level of 95% (p<0.05) was used. The analyses were performed using Statistica 10 software (Statsoft Inc., Tulsa, OK).

2.3   Results and discussion

2.3.1   Characteristics of mealworm larvae

At time of experiment, the average weight each live larva was 89.9 ± 6.4 mg. The proximate composition of fresh and blanched larvae of Yellow mealworm is given in Table 2.1, including moisture, protein, lipid, ash and other components. These results are within the range found in literature, crude proteins from 44.7 to 68.9% (g /g dry matter), lipids from 17.4 to 42.4% (g /g dry matter), and ash from 2.4 to 5.7% (g /g dry matter). The reported moisture content was higher than those found in literature, ranging from 56.3 and 63.5% (g H_2O/g w.b.) (Rumpold and Schlüter, 2013; Yi et al. ,2013; Zielińska et al., 2015). Large variations in nutrient composition of mealworm larvae is not only linked to larval development stage but also to feed quality and rearing conditions, including air moisture and temperature (Nowak et al., 2014).

Table 2.1. Proximate composition of mealworm larvae fresh freeze-dried and blanched freeze-dried mealworm larvae (g/100 g dry matter, n = 2), (mean ± S.D.,); Moisture was determined on fresh larvae (g/100 g wet matter, n = 6).

Component	Fresh	Blanched
Moisture	$68.9^a \pm 0.6$	$70.9^b \pm 0.7$
Crude Protein*	$61.8^a \pm 0.9$	$60.7^a \pm 0.9$
Lipid	$23.4^a \pm 0.8$	$23.0^a \pm 0.5$
Ash	$5.0^a \pm 0.2$	$4.7^a \pm 0.2$

[ab] Different superscripts for the same row indicate significant difference ($p<0.05$)
* includes chitin nitrogen

2.3.2   Effect of blanching treatment on larvae composition

Table 2.1 reports the effect of such treatment on the proximate composition of larvae. From results, the blanching treatment seemed to significantly increase the moisture content of larvae from 68.9 to 70.9%. This effect could be due to absorption and entrapment of water inside the larva, just below the chitinous exoskeleton. To corroborate this result, a series of experiments were conducted blanching the larvae at increasing times. In these tests, larvae blanched for 5 and 10 min showed a moisture content of 73.0 and 75.2% respectively. Several studies indicate a loss of moisture as high as 30% for water blanched shrimps (Erdogdu et al., 2004; Niamnuy et al., 2008) but none of them has explored the effect of the presence or absence of the exoskeleton to support a similar behaviour found in mealworm larvae. In the comparison of chemical constituents between fresh and blanched larvae, no differences were observed. In fact, though protein, ash and lipid content of blanched larvae seemed negatively affected by blanching, from 61.8 to 60.7%, from 23.4 to

23.0% and from 5.0 to 4.7% respectively, these differences were not high enough to be statistically significant (p>0.05). Changes in proximate composition usually occur due to leaching of soluble nutrients in the surrounding medium to the extent of treatment time. In fact, increasing boiling time from 0 to 7 min reduced the protein content in shrimps by 2.9% (Niamnuy et al., 2008). In this case, short blanching time may have been sufficient to increase the moisture content but kept to proximal composition steady. In addition, a containment effect of nutrients exerted by the exoskeleton is plausible.

2.3.3 Modelling of drying curves

The estimated kinetic parameters for each of the proposed model used to fit the experimental data of moisture ratio and the statistical results are reported in Table 2.2. As expected, in all cases the rate constant, k, showed an increasing tendency as the air temperature increased, assuming a trend with temperature. High r^2, low RMSE and low χ^2 attributed the model as of a good quality. With these respects, in this Chapter, all models exhibited high fit quality ($r^2 \geq 0.98$; RMSE ≤ 0.07; $\chi^2 \leq 0.005$) stating that all models could be used to predict experimental data with great accuracy. Nevertheless, the Page model showed the best fit quality, supported by the highest r^2 (0.9972) and the lowest RMSE and χ^2 (0.0261 and 0.0007). On top, having only two parameters, the Page model can be recommended to predict the drying behaviour of larvae of *T. molitor*.

Table 2.2. Mathematical models, kinetic and statistical parameters used to describe the changes in moisture content of mealworm larvae during dehydration at 50, 60 and 70 °C (mean ± S.E.) where k is the drying constant and n is the equation constant. [a] (Martins, Martins, & Pena 2015)

Model name and equation[a]	Kinetic parameters	50 °C	60 °C	70 °C
Lewis	k (min^{-1})	0.0103 ± 0.0002	0.0179 ± 0.0005	0.0284 ± 0.0007
MR = exp(-kt)	r^2	0.9900	0.9799	0.9836
	RMSE	0.0490	0.0678	0.0593
	χ^2	0.0024	0.0046	0.0036
Page	k (min^{-1})	0.0027 ± 0.0003	0.0030 ± 0.0005	0.0068 ± 0.0008
MR = exp(-kt^n)	n	1.2904 ± 0.0225	1.4381 ± 0.0402	1.3873 ± 0.0313
	r^2	0.9972	0.9932	0.9952
	RMSE	0.0261	0.0393	0.0322
	χ^2	0.0007	0.0016	0.0011
Modified Page	k (min^{-1})	0.1113 ± 0.0023	0.1526 ± 0.0041	0.4432 ± 0.0106
MR = exp(-kt)^n	n	0.0928 ± 0.0000	0.1172 ± 0.0000	0.0632 ± 0.0000
	r^2	0.9900	0.9799	0.9836
	RMSE	0.0490	0.0676	0.0593
	χ^2	0.0025	0.0046	0.0036

Figure 2.1 shows experimental moisture ratios and the fits obtained by Page model as a function of drying time in processing of mealworm larvae at 50, 60 and 70°C. At each temperature, the data exhibited a decreasing exponential trend, of which concavity increases with temperature.

Figure 2.1. Experimental and predicted drying curves for mealworm larvae at 50°C, 60°C and 70°C fitted with Page model (bars represent 95% confidence intervals).
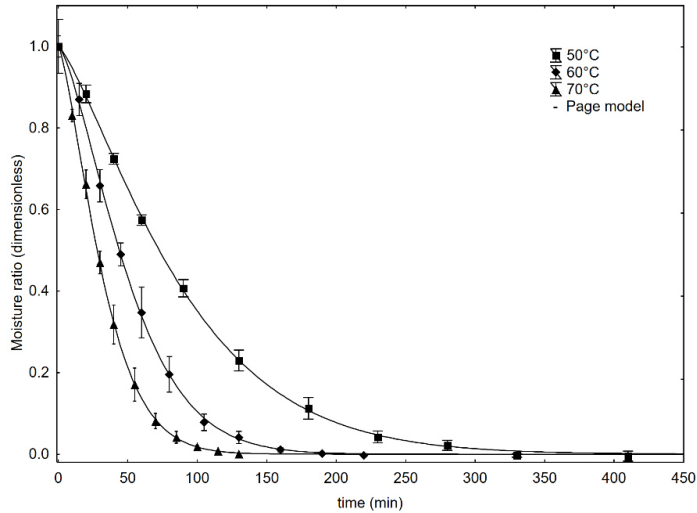
2.3.4   Drying behaviour

Figure 2.2 quantitatively depicts the drying rate curves of samples of mealworm larvae obtained at different working temperatures. After a small peak observed on the 60 and 70°C curves, which may represent the heating period, only a falling rate period for all the working temperatures was observed. Nevertheless, no constant drying rate periods were detected. Similar trends were obtained by other authors on different foods, such as shrimps (Hosseinpour et al., 2013) or pirarucu fish (Martins et al., 2015). Drying of food materials is a complex system that is governed by different moisture transfer mechanisms, including molecular diffusion of water, vapour diffusion or capillary flow (Srikiatden and Roberts, 2007). In the falling drying rate period, the Fick's second law of diffusion can be applied to estimate the "effective moisture diffusivity" (D_{eff}). The latter, based on experimental observations, includes all the possible moisture transfer mechanisms that may be involved in drying of food matters and can be interpreted as a global moisture diffusion coefficient (Sharma and Prasad, 2004).

Figure 2.2. Drying rate curves of mealworm larvae at different temperatures.
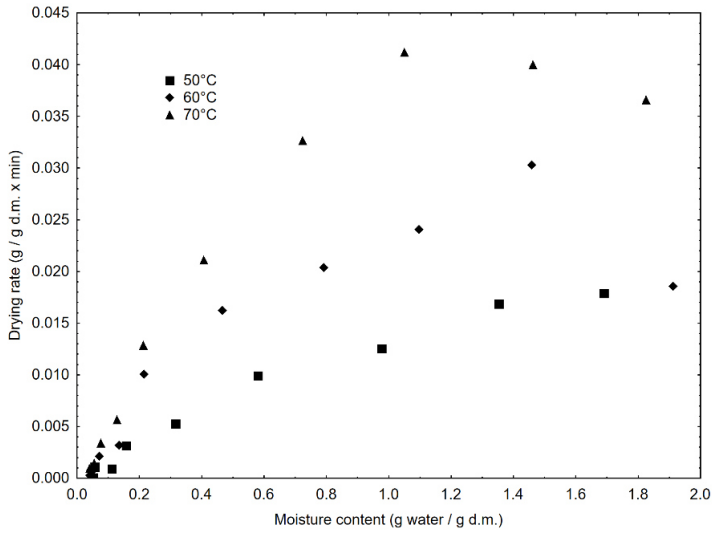
The average values of D_{eff} for larvae of Yellow mealworm obtained by using Equation 4.2 increased progressively from 4.5 x 10^{-11} to 1.10 x 10^{-10} and 1.62 x 10^{-10} m²/s as the temperature increased from 50 to 60 and 70°C respectively ($r^2>0.93$). The D_{eff} values at 60 and 70°C resulted 3.3 and 2.1 times the value at 50°C. These results lie in the range of D_{eff} from 1 x 10^{-11} to 1 x 10^{-9} m²/s found for food materials (Erbay and Icier, 2010). For instance, Xie et al. (2015) observed the D_{eff} value of beef meat increasing from 2.9 to 5.5 x 10^{-10} m²/s at the respective temperature of 50 and 70°C. Among factors affecting D_{eff}, temperature plays a major role, and the temperature dependence is usually described by the Arrhenius equation (Equation 5). In this Chapter, the Arrhenius equation successfully described the temperature dependence of water diffusion rate, showing a correlation coefficient $r^2 = 0.95$. More precisely, a pre-exponential factor (D_0) of $1.38 \times 10^{-2} \pm 7 \times 10^{-4}$ m²/s and an activation energy, E_a, of 52.1 ± 5.2 kJ/mol were estimated. Reflecting the sensibility of D_{eff} to temperature, the higher the E_a, the higher the energy required to activate the moisture diffusion, with consequent increase in industrial processing costs. This result is in accordance with the range from 12.7 to 110 kJ/mol which has been commonly reported for food materials (Erbay and Icier, 2010).

2.3.5 Sorption isotherms

Moisture sorption data of larvae of mealworm larvae dried at different conditions were fitted with the GAB equation. The estimated parameters and the goodness of fit are reported in Table 2.3. In all cases, the GAB model was satisfactory for interpolating the sorption isotherms showing always a determination coefficient greater 0.993. Predicted values of m_0, C and k of isotherms of larvae dried at 50, 60 and 70°C showed no statistical difference (p>0.05). In addition, considering all experimental data detected from samples dried at 50, 60 and 70°C as a single set of data (in common) a similar determination coefficient was estimated, stating as the data obtained at different temperature had the same isotherm behaviour (Table 2.3).

Table2.3. Parameters of GAB equation of mealworm larvae dried at different conditions (mean ± S.E.)

Temperature	m_0	C	k	r^2
50°C	$0.045^a \pm 0.001$	$8.272^{a,b} \pm 2.492$	$0.940^a \pm 0.004$	0.993
60°C	$0.048^a \pm 0.002$	$4.085^a \pm 1.324$	$0.940^a \pm 0.006$	0.996
70°C	$0.051^a \pm 0.004$	$2.198^a \pm 0.643$	$0.928^a \pm 0.008$	0.997
AD (50/60/70°C)	$0.047^a \pm 0.002$	$4.120^a \pm 0.954$	$0.937^a \pm 0.004$	0.995
BFD	$0.044^a \pm 0.001$	$10.847^b \pm 2.020$	$0.956^b \pm 0.002$	0.998
FFD	$0.049^a \pm 0.001$	$6.361^b \pm 0.301$	$0.992^c \pm 0.002$	0.995

[abc] Different superscripts for the same column indicate significant difference ($p<0.05$).
Air-dried (AD), blanched freeze dried (BFD), fresh freeze dried (FFD)

This similarity was well explained by the global curve fitting approach (Table 2.4). In fact, when isotherms of air-dried samples were compared among each other (50 with 60°C, 50 with 70°C, 60 with 70°C), no statistical difference were observed (p>0.05). Thereafter, a single isotherm comprehensive of all air-dried samples of larvae was considered.

Table 2.4. Probability values obtained from the global curve fitting test for different adsorption isotherms

Test	p value
50°C and 60°C	0.9898
50°C and 70°C	0.9884
60°C and 70°C	0.9813
AD and BFD	0.9090
AD and FFD	0.0141
FFD and BFD	0.0450

Air-dried (AD), blanched freeze dried (BFD), fresh freeze dried (FFD)

The sorption isotherms of mealworm larvae dried by different technology were compared in Figure 2.3. For each of the sorption isotherm, an increase in equilibrium moisture content caused an increase in water activity, featuring a sigmoid shape. According to the classification proposed by Salwin (1963), hygroscopic food products rich in proteins tend to exhibit behaviour that are consisting with sigmoid type II isotherms of this kind. Type II isotherms have also been reported for food products like pirarucu fillet (Martins et al., 2015) and lean beef (Trujillo et al., 2003).

Figure. 2.3. Moisture adsorption isotherms of mealworm larvae fitted with GAB model
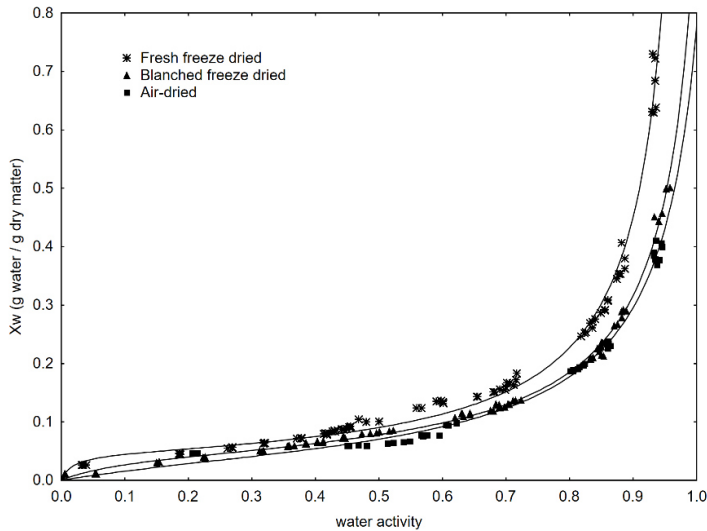
In Figure 2.3, a net distinction for the isotherm of FFD sample is observed, especially at $a_w > 0.6$, compared to the AD and BFD samples that appear overlapped. In addition, FFD larvae adsorbed a higher amount of water, reaching 0.74 g H_2O/g dry matter, followed by 0.50 in BFD and 0.42 in AD g H_2O/g dry matter. The behaviour of the last two samples could be the result of the changes caused by the heat treatment on protein's hydrophilic groups (polar side chains, carbonyl and amino groups), which bind water through hydrogen bond formation (Singh et al., 2001). During blanching and drying of mealworms, as it has been proved for hen meat (Singh et al., 2001), proteins may undergo structural changes, including denaturation, crosslinking and interaction with lipids. Consequently, the number of hydrophilic sites for water binding may be reduced and the sorption properties altered. In addition, if an a_w of 0.6 was chosen to ensure microbiological stability (Gustavo et al., 2008), the GAB equation would estimate values of moisture content of 0.093, 0.099 and 0.110g H_2O/g dry matter for AD, BFD and FFD samples respectively. These levels of

moisture, however, were still too high to avoid undesired phenomena of clumping during powdering operations. In dry products, the monolayer moisture content (m_0) represents the optimal moisture content range to ensure the maximum shelf life, and it is around values of a_w from 0.2 to 0.4 (Gustavo et al., 2008). At moisture content above the monolayer, chemical reactions that require water begin, while above and below it the rate of lipid oxidation increases. Defining the monolayer moisture contents of 0.047, 0.044 and 0.049 (g H_2O/g dry matter), results in the corresponding a_w values 0.35, 0.24 and 0.29 for AD, BFD and FFD samples applying the GAB equation. Therefore, drying mealworm larvae to the monolayer moisture content of around 0.05 g H_2O/g dry matter may be adequate in terms of both food stability and powdering operations. The time to reach the monolayer moisture content was estimated through the Page model and resulted in approximately 355, 180 and 120 min for samples air dried at 50, 60 and 70°C respectively. Since drying is a highly energy-intensive process, a further study on the economic acceptability among different drying techniques is advisable.

2.3.6 Analysis of colour

Colour of food products is of major importance for consumer acceptability, and the incorporation of insects' powder into food items may have a central role to their acceptability (Tan et al., 2015). Figure 2.4 shows the average colour parameters of larvae of Yellow mealworms for blanched, fresh freeze dried, blanched freeze dried, unblanched air-dried and air-dried larvae. Blanched larvae showed values of 46.9, 5.3 and 24.8 respectively for L*, a* and b*. A higher luminosity was observed in fresh freeze dried larvae while lower values were detected for the other cases. This difference can be explained at two levels, of which the first is driven by a physical phenomenon. Water found in fresh tissues has a different refraction index than the air of dry samples. Therefore, the presence of water in blanched samples may have altered the lightness ($L*$), and, as a consequence, dry samples may have appeared darker (Caivano and del Pilar Buera, 2012). Secondly, blanching treatments and a prolonged drying at high temperatures necessary to reach the dehydration equilibrium, probably favoured the well-known non-enzymatic browning reactions which, in turn, caused the reduction in lightness values (Pathare et al., 2013). Freeze drying did not cause significant changes in $a*$ and $b*$ values of larvae (p<0.05). The colour of unblanched larvae was highly affected during the air-drying process, at each of the temperature considered. In particular, the values of lightness and Yellowness of unblanched air-dried larvae decreased to a large extent and such discoloration can be ascribed to formation of brown pigments through melanosis. The reason for the non-inhibition of browning

reactions at a temperature as high as 70°C can be found in their pathway. In fact, once initiated by enzymatic reactions (polyphenol oxidase, PPO) in presence of oxygen, melanosis continue as a chemical reaction of condensation, and this second stage may not be inhibited at the process temperature considered.

Figure 2.4. Effects of different unit operations on L*, a* and b* values of mealworm larvae (bars with different letters are significantly different at p<0.05). Air-dried samples were dried until reaching the monolayer moisture content.
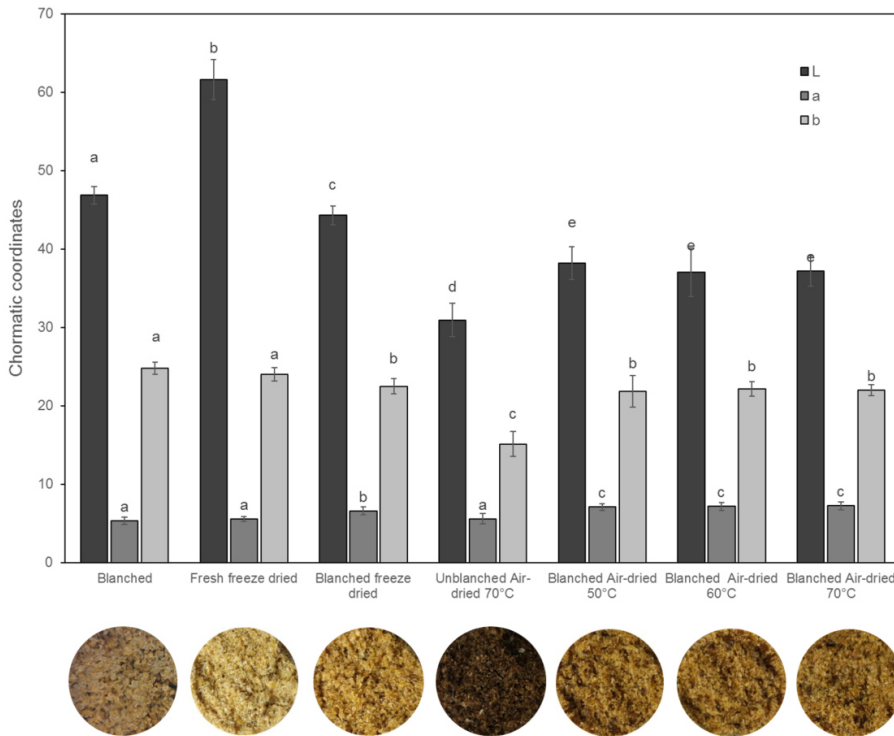
Furthermore, unblanched air-dried larvae presented a highly pungent odour, which may directly preclude their consumption by human. Blanched freeze-dried larvae revealed an increased *a** value, and the same increase, but to a higher extent, was observed in air-dried samples. Differently from the case of unblanched samples, these changes can be reasonable attributed to non-enzymatic browning reactions. For values of *b**, significant influences were found among non-blanched and blanched samples. Larvae of Yellow mealworms are known to contain carotenoids in amounts that depend on their diet. Dietary carotenoids are pigments that impart Yellow (*b**) colour to foods (Pathare et al., 2013). Thus, leaching of these pigments into water during blanching first, and air drying later, could be the cause for this reduction.

It is worth to add that during measurements of sorption isotherms the colour of FFD larvae underwent a colour alteration (data not shown). This type of alteration is presumably linked to enzymatic browning reactions taking place as a result of hydration of enzymes.

2.4   Conclusions

In drying of mealworm larvae, the Page model showed the best fit to the experimental data, obtaining an r^2 higher than 0.9932. The time to reach the monolayer moisture content of 0.05 (g H_2O/g dry matter) for air-dried samples at 70°C was approximately one third the time needed to reach the same level of moisture at 50°C. Estimated effective moisture diffusivity obtained with Fick's second law of diffusion increased with temperature from 4.85×10^{-11} to 1.10×10^{-10} and 1.62×10^{-10} m^2/s at 50, 60 and 70°C respectively. The dependence of the effective moisture diffusivity on temperature was well described by Arrhenius equation ($r^2 = 0.95$), and an activation energy of 52.1 kJ/mol was estimated. Blanching mealworm larvae in boiling water for 3 minutes increased their moisture content without affecting the proximate composition. Gab model well described sorption isotherm of all samples, obtaining an r^2 always higher than 0.995. Larvae of Yellow mealworms presented type II sorption isotherms, and blanching treatment reduced their hygroscopicity more than the employed drying methods. In light of reported observations, lyophilisation preserved the colour of fresh larvae the most. In order to properly utilize mealworm proteins, either as replacement in conventional food systems or for their direct consumption, a study of their functional properties is necessary. Since in these experiments colour alteration occurred for freeze dried fresh larvae after rehydration, we suspect this to be due to enzymatic browning reactions occurring due to recovery of enzymatic activities. Therefore, enriching high-moisture food products with fresh freeze dried mealworm powder, may trigger microbial spoilage and speed up degradative reactions. Furthermore, a study on the inhibition of PPOs by means of higher drying temperature, removal of oxygen by applying vacuum-drying technology or use of appropriate PPOs' inhibitors should be implemented. Moreover, in order to properly utilize mealworm's powder, either as replacement in conventional food systems or for their direct consumption further research on sensory aspects and functional properties are needed.

Chapter *3*

— Insect-enriched extruded snacks: mapping structure, texture and digestibility as a function of formulation and processing conditions—

Azzollini, D.[1], Derossi, A.[1], Fogliano, V.[2], Lakemond, C.M.M.[2], Severini, C.[1]
[1] Department of Science of Agriculture, Food and Environment, University of Foggia, Italy
[2] Food Quality & Design group, Wageningen University & Research, Wageningen, The Netherlands

Abstract:

Extruded cereals made of wheat flour and grinded Yellow mealworm larvea (*Tenebrio molitor*) were produced to investigate the effect of *T. molitor* inclusion (0%, 10%, 20%) and processing conditions (barrel temperature and screw speed) on their nutritional content, microstructure, texture and digestibility. At 10% insect substitution, protein content increased by 35%, high enough to claim the food as "source of protein" according to European food regulation. At 20% substitution, snacks showed poor expansion properties. Instead, at 10% inclusion, the adoption of high barrel tempearature and screw speed significantly improved microstructure in terms of expansion, porosity and pore structure, delivering acceptable textural qualities. Starch and protein digestibility was negatively correlated to pore wall thickness/pore size ratio (r^2 0.84, 0.83 respectively), confirming the role of microstructure in controlling digestibility of extruded snacks. These results reveal that by tailoring processing conditions and substitution level, insects can be successfully incorporated into extruded cereal snacks.

3.1   Introduction

Insects are highly valued as tasty and nutritious food by over 2 billion people mostly living in Asia, Africa and South America. In such areas, insects are mainly harvested from the wild and provide a significant amount of both macro- and micronutrients (FAO, 2013). Given the wide range of edible insect species, over 2000 reported by Jongema (2013), insects vary largely in their nutritional composition. Insects show a high nutritional variability, displaying a broad range of protein, fat and carbohydrate concentrations (Raubenheimer et al., 2014). Consequently, some species containing high amounts of specific nutrients represent a promising, yet underexploited food source. For instance, species of the order Orthoptera (grasshoppers, locusts, crickets) can contain up to 77% protein (dry basis) while a fat content of about 77% fat was reported for larvae of *Phasus triangularis*, Lepidopteran (moths and butterflies) (Ramos-Elorduy, et al., 1998). Furthermore, insects are also rich in important minerals, including copper, selenium, iron, zinc, magnesium, manganese, phosphorous, and vitamins like biotin, riboflavin, pantothenic acid, and folic acid (Rumpold & Schlüter, 2013). Recently, insects have gained much interest in Western societies as an alternative source of protein: one of the main advantages over other protein sources is the low environmental costs of production, which becomes essential to satisfy the rise in the global proteins demand (van Huis, 2013). Nevertheless, for distribution of edible insects on industrial scale different challenges need to be addressed, covering the development of automated rearing facilities, safe hygienic processing practices, and the establishment of international food regulations (Birgit a. Rumpold & Schlüter, 2013). Westerners show a great aversion towards the consumption of insects. Rejection towards insects has been mainly attributed to cultural and psychological barriers (Harris, 1985) and association with unhygienic or rotten foods (Caparros Megido et al., 2016). Several studies show that presenting insects invisibly within familiar preparations may be effective to reduce negative perceptions and to increase their acceptance (Hartmann & Siegrist, 2016; Looy et al., 2014; Tan et al., 2015; Tan, van den Berg, & Stieger, 2016b). Recently, Le Goff & Delarue (2015) reported that consumers reject the idea of tasting chips made by an invisible insect based flour, but they accept it after the first bite, suggesting that processing insects to create appealing products may be a good strategy to vehicle insect into food designed for Western consumers.

Ready-to-eat expanded snacks are very popular among Western consumers principally due to their convenience, attractive appearance and unique texture attributes. In fact, the consumption of expanded products have increased tremendously in recent years and their global market is projected to reach 31 billion dollars by 2019 (marketsandmarkets, 2014).

Expanded snacks are produced through the extrusion-cooking technology, which is an efficient manufacturing process. By combination of mechanical shear, high temperature and high pressure, starch solid materials are converted into a viscoelastic fluid that is pushed by a screw through a die. The sudden decrease in pressure vaporizes the water embedded in the fluid, leading to the formation of a solid foam with specific structural characteristics (pore wall size and thickness, porosity, density) and mechanical properties (Guy, 2001). Although starchy materials are the most suitable to deliver good technological features for production of acceptable snacks, they are often low in protein and dietary fibre being unable to satisfy the needs of an increasing number of health-conscious consumers (Brennan, Derbyshire, Tiwari, & Brennan, 2013). Improving the nutritional value of these types of snacks is a twofold opportunity either for consumers' health and food industries. Up to now the focus of the nutritional improvement was on whole grains, addition of legumes and other functional ingredients, which cause a decrease of sectional expansion and density, thereby increasing hardness of extruded products (Chanvrier, Desbois, et al., 2013; Lazou, Michailidis, Thymi, Krokida, & Bisharat, 2007; Ramos Diaz et al., 2015; Robin et al., 2012; Sumargo, Gulati, Weier, Clarke, & Rose, 2016; Yu, Ramaswamy, & Boye, 2013). To date, the use of edible insects in expanded extruded snacks has not yet been investigated. Besides the foreseen progress of insects' fractionation systems to obtain protein, fat and chitin, the incorporation of insects invisibly into familiar foods like snacks may be a valid strategy to speed their adoption among consumers.

The objective of this Chapter was to investigate the effects of different blends of wheat flour-Yellow mealworm larvae and processing conditions on structure, texture and digestibility of extruded snacks. Recipes containing 0-10-20% of grinded *T. molitor* first studied, and the 10% formulation was processed using different extrusion conditions. Extruded snacks properties were analysed by X-ray microtomography and compression test. Moreover, starch and protein digestibility of the snacks were evaluated by the in-vitro INFOGEST protocol.

3.2   Materials and methods

3.2.1   Materials

Wheat flour of type 0 was supplied by Molino Taramazzo (Pezzolo Valle Uzzone, Cuneo, Italy). Larvae of Yellow mealworms were supplied in dry form by from HaoCheng Mealworm Inc. (Xiangtan, Hunan, China). Larvae were microwave dried by the provider maintaining the temperature below 80°C. Dry larvae were ground for 60 s at 6000 rpm in a knife mill (Grindomix GM 200, Retsch, Germany) to pass through 900 μm sieves. Three blends of wheat flour and mealworm powder were formulated in mass ratios of 100:0, 90:10 and 80:20 on a dry matter basis (Table 3.1). Before use, the blends were mixed through a planetary mixer (cooking chef, Kenwood Ltd. UK).

3.2.2   Extrusion processing

The extrusion trials were conducted using a co-rotating twin-screw extruder (BC-21 extruder, Clextral, Firminy, France) consisting of nine independent zones with a total barrel length of 900 mm, a distance between shafts of 21 mm (L/D = 36:1), and a circular die opening of 5 mm. Further specifications are described by De Pilli et al. (2008). The extruder was operated at a constant feed rate of 10 kg/h and 18% moisture dry bases. Blends were extruded in two sets of experiments as reported in Table 3.1 and herein referred to as Exp1 and Exp2. In the first experiment three different formulations containing a mass fraction of 0, 10 and 20% of grinded mealworms were extruded as reported above, whilst in the second experiment the formulation containing 10% grinded mealworms was processed with 9 different combination of extruder screw speed and barrel temperature. The rationale for choosing the formulation of 10% was to fully study the effect of temperature and screw speed, and build a complete design of experiments with these factors while still maintaining an average level of insect enrichment. In all experiments, temperature profile of the first six zones was set at 30, 30, 50, 60, 80 and 100°C in forward order, while temperature of the last three zones and screw speed were set as reported in Table 3.1. Specific mechanical energy (SME) was computed according to De Pilli et al. (2008). After extrusion, samples were dried at 50°C for 6 hours, sealed in plastic bags and stored at -20°C till the experiments.

Table 3.1. Formulation and extrusion conditions used for the processing of Exp1 and Exp2 and moisture loss of extrudates at the die. Temperature of the last three zones are reported.

Samples	Wheat: mealworm ratio	Barrel temperature (°C)	Screw speed (rpm)	SME (kJ/kg)	Moisture loss (%)
Experiment 1					
i0	100:0	120, 150, 160	400	485	40.3 ± 0.3
i10	90:10	120, 150, 160	400	339	32.3 ± 0.3
i20	80:20	120, 150, 160	400	166	9.9 ± 0.4
Experiment 2					
i1	10	100, 110, 120	240	155	17.8 ± 0.3
i2	10	100, 110, 120	320	244	27.0 ± 0.2
i3	10	100, 110, 120	400	445	26.9 ± 0.2
i4	10	110, 130, 140	240	127	18.7 ± 0.1
i5	10	110, 130, 140	320	197	27.4 ± 0.2
i6	10	110, 130, 140	400	392	28.8 ± 0.1
i7	10	120, 150, 160	240	104	32.4 ± 0.1
i8	10	120, 150, 160	320	170	35.6 ± 0.1
i10	10	120, 150, 160	400	339	32.3 ± 0.3

(SME: specific mechanical energy)

3.2.3   Nutritional analysis of extruded products

Extruded snacks were milled to pass through 90 μm sieves and analysed for: total starch by Megazyme total starch kit K-TSTA 09/14 (AOAC, 2005); lipid by Soxhlet extraction (AOAC, 1920); ash by gravimetric method (AOAC, 1923). Protein content was analysed by Dumas method of combustion (AOAC, 1996) using a Nitrogen/Protein analyser (model FP-528, Leco St. Joseph, USA). EDTA was used as standard (Elemental Microanalysis Ltd, Okehampton, UK). Different nitrogen-protein conversion factors were used for each formulation. Proteins in wheat flour and mealworm powder were calculated by using respectively 5.71 and 6.25 N conversion factor. For blends, the N-conversion factors were computed as weight average between single N-factors and protein content.

3.2.4 Expansion characterization

Moisture analysis

Moisture loss corresponds to the moisture content of extruded snacks at the die exit and was computed by subtracting the residual moisture from the in-barrel moisture. Moisture was measured according to AOAC (1999) on six replicates.

Microstructure

Microstructural features of the extruded products were analysed using X-ray microtomography. Three pieces of snacks from each treatment were stuck on a sample holder and scanned by a micro-CT scan (SkyScan 1174, Brüker, Kontich, Belgium) under the following settings: voltage 50 kV, current 800 µA, sample rotation 360°, rotation step 0.6°, average frame 3, magnification 28.5 µm, exposure time 1600 ms. Scans were performed with the Skyscan software (version 2), reconstruction with the Skyscan NRecon software (version 1.6.2.0) and 3D image analysis with CTAn software (version 1.12.0.0). A number of 300 cross sectional greyscale images were reconstructed and converted into binary images by applying Otsu's method. The volume of interest was selected by the shrink-wrap function and the volume was eroded automatically to adjust to the surface of the sample. Product diameter was computed from the average area of extruded products as obtained by 2D analysis assuming samples had a circular shape. From that, expansion ratio was computed as the ratio between the square of product diameter and the square of die diameter. The pore size distribution (PS) was obtained by the structure separation function and the pore wall thickness distribution (PWT) was obtained by the structure thickness function. To reduce the error from noise and artefacts only voxels larger than 3*3*3 pixels were considered pores. Porosity was calculated as the ratio of the volume of pores and the total volume of the object. Pore density was expressed as ratio among number of pores per cubic millimetre. The total volume was subdivided into two regions, each of 300 images from bottom up.

3.2.5 Texture

Mechanical properties of the snacks were measured with a texture analyser (model TA-XTplus) equipped with a 50.00 kg load cell and operating with the software Exponent 6.1.4.0 software (Stable Micro Systems, Surrey, UK). Six dried pieces obtained from each extrusion condition were compressed to 70% of their initial diameter using a 75 mm compression plate (test speed of 1.0 mm/s). From the force-displacement curves, the maximum peak of the curve corresponded to the maximum compression force (*Fmax*) (N).

The area under the curve (S) and the number of peaks (n) were used to calculate the spatial frequency of ruptures (N_{sr}) as in Eq. 1, the average crushing force (F_{cr}) as in Eq. 2 and crispness work (W_c) as in Eq. 3 (Agbisit et al., 2007; Karkle et al., 2012)

$$N_{sr} = n/d \ (mm^{-1})$$

<div align="right">Eq. 1</div>

$$F_{sr} = S/d \ (N)$$

<div align="right">Eq. 2</div>

$$W_c = F_{cr}/N_{sr} \ (N \ mm)$$

<div align="right">Eq. 3</div>

where d corresponds to the probe travel distance.

3.2.6 Static *in vitro* gastrointestinal digestion

To evaluate the digestibility of extruded products, the standardised static *in vitro* digestion protocol developed within the COST FA1005 INFOGEST Network was adopted (Minekus et al., 2014). The protocol holds an international consensus and it is based on human gastrointestinal physiological conditions. Before digestion, samples from Exp1 and Exp2 were obtained using a laboratory mill (model A 11, IKA, Staufen, Germany) and sieved through stainless steel sieves to obtain a particle size between 0.9 and 1.4 mm. The reasoning for choosing this range of particle size was to retain intact snack microstructure while being consistent with the particle size reduction after the mastication (Jalabert-Malbos et al. 2007). Additional digestion was performed on snack samples with a particle size below 0.09 mm in order to investigate digestibility in a condition in which the effect of the pore segments on digestibility is reduced. Stock solutions of concentrated simulated salivary (SSF), gastric (SGF) and duodenal fluids (SDF) were prepared according to Minekus et al., (2014). An amount of 0.5 g of ground snacks were hydrated with 2.0 mL of deionized water in centrifuge tubes. Subsequently, 1.75 mL of SSF were added, the pH was adjusted to 7.0, followed by the addition of a solution of Ca_2Cl to achieve 0.75 mM in the final mixture and the necessary amount of deionized water to reach 50:50 ratio (w/v) between the sample solution and SSF. The solution was agitated for 2 min at 37°C to reproduce the oral phase. In this study salivary α-amylase was not added since the salivary hydrolysis of starch is negligible respect to the amount degraded by pancreatin in the intestinal phase (Woolnough et al., 2010). Bolus derived from the oral phase was mixed with 3.75 mL of SGF supplemented with pepsin (P6887 from Sigma, CAS n. 9001-75-6) to achieve 2000 U ml^{-1} in the final digestion mixture. The solution was adjusted to pH 3.0, Ca_2Cl was added (to achieve 0.075 mM in the final mixture), followed by deionized water

as indicated above. The digestate was kept at 37 °C for 2 hours followed by a gentle agitation at 20 rpm with an overhead shaker. Subsequently, 9.25 mL of SDF containing pancreatin (100 U trypsin activity/mL of digestate) and bile (10 mM in the total digesta) was added to the gastric chyme, the pH was adjusted to 7.0 followed by the addition of Ca_2Cl to achieve 0.3 M in the final mixture and deionized water. Samples were then incubated for 120 min as indicated above. Trypsin activity of pancreatin (P1750 4 x USP, from Sigma) was assayed using the p-toluene-sulfonyl-L-arginine methyl ester (TAME) assay as recommended by Minekus et al. (2014). The intestinal phase was stopped by adding 4 μL of 5 mM the protease inhibitor (Pefabloc® SC – 76307) and immediately centrifuged at 2000 g for 5 min at 4°C to remove unreacted starch (Warren et al., 2015). Thereafter the supernatant was filtered through a 0.45 μm Phenex-PTFE filter, snap-freezed in liquid nitrogen and stored at -20°C until analysis. The digestion was performed in triplicate and the degree to which protein and starch were digested were determined according to the methods described below

Determination of protein digestibility
The degree of protein hydrolysis after *in vitro* digestion was analysed by determining the content of free α-amino groups (NH_2) in the digestate supernatant. Free α-amino groups were determined after reaction with ortho-phthalaldehyde (OPA) following the method of Nielsen et al. (2001). Complete hydrolysis of samples was performed in 6 N HCl at 110°C for 24 h for obtaining the number of total NH_2 groups. For quantification of NH_2 groups, a calibration curve of L-serine (0.1 to 1.6 mM) was made and values of digestibility were computed as in Eq. 4

$$Protein\ dig. = \left(free\ NH_{2_{after\ INFOGEST\ digestion}} \middle/ free\ NH_{2_{after\ acid\ digestion}} \right) * 100 \qquad \text{Eq. 4}$$

Determination of starch digestibility

The degree of starch hydrolysis, after *in vitro* digestion, was assessed by determining the content of glucose. To this purpose, sugars in the supernatant, released from the pancreatic phase, were hydrolysed to glucose. Hydrolysis was performed with excess of amyloglucosidase from *Aspergillus niger* (800 U/mL of supernatant; 10113, Sigma) in 10 mM Na-acetate buffer, pH 4.8, at 60°C for 3 hours. Glucose was quantified using a glucose oxidase kit (GOPOD format, Megazyme Wicklow, Ireland) and converted to starch by a multiplication factor of 0.9. Starch digestibility was computed as in Eq.5

$$Starch\ dig. = \left(Starch_{after\ INFOGEST\ digestion} / Total\ starch_{extruded\ snacks}\right) * 100 \qquad \text{Eq. 5}$$

were total starch was measured as reported in the nutritional analysis section.

3.2.7 Statistical analysis

The data analysis was aimed at understanding the product characteristics (structure, texture and digestibility) as a function of formulation and process parameters. Analysis of variance (ANOVA) was performed to identify the main effect (Statistica, Statsoft, Inc, USA). Post-hoc analyses (Turkey HSD) were performed to assess the significance of difference at 95% significance.

3. Results and discussion

3.3.1 Composition of extruded snacks

The proximate composition of the extruded snacks obtained with different formulations is provided in Table 3.2. By increasing the percentage of mealworms, the protein content increased from 11.8 to 20.4 g/100g and the lipid content from 0.9 to 5.4 g/100g with a corresponding decrease of starch from 81.1 to 66.0 g/100g. As shown in Table 2, snack enrichment with mealworm powder improved their macronutrient composition towards the recommended ratio of nutrients for human diet as reported in the Acceptable Macronutrient Distribution Ranges of Food and Nutrition Board (2002). The high concentration of protein and lipid in mealworm powder led to a considerable increase in the same components in the extruded snack: protein in i10 and i20 accounts for respectively 16 and 21% of the total energy value, enough to claim the food respectively as "source of protein" and "high protein" according to European food law n. 1924/2006. A lipid concentration of 5.4% as present in i20 was still lower than those found in many extruded commercial products, in which lipid content may reach 35% of total weight (Ilo et al., 2000).

Table 3.2. Nutritional composition of snacks and grounded Yellow mealworms. Data are expressed as g/100g (dry basis). Values in brackets (%) correspond to the percentage of energy provided by the nutrient in the formulation.

Nutritional composition	i0	i10	i20	Yellow mealworms	AMDR (%) ***
Starch	81.1[a] (85.5)	73.3[b] (75.5)	66.0[c] (67.0)	5.3 (4.4)	45-65
Protein	11.8[a] (12.5)	15.9[b] (16.4)	20.4[c] (20.7)	54.2 (44.8)	10-35
Lipid	0.9[a] (2.1)	3.5[b] (8.1)	5.4[c] (12.3)	27.4 (50.9)	20-35
Ash	0.7[a]	1.1[b]	1.4[c]	4.0	-
Other*	5.5	6.2	6.8	9.1	-
Energy value (kCal/100g)**	379	387	394	484	-

Means (n = 3) with different subscript within the same row are significantly different (p<0.05)
*Includes fibre, other carbohydrates and vitamins.
** Heat of combustion considered: starch (4 kCal/100g), protein (4 kCal/100g), lipid (9 kCal/100g).
*** Acceptable Macronutrient Distribution Ranges of Food (Food and Nutrition Board, 2002).

### 3.3.2 Microstructure of extruded snacks

The representative cross-sectional X-ray images of the extruded products from Exp.1 and Exp.2 reported in Figure 3.1 showed that the extruded product obtained from only wheat flour was the largest and the most aerated one. The addition of grinded mealworms progressively reduced the size of extruded snacks and increased their compactness. The analysis of 3D reconstructed X-ray images was performed in order to quantify the main structural parameters, allowing a more objective comparison of extruded snacks than pure visual judgement.

Figure 3.1. Representative cross-sectional X-ray tomography images of extrudates from Exp.1 and Exp. 2. Coded values are reported in Table 1.
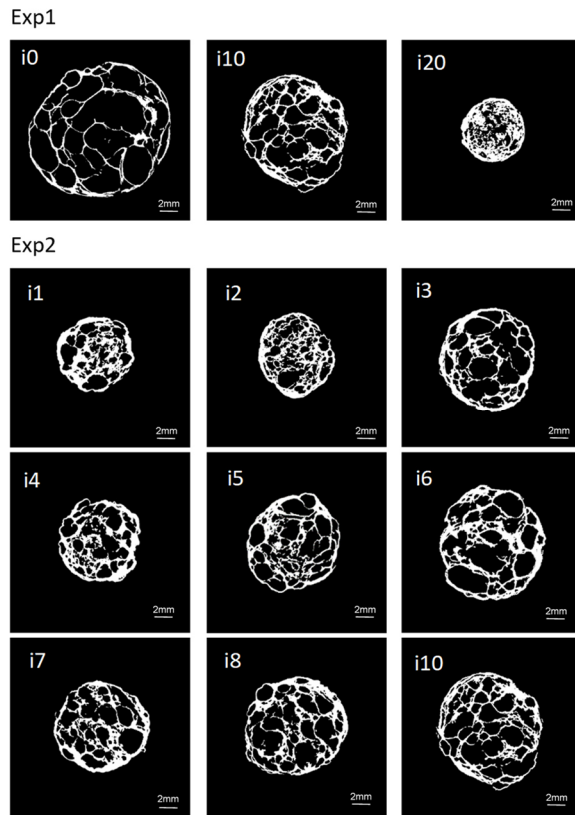
The main effects of formulation and processing conditions on microstructure are shown in Figure 3.2. From the first set of experiments, expansion ratio of snacks, shown in Figure 2b, changed from 2.95 to 2.42 and 1.45 respectively for i0, i10 and i20, indicating a negative linear relationship with the level of mealworm enrichment (r^2 0.97). For a fixed amount of mealworm powder (i.e. 10% as in Exp.2) different processing conditions were applied. Data show that the increase of barrel temperature and screw speed induced a higher expansion and increased the apparent pore size. In this experiment, the most compact product was obtained with the lowest barrel temperature and screw speed and *vice versa*. As visible in figure 3.1, a series of knot-like formations were found, especially in products obtained with mealworms and also for low processing temperature and low screw speed. Such knots are likely the results of poor product expansion, caused by limited starch conversion and the increase in protein and lipid content after insect enrichment (Ramos Diaz et al., 2015). Snacks extruded at 160°C and 400 rpm were 80% more expanded that those obtained at 120°C and 320 rpm (Table S.3.1 in supplementary material). Results show that both formulation and processing conditions altered the microstructure of snacks. In Exp.1, similar to the expansion ratio, porosity of snacks decreased with added Yellow mealworm. Interestingly compared to i0, the drop in porosity by 12% for i10 was significant but limited compared to i20, whose porosity was almost halved.

Figure 3.2. Main effects of formulation and process conditions on specific mechanical energy (SME) and structural characteristics of extrudates from Exp. 1 and 2. MW (percent of mealworm), BT (barrel temperature), SS (screw speed).
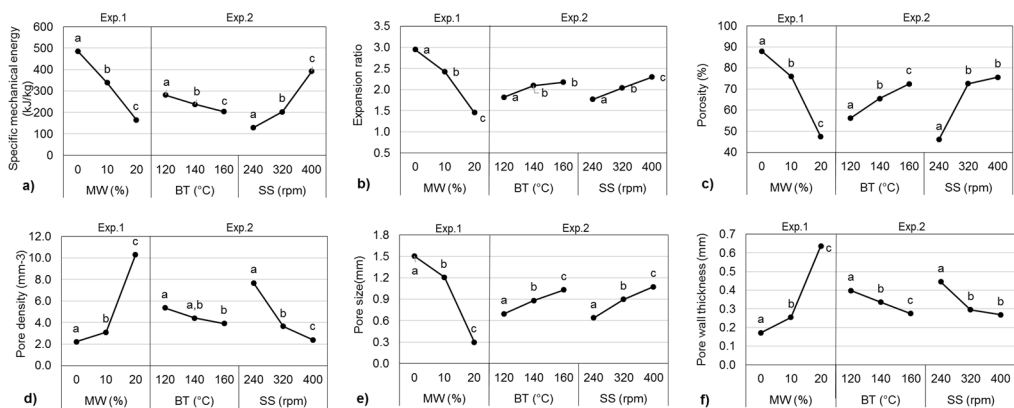

Points with different subscript within the same independent variable are significantly different (p<0.05).

Furthermore, increase of mealworms content from 10 to 20% resulted in a proportional decrease in the average pore size (PS) and an increase in average pore wall thickness (PWT). These observations reinforce intuitive expectations upon addition of oily and protein rich ingredients to an extruded product (Ilo et al., 2000; Robin et al., 2011). Structural properties are the result of viscoelastic properties of the melt, which depend on the characteristics of the raw materials (Moraru & Kokini, 2003). Looking at results of Exp.1, changes in microstructural properties could be mainly attributed to the lipid content. Concentrations of lipids below 1% lubricate and stabilize the extrusion process and favour the snack expansion, while higher concentrations reduce the melt viscosity causing a loss in mechanical energy (SME) conveyed to the melt (Ilo et al., 2000). The lower SME for blends in Exp.1 very likely reflects the effect of lipids in reducing the viscosity of the melt and hindering the hydration of starch, which is necessary for its gelatinization and expansion. The parallel increase in protein concentration may also have had a negative effect on expansion (Moraru & Kokini, 2003). Similar findings on extrusion of spirulina-corn (Joshi et al., 2014) and soy-rice (Yu et al., 2013) enriched extruded products were previously reported. During extrusion, proteins affect water distribution in the matrix and create a network through covalent and nonbonding interactions that changes extensional properties of the melt, limiting its expansion (Moraru & Kokini, 2003). Furthermore, although the observed changes can be mainly attributed to the increase of lipids and proteins, the lower expansion may also partially arise from the lower starch content in the recipes. Pore density increased as the mealworm level increased, from 2.2 to 10.3 pores per cubic millimetre in i0 and i20 respectively. Of course, this effect is strictly related with the reduction in average PS above discussed. Microstructural attributes of extruded products from Exp.1 were further characterized in terms of volumic frequency of pore wall thickness and pore size. Results are presented in Figure 3.3 and showed a clear decrease in pore size as mealworm concentration increased. In detail, the largest 20% of the pores were between 2.1 and 3.0 mm, 1.5 and 2.5 mm, 0.3 and 1.2 mm, in i0, i10 and i20, respectively. Similarly, the PWT increased as mealworm increased. Product having 20% grinded mealworm displayed the broadest spread as compared to those having 10 and 0% of mealworm.

These results confirm that thicker pore walls and smaller pore sizes were the result of limited expansion at the die caused by poor viscoelastic properties of the melt (Chanvrier et al., 2013) and low specific mechanical energy (SME) (Chanvrier et al., 2007).

Figure 3.3. a) cumulative cell size-volumetric distribution; b) cell wall thickness volumetric-distribution of extruded snacks from Exp.1.
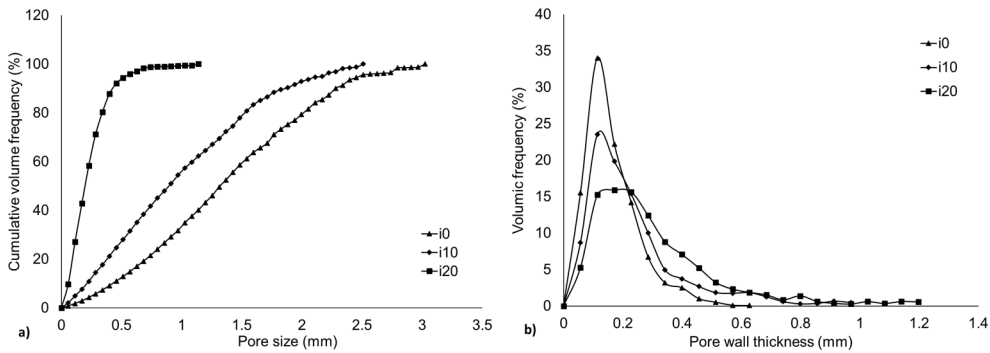

Data of Exp.2 showed a dependency between processing conditions and microstructure (Figure 3.2). The raise in temperature from 120 to 160°C increased the porosity from 56 to 72% and decreased pore density from 5.4 to 3.9 pores per cubic millimetre. Porosity was positively and linearly correlated with mean pore size ($r^2 = 0.78$) while an inverse relationship was observed with mean pore wall thickness ($r^2 = 0.95$). The measured SME decreased with increasing temperature. More specifically, a drop in SME 280 to 204 kJ/kg was recorded when temperature raised from 120 to 160°C. These results are in line with those of Altan et al., (2008) and Moraru & Kokini (2003), who found that that an increase in temperature leads to a lower melt viscosity and a consequent reduced SME. Although a reduced SME upon increasing temperature may suggest a loss in expansion, as found in Exp.1, this effect was not observed. Bhattacharya (1997) justified this behaviour with two hypotheses. At first, high temperatures could increase the extent of starch gelatinization, improving the melt homogeneity and its extensional properties. Secondly, a higher input of thermal energy enhances the amount of superheated steam. Hence, moisture flashes off more easily, providing a more expanded and porous structure to snacks. Data on moisture loss confirmed this hypothesis (see Table 3.1) showing that only the 9.9% of initial moisture was lost in 20% mealworms snacks, compared with a loss of 40.3% for samples having 0% mealworms. As for barrel temperature, similar observation can be made when increasing

screw speed which generally has a positive effect on product expansion (Moraru & Kokini, 2003). In this Chapter, the increase in screw speed from 240 to 400 rpm favoured the porosity, changing from 46% to 75% while a negative effect was observed for pore density which decreased from 7.7 to 2.4 pores per cubic millimetre respectively. Robin et al. (2012) observed a similar trend and they attributed the effect of screw speed on SME to a higher mechanical stress and shear rate transmitted from the screws to the melt, allowing a better hydration of starch and improved expansion. The increasing mechanical input with screw speed observed in these experiments can explain the differences in microstructural parameters.

3.3.3   Mechanical properties of extruded snacks

Textural attributes from a force-deformation curve are summarized in Table S.3.1 (supplementary material). The maximum compression force of extruded products is usually associated with the sensory perception of hardness during chewing (Roudaut et al., 2002). In these experiments, compression force increased with level of Yellow mealworm and decreased with barrel temperature and screw speed. For a more visual interpretation of the trend, values of compression force were plotted against the total porosity (Fig. 3.4a). The graph clearly suggested that in both experiments, regardless the formulation and processing conditions, the compression force is negatively correlated with porosity, following the global solid foam model (Gibson & Ashby, 1997). Samples with porosity below 50% stand above, exceeding a hardness of 400 N, while snacks corresponding to i0 and i10 showed the lowest Fmax.

Figure 3.4. Mechanical properties of extrudates from Exp.1 and Exp.2: (a) maximum compression force (Fmax) versus total porosity and (b) crispness work versus PWT/PS. Error bars represent one standard deviation from the mean.
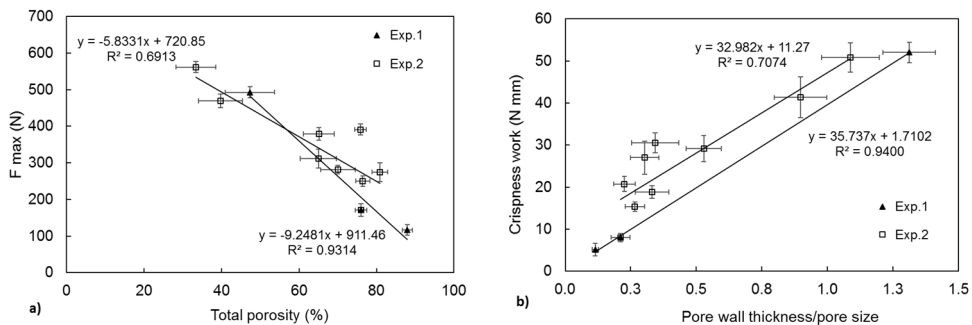
A similar behaviour was reported by Chanvrier et al. (2013) who showed that beside porosity, protein content further increased hardness. This effect was associated with modification of the pore wall composition and their morphology. Changes in protein content also occur in Exp.1, due to the increase of the mealworm concentration. However, the effect of protein cannot be stated in this case, probably due to the co-presence of proteins and lipids within the formulation. Data of Table S.3.1 indicated that low porosity products also exhibited the lowest spatial frequency of ruptures . This measure describes the number of fracture events occurring during compression and it is positively correlated with microstructural attributes of pores size (r^2 0.75). This is in line with findings of Chanvrier et al. (2006), who related this behaviour to the propagation of fractures at the phase interface, so that large pores exhibit a higher interfacial area and give more peaks. Crispness work (W_c), can be interpreted as the sensory parameter of fracturability and describes the work required to fracture one pore or a group of pores. Processing conditions and mealworm enrichment had an impact on W_c (Table S.3.1). In particular, snacks processed at lower barrel temperature and screw speed showed a high W_c. A strong relationship was found between W_c and the ratio between pore wall thickness and pore size (PWT/PS) (Fig. 3.4b). The graph shows that the average force required to break a pore was lower when pores were larger and had thinner walls. Furthermore, samples of Exp.1 had an overall lower W_c than those of Exp.2, displaying a parallel trend with reduced intercept. It should be remembered that snacks were obtained at the highest screw speed and barrel temperature, which may explain the lower values. Interestingly, no significant differences were observed between crispness of i0 and i10 (Table 3S..1).

## 3.3   *In-vitro* digestibility of extruded snacks

Digestion of extruded snacks was performed with the standardized *in vitro* INFOGEST protocol. To properly mimic the oral processing occurring during human consumption, it is important that also particle size of the digestate is considered. During mastication, food is broken into small particles. For snacks, the average particle size before swallowing is in the range between 0.9 and 1.4 mm (Jalabert-Malbos et al., 2007). In order to highlight the importance of microstructure, the determination of starch and protein digestibility was conducted on both fine (0.09 mm) and coarse (0.9-1.4 mm) extruded snacks. Therefore, to

improve readability, the results on digestibility of snacks with different particle sizes will be discussed in two different sections.

3.3.1   In-vitro starch and protein digestibility of the fine particle of the snacks

Results of fine particle starch digestibility (FSD) are reported in Figure 3.5a. In Exp.1 values of FSD ranged from 55.9 to 52.7% with the highest FSD measured for snack obtained without insects. The addition of 10% insects did not influence the FSD (p >0.05), while a significant decrease to 53.3% was observed at 20% addition. The degree of starch digestibility in extruded products is mainly linked to its gelatinization (Altan et al., 2009). The reduction of FSD with insect addition is likely due to the effect of lipids on the mechanical energy input and the consequent limited starch transformation. Lin et al., (1998) reported that the presence of 5% fat, similar to that found in i20, reduced the SME and the melt temperature, causing the decreasing of starch gelatinization from 100% to 82%. Furthermore, fat was also hypothesized to prevent absorption of moisture and gelatinization by forming a hydrophobic layer outside starch granules.

Figure 3.5. Comparison of a) starch and b) protein digestibility between extruded snacks at fine (<0.09 mm) and coarse (0.9-1.4 mm) particle size from Exp.1 and Exp.2. Error bars represent one standard deviation from the mean.
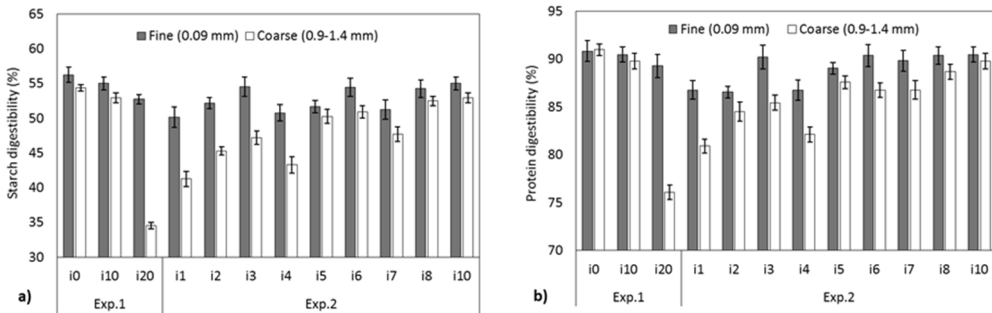

According to Guha et al. (1998) and Altan et al. (2009), protein-starch networks, developed during extrusion, may also decrease starch digestibility by trapping starch granules and reducing their susceptibility to enzymatic attack. In Exp.2, FSD decreased significantly (p<0.05) as screw speed increased, while no significant effects were observed for changes in barrel temperature. Snacks processed at 240 rpm had an average FSD of 50.7%, while increasing the screw speed at 320 and 400 rpm raised the FSD by 3.9% and 7.8%

respectively (see Figure 3.5a). Screw speed is known to play an important role in starch gelatinization (Lin et al., 1998; Moraru & Kokini, 2003). As previously discussed, a faster screw speed generates a higher friction, which tears starch granules apart and makes them more easily digestible. In this case a linear relationship was found between SME and FSD (r^2 0.62). These results are in agreement with Lin et al., (1998), who demonstrated that at 2.5% fat, a high screw speed significantly increased SME and starch gelatinization. The values of protein digestibility (FPD) were not significantly affected by snack formulation, remaining stable at 90.2% (see Figure 3.5 panel b). A lower protein digestibility for formulation containing insects was expected. Yi et al., (2016) found that in Yellow mealworm larvae, only 54% of undenatured yellow mealworm proteins were digestible after duodenal tract, while Marono et al., (2015) identified at 66% the level of protein digestibility. The higher protein digestibility found in these experiments may be due to denaturation of proteins. In addition low values of protein digestibility can be explained by the distribution of proteins in the larvae. Finke (2007) found out that a significant amount of amino acids (from 9.3 to 32.7%) in insects are either highly sclerotized or bound to chitin, and therefore may be difficult to digest. In i10 and i20, insect proteins accounted respectively for 35% and 50% of total proteins. Hence their presence was expected to lower the FPD. Since no difference in FPD was found among formulations, it is possible that as for other plant-based proteins (Day & Swanson, 2013), the shear forces in the extrusion may have mechanically ruptured these links and improved the digestibility. This hypothesis finds confirmation in the data coming from samples of the Exp.2. As shown in Figure 3.5 (panel b), also in this case, FPD was the highest at elevated screw speed and barrel temperature. When the percent values of protein digestibility were multiplied with the amount of protein in the respective formulation, a substantial increase in net digestible proteins was observed. In this case, snacks obtained with only wheat flour had the lowest net digestible protein content of 10.3 g $100g^{-1}$, while in those enriched at 10% and 20% mealworms, net digestible protein significantly increased to 13.7 and 14.8 g 100 g^{-1} respectively.

3.3.2 *In-vitro* digestibility of the coarse particle of the extruded snacks

The two panels of Figure 3.5 showed the values of starch (CSD) and protein (CPD) digestibility of snacks at this specific particle size. Both starch and protein digestibility of i0 and i10 did not differ from their respective FSD and FPD. Interestingly, the situation is different for the samples prepared with 20% grinded mealworm. In this case CSD and CPD were significantly lower than the respective values of digestibility measured on the fine particle size. In i20, CSD was of 18 percent point lower than FSD, while CPD decreased of 14 percent points compared to FPD, as reported in Figure 3.5 Panel a) and b). This could be an effect of different microstructure. Chanvrier et al. (2007) hypothesised that microstructure may govern accessibility of the digestive enzymes towards macromolecules, and therefore their digestion. For i0 and i10, similarities between fine and coarse digestibility were probably due to their high porosity, which produces a high surface contact area (i.e. small wall thickness) and so a higher diffusion of enzymes. Contrarily, i20 showed a high compactness, and its analysis it at fine particle dimension may have reduced the diffusion path length of enzymes, leading to an increase of digestibility. This concept was generalized and schematized in Figure 3.6, showing the internal structure of snacks in the range of wall thickness and pore size found in Exp.1 and Exp.2.

Table 3.4. Design of pore size (PS) vs pore wall thickness (PWT) within the range found in snacks. Values in the box correspond to the ratio PWT/PS. The image is purely indicative and does not reflect the real microstructure of snacks.
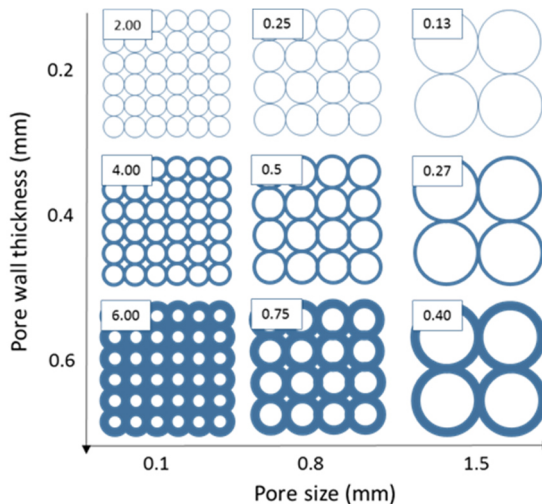
It should be noted that Figure 3.6 is only a schematic representation and does only reflect partly the real situation of the microstructure of extruded snack. It can be hypothesised that the pore thickness (PWT) describes the diffusion path length of enzymes while the pore size (PS) provides a measure of structure compactness. Therefore, the higher their ratio (PWT/PS) the less accessible molecules are to digestive enzymes. At large, if the wall thickness (PWT) describes the diffusion path length of enzymes, and pore size (PS) is considered as a measure of structure compactness, the higher their ratio (PWT/PS) the less accessible molecules are to digestive enzymes.

In Figure 3.7 digestibility data were analysed with respect to microstructural properties, and an inverse correlation was found (CSD r^2 = 0.827; CPD r^2 = 0.843; Fig. 7). Snacks with a high PWT/PS ratio, small pores and thick walls, had the most compact structure and lower digestibility values. For the same formulation, FSD decreased from 53.9% to 41.2% and CPD decreased from 89.8% to 80.9% in i10 and i1 respectively. No difference between fine and coarse size on protein digestibility was observed for i0 and i10. Since these snacks had the lowest PWT/PS ratio, it is likely that their structure did not limit the accessibility to digestive enzymes. A similar correlation (r^2 > 0.70) between PWT/PS and CPD or CSD was found when values from Exp.1 and Exp.2 were considered separately.

Table 3.7. Protein and starch digestibility of snacks obtained from both Exp.1 and Exp.2 versus ratio of pore wall thickness to pore size. Error bars represent one standard deviation from the mean.
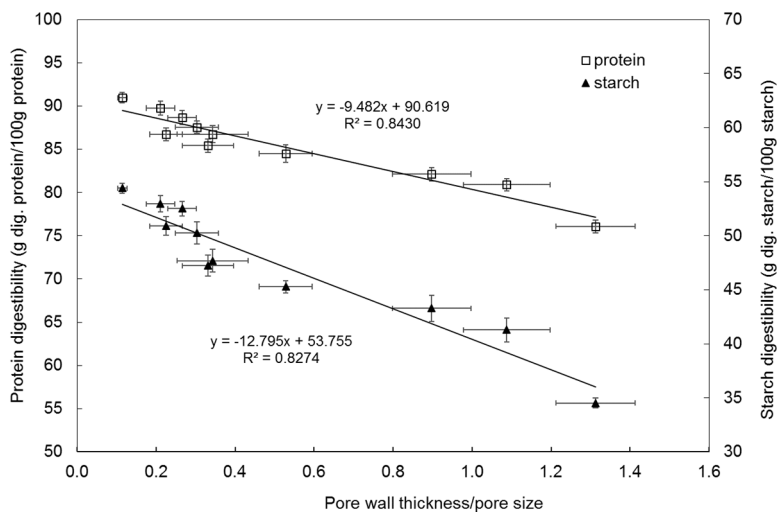
Values of digestibility were also negatively correlated to snack porosity, but to a lower extent (r^2 = 0.684 and 0.670, respectively). Furthermore, considering samples as i2 and i7 with a similar porosity (table S.1), protein digestibility was significantly different at 84.6 and 86.8% respectively only at p < 0.1. When looking at their pore structure, i7 had larger pores that may justify its higher digestibility, while a similar PWT was observed. These results are in line with Karkle et al. (2012), who proved the influence of microstructure on digestibility of extruded products and confirm the possibility of combining microstructural properties to control digestibility.

The use of an in vitro digestion procedure to assess the digestibility is surely a limitation of this work. However INFOGEST is now considered the most reliable procedure for in vitro assessment of digestibility. Due to the novelty of the INFOGEST protocol, these results are difficult to compare with data from the literature. The only record on adoption of the same digestive procedure is found in Stuknytė et al. (2014). In their work, a value of digested starch of about 15.9 g 100 g^{-1} was found in durum wheat pasta. This amount was lower than 45.8 g 100 g^{-1} (d.m.) of digestible starch found in snacks produced with only wheat flour (i0), probably due to different raw material and processing condition.

3.4   Conclusions

In this work the physico chemical and nutritional characteristics of extruded wheat-based snack enriched with insect powder (*T. molitor*) are reported. Microstructural properties of snacks were highly affected by formulation and processing conditions. At an inclusion of 20%, Yellow mealworm snack showed poor expansion properties, while for 10% inclusion, the adoption of high barrel tempearature and screw speed significantly improved microstructure in terms of expansion, porosity, pore wall thickness and pore size. Microstructure was the major attribute impacting mechanical properties of snacks, i.e. porosity was highly correlated with hardness of snacks. Microstructure was the major attribute impacting mechanical properties of snacks, i.e. porosity was highly correlated with hardness of snacks. Changes in microstructure were mainly attributed to high lipid content in mealworms. Data obtained by the *in vitro* INFOGEST protocol of digestion showed the role of microstructure in controlling protein and starch digestibility of extruded products, decreasing with the increase of the ratio pore wall thickness/pore size. Thanks to flexibility of the cooking extrusion proces, these results pave the way for designing of innvoative food microstructures with tailored digestibility characteristics. To date, insects are only allowed in their entire form in some EU countries. Hence, although their use in any form like protein isolate would probably overcome technological issues or possible lipid oxidation, their adoption for final market would currently be denied. The addition of grinded mealworm significantly improved the nutritional profile of the extruded product and the protein concentration of snacks added with 10% mealworm allows to use the claim "source of protein" according to European food law.

Supplementary material

Table S1. Microstructure, mechanical properties and digestibility (fine and coarse particle size) values of samples from Exp.1 and Exp.2.

Samples	Microstructure			Mechanical properties				Digestibility			
	Mean pore wall thickness (mm)	Mean pore size (mm)	Porosity (%)	F max (N)	N_{sr} (mm^{-1})	F_{cr} (N)	W_c (N mm)	Digested starch (g/100 g starch)		Digested protein (g/100 g protein)	
								Coarse	Fine	Coarse	Fine
Exp1											
i0	0.17	1.50	88	116	12.51	64	5.1	54.4	56.25	91.0	90.83
i10	0.25	1.21	76	171	10.56	85	8.0	53.0	55.01	89.8	90.47
i20	0.33	0.25	47	493	4.23	219	52.0	34.5	52.75	76.1	89.28
Exp2											
i1	0.57	0.52	33	561	4.37	221	50.8	41.3	50.14	80.9	86.75
i2	0.33	0.63	65	379	6.12	177	29.2	45.3	52.19	84.5	86.53
i3	0.29	0.89	70	281	7.70	144	18.8	47.2	54.54	85.4	90.18
i4	0.46	0.52	40	469	4.87	200	41.3	43.3	50.77	82.1	86.76
i5	0.29	0.95	76	391	6.71	179	27.0	50.2	51.65	87.6	89.02
i6	0.26	1.13	81	274	7.00	145	20.7	50.9	54.45	86.7	90.37
i7	0.30	0.88	65	312	5.53	169	30.6	47.7	51.24	86.8	89.81
i8	0.27	1.01	76	250	8.66	133	15.4	52.5	54.24	88.7	90.37
i10	0.25	1.21	76	171	10.56	85	8.0	54.4	55.01	89.8	90.47

F max: maximum compression force; Nsr: spatial frequency of ruptures; Fcr: average crushing force; Wc: crispness work.

Variables affecting the printability of foods: preliminary tests on cereal-based products

Chapter 4

Abstract

3D printing technology was employed to obtain cereal-based snacks having a desired shape and dimension. The printability of the dough and the quality of baked samples were studied as a function of two main variables: infill percentage and layer height. The obtained snacks well matched the designed structures but some dimensional changes were observed. The increase of layer height produced a reduction in the height of samples from 20 to 18 mm, as well as an increase of their diameter from 15.5 to 19 mm. This was attributed to the irregular deposition of the dough as the layer height increased. On the other hand, the infill level was more important for the changes in solid fraction of both raw and baked snacks exhibiting values of ∼84% and ∼24%, respectively. The breaking strength of samples was strongly related to the infill level, although a significant variability resided in the level of layer height used during 3D printing.

4.1   Introduction

In the last 20 years the growing development in printing technology has enabled to overcome the gap between the traditional bi-dimensional surface and three-dimensional space. The so-called 'Additive Manufacturing' (AM), also known as rapid prototyping, is the process by which 3D objects are built through the deposition layer-by-layer of several cross-sectional slices. From an economic point of view, 3D printing technologies are at least of two types, the commercial 3D printers with a cost lower than $ 10,000 and rapid prototype machines of up to $ 500,000 or further. Additionally, 3D printers of lower costs usually necessitate a computer-assisted design (CAD) software to save a design model as standard-stereo-lithography (STL) file, while the rapid prototyping use native CAD, Blender or Google SketchUp files (Berman, 2012). The first 3D printing technology developed at MIT was the powder deposition method (Sachs et al., 1992) (Cambridge, MA). This method is based on the deposition of a thin layer of a specific powder formula followed by the deposition of a suitable binding agent. The latter was essential to create links within the consequential powder elements. The quality of 3D printed objects is greatly affected by several variables, including the deposition method itself, binding criteria, liquid formulation, printing options (i.e. Drops-on-demand, DoD, or continuous-jet, CJ) as well as post-printing treatments (Utela et al., 2008, Bose et al., 2013).

More recently, several 3D printing technologies have been developed. These include laser sintering (SLS), fused deposition model (FDM), robotic assisted deposition, direct ink writing, laser-assisted bioprinting (LAB) and micro-extrusion (Bose et al. 2013; Murphy and Atala, 2014). To date, the most interesting researches and technical application of 3D printing focus on materials science such as polymers, metals, production of pharmaceutical dosage forms (Wang et al., 2006; Gbureck et al., 2007) and scaffolds for tissues generation (Sobral et al. 2011; Bose et al., 2013; Murphy and Atala, 2014). Goyanes et al. (2014) investigated the application of FDM technique to obtain drug-loaded tablets. The authors explored the effects of different 3D structures on the kinetic of chemical compounds release. The results proved that 3D printing could be an effective method to manage personalized-dose medicines. Studying the application of 3D printing for tissue generation, Sobral and co-authors (2011) produced several 3D scaffold architectures able to improve the cell seeding efficiency and cell distribution. Other interesting results in the field of biomaterials fabrication, animal tissues as well as edible polymers are available in literature (Mironov et al., 2009; Tessmar et al., 2009).

In food applications, 3D printing technology may provide opportunity to develop foods at low environmental cost and better quality (Yang et al., 2015) or to fabricate food structures with complex geometries and tailored nutritional contents (Godoi et al., 2016). Moreover, apart the type of technology, several variables significantly affects the performance of 3D printed structures. For instance, in the case of fused deposition material, the printer setting should be optimized in terms of extrusion temperature (°C), extrusion speed (mm), traveling speed (mm/s), layer height (mm), fill density (%), nozzle size (mm), shell thickness (mm), etc. Goyaned et al. (2014) studied the effect of different infill percentages (from 0% to 100%) on the quality of drug-loaded tablets proving that the infill level has a significant effect on the dissolution kinetic. This was probably due to the changes in the extrusion pattern during printing. Given these promising results, the interest in the application of 3D printing technology in food science is increasing (Wegrzyn et al., 2012). Among the above discussed technologies, laser-sintering, fused deposition material and extrusion deposition have been used in some cases in order to obtain 3D printed food structures. Sugar-based powders are the best materials to obtain complex shape structures through laser sintering technology (The CanyFab-Project, 2008). A like-FDM technique was used in order to produce 3D chocolate objects (Causer, 2009; Hao et al., 2010). The Netherlands Organization for Applied Scientific Research (TNO, 2015) proposed a 3D printer based on the deposition of pastes obtained by mixing several food ingredients. Lipton et al. (2010) obtained a cake shape by using a twin head extrusion and post-baking. However, all the above examples were focused on the production of commercial 3D food printer systems according to the consumer interests. On the other hand, in order to improve the knowledge of this technology when applied in food science, very few experiments have been performed in detail. Hao and co-authors (2010) found a linear relationship between extrusion speed and both bead diameter and mass of printed chocolate. Grazia-Julia et al., (2015) studied the behaviour of three food materials such as beef burger preparations, cheese cracker dough and pizza dough during 3D printing. The results showed that beef preparation and pizza dough were only printable by using a 4 mm nozzle while the cheese crackers were extruded with nozzles between 1.5 and 4 mm. Also, beef preparation was better printed by increasing the amount of salt and pepper probably due to the solubilisation of myofibrillar proteins, which decrease the force required for the extrusion. Vancauwenberghe et al. (2015) studied different formulation of bio-inks based on pectin with the aim to obtain 3D printed edible objects. In a first step, a bio-ink formulated with pectin, sugar syrup, bovine serum and $CaCl_2$ was printed. Then a post-processing consisting

in the incubation of the object in a CaCl$_2$ solution was performed to solidify the structure. Aregawi et al. (2015a) printed cookies by using the selective laser sintering technique (SLS). Other interesting examples were reported from Wegrzyn et al. (2012), Aregawi et al., (2015b), Vallons et al., (2015), Klomp et al. (2015) and Diaz et al., (2015).

From the above papers limited information on the effects of the printer variables such as travel speed, print speed, infill levels, layer eight, etc., on the printing performances of the food are available. Given these considerations, the main aim of this paper was to study the printability of a wheat-based food product as affected by some printing variables. More specifically, the printing performances of the dough as well as the characteristics of the baked samples were studied by analysing the changes in dimension, shape, microstructure and texture properties.

4.2 Material and Methods

4.2.1 Dough preparation

Commercial wheat flour 0 type (according to the Italian Food Regulation, 2001) was purchased locally and used for this study. Farinograph test was performed according to the standard AACC Method 54-21 (AACC, 2000) (Brabender, Duisburg, Germany) to determine the optimal mixing time and water absorption capacity of the flour to reach 500 BU. The farinograph analysis showed a development time of 4 min and a stability of 10 min, which is typical of strong flours. For experiments, the dough was prepared by mixing 100 g of wheat flour with 54 g of distilled water (according to farinograph absorption) in a planetary kneader (model cooking chef, Kenwood Ltd. UK). Ingredients were initially mixed for 1 min at low speed (60 rpm), the bowl was then scraped down, and mixed again for 3 min at the same speed. The dough was then covered with plastic wrap and left to rest for 30 min before use.

4.2.2 Experimental design

A Box-Behnken design of two variables, infill level (%) and layer height (mm), and three levels of variation were used for experiments (Box and Hunter, 1978). More specifically, the infill level refers to the solid fraction in the inner part of the designed structure and can be interpreted as the reciprocal of porosity. The layer height represents the distance, on the z-axis, between two successive layers, and it is the main parameter affecting print quality. A full factorial design of 3(k-p) experiments was performed, where k is the number of

independent variables and p is a parameter which refers to the interaction effects that are confounded with any other. In our case a total number of experiments N = 3(2-0) = 9 were performed (Box and Hunter, 1978). Table 4.1 shows the Box-Behnken design with the coded values for each independent variable and each experimental condition used during experiments.

Table 4.1. The arrangement of Box-Behnken design

Experiments	Codes		Variables	
	Layer height	Infill	Layer height (mm)	Infill (%)
1	0	+1	0.4	20
2	+1	0	0.5	15
3	-1	-1	0.3	10
4	-1	0	0.3	15
5	+1	+1	0.5	20
6	0	-1	0.4	10
7	+1	-1	0.5	10
8	-1	+1	0.3	20
9	0	0	0.4	15

In this case, the response surface methodology was not used to model or optimize but to investigate the effect of the two independent variables on the main properties of 3D printed objects. The experimental conditions of Table 4.1 were repeated in triplicate for a total of 27 printing tests. The other printing variables were set as follows: extrusion at room temperature, print speed (30 mm/s), travel speed (50 mm/s), number of shells of 1 and nozzle size of 0.6 mm. The three-dimensional structure used for food printing was designed by using the browser based 3D design Tinkercad (Autodesk, Inc.). A simple structure consisting in a cylinder with a diameter of 17 mm and a height of 25 mm was chosen for printing the snack. From Tinkercad, a stereolithography interface format file, .stl, was obtained and used as basis for changes infill and layer height in accordance with Table 4.1. CURA 15.04.2 (Ultimaker B.V., The Netherlands) software was used to modify the setting of .stl file obtaining the 9 different 3D structures of Box-Behnken.

4.2.3   Production of snacks by 3D printing

After resting, the dough was loaded into a tight piston chamber on which 4 bars pressure were continuously applied to convey the dough to the micro extruder for printing. A 3D Printer mod. Delta 2040 (Wasp project, Italy) equipped with the Clay extruder kit 2.00 (Wasproject, Italy) was employed for 3D printing experiments. The objects were printed on a stainless steel screen (2 mm mesh) and immediately frozen at -18°C until being baked and analysed. Samples were baked in a convection oven (mod. Vitality CE116KT - SAMSUNG, South Korea) at 200°C for 15 min.

4.2.4   Analysis of macrostructure and microstructure

Moisture content was analysed gravimetrically by drying 3 g of the printed samples at 105°C until constant weight. Weight loss was measured by measuring the changes in weight after baking in the oven. X-ray microtomography scans were acquired with a SkyScan 1174 (Brüker, Kontich, Belgium) with a voltage of 50 kV and a current of 800 μA. For a resolution of 28.5 μm, the camera was set up at 1304×1024 pixels with an exposure time of 1600 ms. Scans of raw and baked 3D printed specimens were acquired over 360°, with a rotation step of 0.6° and an averaging frame of 3. Cross section of the images was used to reconstruct the 3D image by using the Nrecon 1.6.2.0 (Bruker, Kontich, Belgium). Three dimensional stacks of several hundreds of gray scale images were obtained, representing the entire volume of each 3D printed sample. 2D and 3D analysis were performed using CTAn 1.12.0.0 (Bruker microCT, Kontich, Belgium). The 2D analysis of diameter was conducted on 5 different slices chosen every 150 images from the bottom to the top object to ensure sample representativeness; also, 3 diameters were measured for each slice. Similarly, 2 measurements of height were taken on 5 different coronal plane images. For 3D analysis, a cylindrical volume of interest (VOI) of about 400 mm³ was set and randomly applied 5 times on different parts of each food object. The grayscale images were converted into binary images with the software automatic thresholding algorithm and total porosity was obtained measurement by using the CTan software.

4.2.5   Instrumental analysis of texture

Texture properties of the 3D printed objects were measured with a texture analyser (model TA-XTplus) equipped with a 50.00 kg load cell and operating with the software Exponent 6.1.4.0 software (Stable Micro Systems, Surrey, UK). Baked objects were dried at 50°C to constant weight to avoid the effect of the water content, placed horizontally and compressed until the 70% of their initial diameter by using a 75 mm compression plate. A test speed of 1.0 mm/s was always used for all experiments. Three replicates were performed for each sample. From for force-displacement curves, the Fmax (Newton), corresponding to the maximum peak of the curve was extracted.

4.2.6   Statistical analysis

After each printing, the experimental data were fitted with a polynomial model in order to define the effects of independent variables on the quality attributes of snack. In particular, the following polynomial model was used:

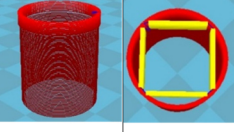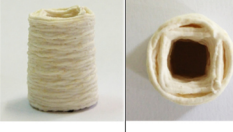$$y = B_0 + \sum B_i x_i + \sum B_{ii} x^2_{ii} + \sum B_{ij} x_{ij} \qquad\qquad \text{Eq.1}$$
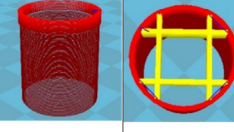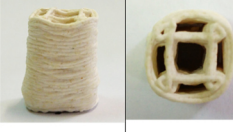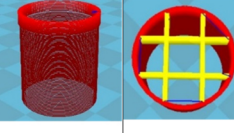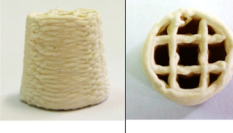
Where B0 is the initial value of the dependent variables, B_i, B_{ii}, B_{ij} are the regression coefficients, x_i and x_j indicates the linear effect of the independent variables, x_i^2 refers to the non linear (quadratic) effect of the independent variables while x_{ij} refers to the interactive effect of two independent variables. The goodness of fitting was evaluated by correlation coefficient (r), significance (p-level) and corresponding standard error (SE) of each regression coefficient estimated. With the aim to show the individual (linear or quadratic) and combined effects of the independent variables on the quality attributes of 3D printed snacks, three-dimensional plots were used. The principal component analysis (PCA) was used for discriminating the 3D printed samples on the basis of their physical, chemical and microstructure properties. All statistical analyses were performed using Statsoft ver. 10.0 (Tulsa, USA, 2011).

4.3   Result and Discussion

4.3.1   Changes in appearance of 3D printed products

At first, the visual aspect and the main dimensional properties of the 3D designed structures as well as the corresponding printed samples are shown in Figure 4.1. The designed structure has a total surface of 9.07 cm², a shell surface of 6.53 cm² and a surface of the inner part of 2.54 cm². Since the variable infill refers to the filling of the only inner part of the structure, without considering the external shell, a total solid fraction of 74.8, 76.2 and 77.6% may be calculated when the infill was respectively set at values of 10, 15 and 20%.

Figure 4.1. Three-dimensional designed structures, printed and baked snacks obtained in different operative conditions.

Layer height (mm)	Infill (%)	Calculated solid fraction (%)	Designed objects		Printed raw objects		Printed baked objects	
0.3	10	74.8						
0.4	20	76.2						
0.5	30	77.6						

Moreover, from the figure (on the left hand) the changes of the pathway performed by the extruder to obtain the different infill levels may be observed. Also, the Figure shows the distance between the transversal slices when layer height increases from 0.3 to 0.5 mm. On the right hand the printed raw and baked samples are shown. Both the samples showed a high accuracy being very similar to the designed structures. The external aspect and the internal design (i.e. the pathway of the extruder) were accurate stating as wheat-based products can be obtained by using 3D printing technology. However, visually speaking the samples appeared to be rougher as the layer height increased. Furthermore, it was observed that the diameter of samples increased as a function of the infill percentage and/or the layer height. This means that both the independent variables affected the printing performance thus the quality of final products. Furthermore, the figure shows the samples

after baking. In comparison with the printed dough, some modifications may be observed. Of course, these have been caused by the chemical and physical changes occurred during baking such as dehydration, protein denaturation, starch gelatinization, etc. However, the snacks captured the overall morphological properties of the designed structure stating as 3D printing is a useful technique to obtain wheat-based snacks with desired shape and dimension. In order to better discuss the printing performance of the dough, in the following sections the effects of the printing variables on the main dimensional and physical attributes as well as their microstructure will be analysed.

4.3.2 Effects of printing variables on dimensional properties of samples

Figure 4.2 shows the Pareto chart describing the effects of independent variables on the diameter of 3D printed samples. The linear effect of layer height was the stronger with an estimated effect of 13.456, followed by the nonlinear and linear effects of the infill percentage with values respectively of 2.723 and -2.282. It is interesting to observe that the linear effect of layer height and infill showed respectively a positive and negative sign, stating as the diameter of unbaked samples increased with layer height while it decreased with the infill percentage.

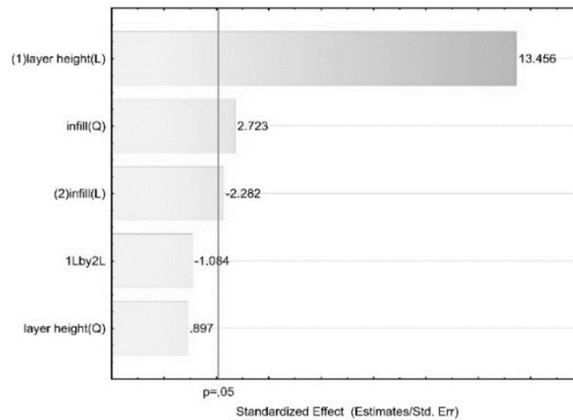**Figure 4.2** Pareto chart describing the effects of infill and layer height on the diameter of 3D printed snacks

Figure 4.3 shows the three-dimensional plot describing the effect of the infill and layer height on the diameter of 3D printed snacks.

Figure 4.3. Three dimensional plot describing the effect of infill and layer height levels on the diameter of 3D printed snacks.
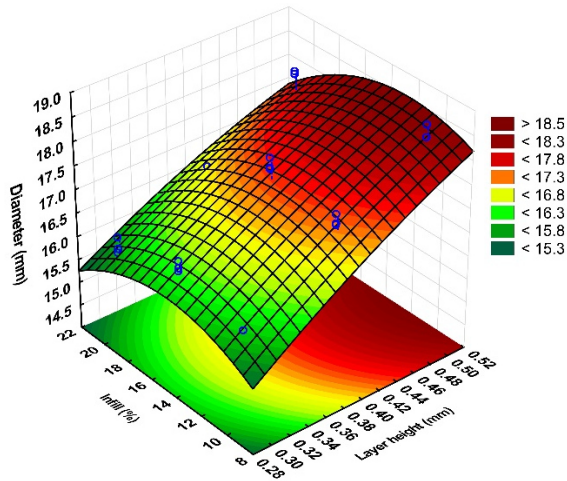
The polynomial model of Eq. 1 sufficiently described the changes in diameter showing a correlation coefficient of 0.90. Also, according to the Pareto chart, the effect of the infill was light giving a maximum change in diameter of ∼ 1 mm when the infill increased from 10 to 20%. This was expected since the infill only modifies what is printed inside the shell of the samples. Goyanes et al. (2014), by studying the effects of the infill level on the quality of printed drug-loaded tablets with a cylindrical shape, showed that any dimensional differences were not observed. In fact, the variation of the infill percentage from 0% to 100% produced a small variation of diameter from 10.55 mm to 10.67 mm respectively. In our case, when layer height was reduced from 0.5 mm to 0.3 mm, the diameter of samples significantly decreased from ∼ 18.5 mm to ∼ 15.3 mm. These values were respectively greater and lower in size than the designed 3D structure which was projected with a diameter of 17 mm. Only by using a layer height of ∼ 0.4 mm the diameter of printed samples well matched the desired structure. To better explain these discrepancies some considerations should be taken into account. In general, the layer height is greater, the time needed for the deposition of a new layer of material increased. In these conditions, the extruder automatically increases the print speed, enabling to maintain equilibrium between the amount of material extruded and the travel speeds. This equilibrium enables to obtain a good printing quality.

Nevertheless, commercial 3D printers are commonly set for synthetic materials such as PLA, ABS, PC, nylon, PET, etc. and these settings are not specific for food-like material; furthermore, no scientific information are available on possible setting of 3D printer when using food materials. In our case, the change in layer height led to three scenarios reported in Figure 4.4.

Figure 4.4. Schematic representation of three scenarios obtained during 3D printing with different layer height; Case A (layer height = 0.4 mm), Case B (layer height = 0.5 mm), Case C (layer height = 0.6 mm).
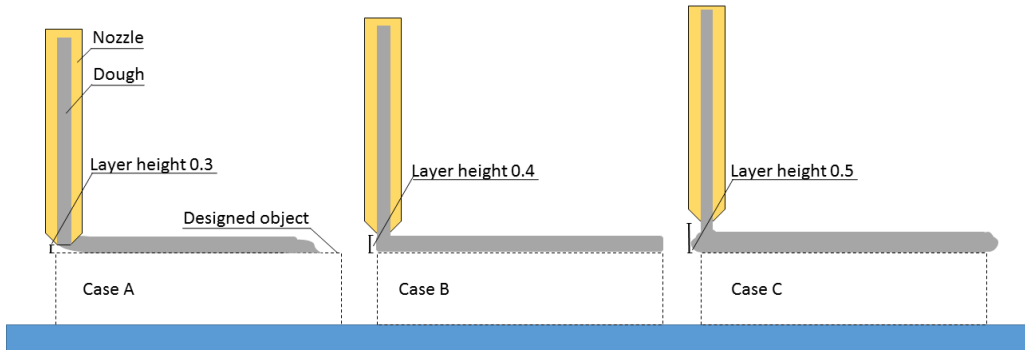
As shown in the case A, when layer height decreased until values lower than 0.4 mm, the deposition of dough occurred inside the underlying layer of dough. Consequently, the above reported reduction in printing speed was too high generating a situation in which not sufficient dough was extruded while the extruder travels with a speed of 50 mm/s. In this scenario, the dough was dragged during printing with the consequence reduction in diameter of samples. Instead, when the layer height was > 0.4 mm (Figure 4.4, case C) the dough settled irregularly on the underlying layer, particularly on the external surface of the shell leading to the observed increase of diameter of sample. An optimal deposition was achieved at layer height 0.4 (Figure 4.4, Case B), in which the dough was deposited in line with the underlying layer thanks to a sufficiently spaced layer height and to the equilibrium between the dough flow and printing speed. After baking, a similar trend of diameter values was observed. In this case, however, the results showed that the layer height was the only variable significantly affecting the diameter of samples with an estimated standardized effect of 12.155 (data not shown). In general, the experimental diameter of baked samples was lower than the unbaked material with values in the range of 14.0 mm and 16.5 mm. Of course, this may be considered as an effect of the water removal during baking process, which induced the reduction of dimension of samples (Figure 4.5).

Figure 4.5. Three-dimensional plot describing the effect of infill and layer height levels on the diameter of baked snacks.
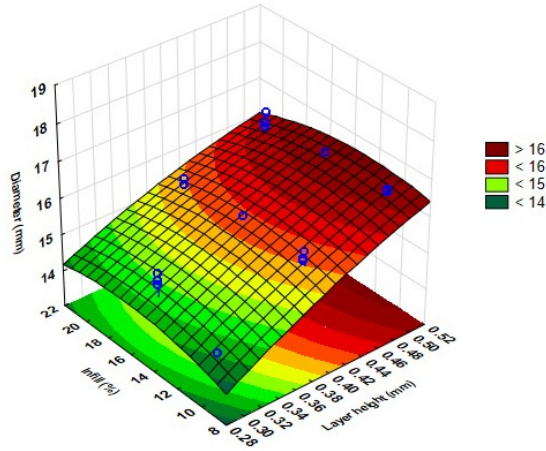

Figure 4.6 shows the effects of both infill and layer height on the height of baked samples. The model of Eq. 1 accounted for the 83.2% of the variance of experimental data showing a good ability in describing the changes of this attribute. Although both the independent variables resulted to be statistically significant ($p<0.05$) (data not shown), the figure clearly shows that infill percentage had only a slight effect.

Figure 4.6. Three-dimensional plot describing the effect of infill and layer height levels on the height of 3D printed snacks.
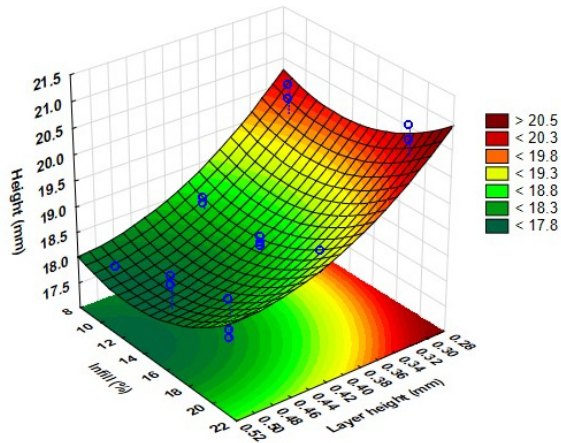
A maximum increase in height of samples of 0.5 mm was observed by increasing infill values. When modifying the layer height, important changes were detected showing its inverse relationship with the height of samples which exhibited values between ~ 20.5 mm and ~ 17.5 mm for layer height of 0.3 and 0.5 mm, respectively. This behaviour may be

explained in accordance with the above discussion. For simplicity, let us consider the deposition of the nth layer of dough during printing occurring after the (n-1)th layer. When layer height is high, the nth layer was irregularly deposited falling toward the external face of the shell. This, of course, reduced the expected increase in height of the samples. By repeating this phenomena n-time as there are the remaining n-layers of the 3D samples, it is clear as the experimental data showed an overall reduction in height. Furthermore, by progressively increasing the layer height this phenomenon increased, showing the reduction in height of the samples reported in Figure 4.6.

4.3.3   Changes in microstructure of samples upon baking

By fitting the solid fraction of raw and baked samples, the polynomial model of Eq. 1 precisely described the experimental changes showing a correlation coefficient greater than 0.965. Figure 7a and 7b report the standardized effects of the infill percentage and layer height on the solid fraction of raw and baked samples, respectively.

Figure 4.7. a) Pareto chart describing the effects of infill and layer height on the solid fraction of 3D printed snacks; b) Pareto chart describing the effects of infill and layer height on the solid fraction of 3D printed snacks after baking.
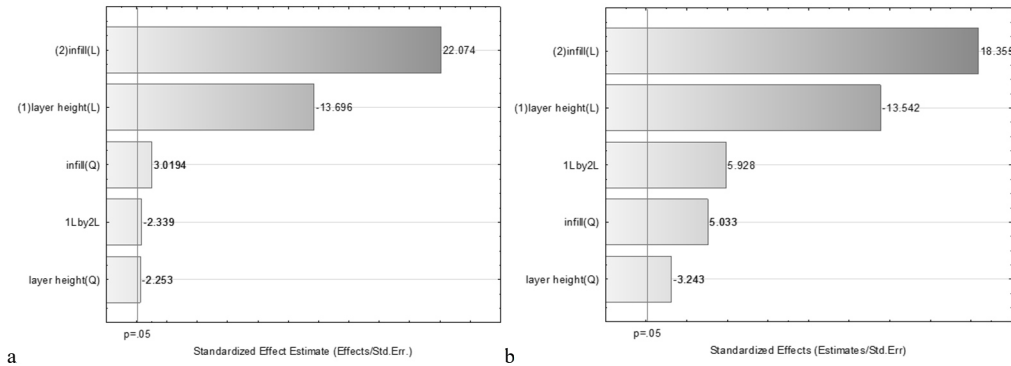
The infill was directly related with the solid fraction of samples showing also the greater effect. Of course, this was expected since that the greater is the infill percentage, the greater is the amount of dough used to fill the inner part of samples. On the other hand, the layer height showed an inverse relationship with the solid fraction of samples exhibiting estimated effect of -13.696 and – 13.542 respectively for raw and baked samples. This behaviour could be explained taking into account that when the layer height increased the not accurate deposition of the dough above reported created many pores among the layers of the snacks leading to the reduction in solid fraction. Figure 4.8 shows the three-

dimensional plot describing the effects of infill and layer height on the solid fraction of raw samples.

**Figure 4.8.** Three-dimensional plot describing the effects of infill and layer height levels on the solid fraction of raw 3D printed snacks.
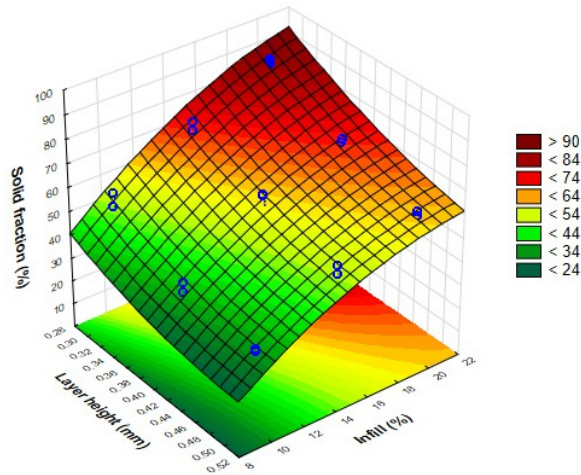
In accordance with the standardized effects of figures 4.7a and 4.7b the infill percentage had the most important effect on the solid fraction of samples. With a low layer height of 0.3 mm, the increase in the infill produced an increase in the solid fraction of samples from ∼54% to ∼90%. Moreover, when considering the highest layer height of 0.50 mm, solid fraction values between ∼ 24% and ∼ 64% were obtained. In general, these results are significantly lower than the expected values. As reported in Figure 4.1, when infill values of 10, 15 and 20% were applied, the corresponding solid fractions of the designed structure were respectively of 74.8, 76.2 and 77.6%. Again, it should be considered that the common 3D printers are used to perform the fused-deposition of synthetic material such as filament of PLA, nylon, etc. These materials during 3D printing maintain constant their density enabling to obtain 3D structures without any changes in void/solid fractions. In our case the dough imply differently behavior; the lower solid fraction may be caused by two main contributions. As well known, during kneading time a significant amount of pores, generally recognized to be in a range of 10 – 20% of voids, are randomly dispersed in the dough. That means that our solid matrix (the dough) contains a 10 – 20% of void spaces before being used to print the samples. Moreover, it is reasonable to suppose that several new pores may be created during the layer-by-layer deposition of the dough producing an additional decrease in solid fraction of samples. Furthermore, the fitted surface clearly

describes a reduction in solid fraction of samples by increasing the layer height for any infill value. However, in this case the changes were slight with values from 45% to 34% for the lower infill level (10%) while values between 90% and 64% were observed by using the maximum infill of 20%. On these bases, it can be stated that when the layer height increased, the not accurate deposition thread deposition of the dough, produced a structure having a major amount of voids. Figure 4.9 shows the solid fraction of baked samples as a function of designed infill and layer height.

Figure 4.9. Three-dimensional plot describing the effects of infill and layer eight levels on the solid fraction of baked 3D printed snacks.
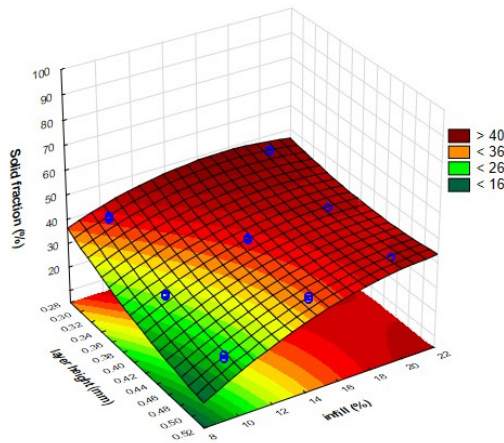
Although the trend was close to that reported in Figure 4.8, the experimental data were significantly lower than raw samples showing values ranged between 45% and 21%. Of course, this is because the vapor produced during baking greatly increased the dimension of the pre-existing pores as wells it created new ones. Also, by comparing Figures 4.8 and 4.9, the major differences are shown for the samples printed with the highest infill levels. For instance, when using an infill of 10% and by increasing the layer height values, solid fractions reduced from 24 - 44% to 16 - 36% for raw to baked samples, while ranges of 74 - 90% and 40 - 45% were observed by using the maximum infill of 20%. Obviously, when a greater infill was used, a major fraction of dough was extruded and a greater amount of new pores were created during baking under the action of forming vapor. Furthermore, the major differences in solid fractions as a function of layer height and infill level were observed for raw samples (Figure 4.8) because after baking the abruptly increase in void fraction significantly reduced the effect of independent variables on the structure of samples. However, to better study the behaviour of samples after baking, the difference in

porosity (DP%) after baking was evaluated as the difference between the porosity of baked samples (Pc) and the porosity of raw samples (Pr), and plotted against the infill values (Figure 4.10).

Figure 4.10. Changes in porosity fraction of 3D printed snack after baking as a function of infill levels
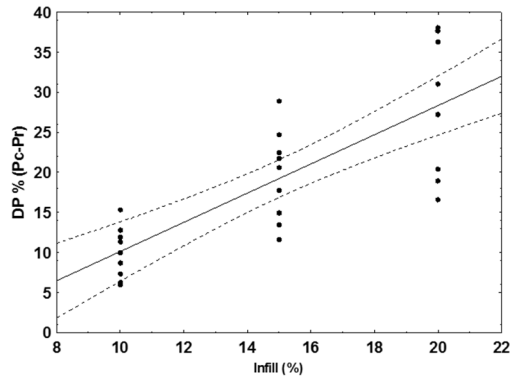
The data were well structured with the infill showing as a simple linear model accounted for the 60% of the variance of experimental data (data not shown). This proved as the amount of dough extruded during printing greatly positively affected the increase in porosity observed after baking. However, the figure shows a high variability of experimental data, particularly when the highest infill values were used. This variability resides in the effect of layer height which, as reported in Figure 4.8, produced a significantly reduction in solid fraction (increase in porosity) as layer height increased. Of course, during the 3D printing of samples, the changes in porosity fraction of samples when increasing the layer height became bigger and bigger with the increase of infill level.

Figure 4.11 shows the transversal section of micro-CT images of samples obtained by 3D printing in different conditions. The images refer to a single slice randomly chosen inside the sample. For raw samples, we can observe a good match between the micro-CT image and the picture reported in figure 1 stating as the internal structure of the snacks well matched the designed structure of samples. Only in the case of the samples printed with an infill of 20% it seems that the internal structure does not sufficiently capture the general features of figure 1. However, it should be taken into account that the two images refer to samples obtained with different layer heights of 0.5 mm for of picture of figure 1 and of 0.3 mm for the micro-CT images.

Figure 4.11. Original X-ray micro CT virtual transversal-sectional images of 3D printed snacks. A) Sample obtained with an infill of 10% and layer height of 0.5 mm; B) Sample obtained with an infill of 15% and layer height of 0.4 mm; C) Sample obtained with an infill.
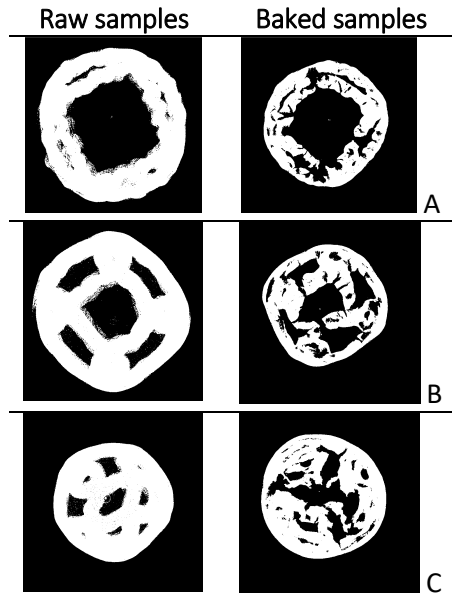
As previously discussed by using the lower layer height the reduction in printing speed was too high in comparison with the travel speed of the extruder, leading to the dragging of the dough toward the inner part of the snacks. That means that the raw samples C reported in Figure 4.11 exhibited the unexpected level of filling in comparison with designed structure and/or the snack printed with layer height of 0.5 mm. According to the results of Figures 4.8 and 4.9, a great increase in porosity was observed after baking as a consequence of the action of vapor, which created new pores. Also, as clearly observed, the fractional increase in porosity was higher for samples printed with an infill of 20%, while, for the raw samples obtained with an infill of 10% (the highest void fraction), only a slight increase was observed after baking. Moreover, it is possible to observe an increase in diameter as layer height increased, due to the not accurate deposition of the dough toward the external surface of the shell.

The breaking strength of samples printed by using a layer height of 0.4 mm and different infill levels are shown in Figure 4.12.

Figure 4.12. Breaking strength of baked 3D printed snacks obtained with different infill levels.
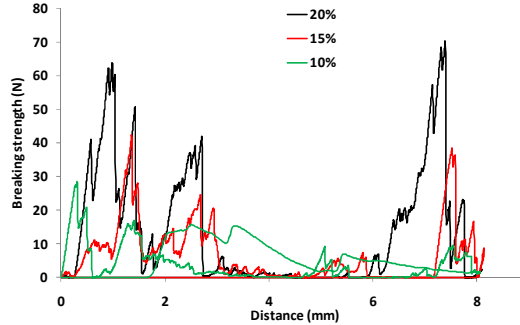
In all cases a first series of peaks were detected while the compression plate travelled from 0 to ∼3 mm. Then negligible values were observed until reaching 6 mm of displacement. Of course, in the first 3 mm the most important fractures were observed, while the second series of peaks, between 6 and 8 mm, are the result of the compression of many small pieces of samples randomly rearranged in the cell during the experiments. In the middle, the data are close to zero because the pieces of samples are far from the plate. However, as expected, a reduction of breaking strength was observed when reducing the infill level. Analysing the first 3 mm of the profile the 3D samples exhibited maximum values of 62.62 N, 40.79 N and 26.31 N for infill values respectively of 20%, 15% and 10% stating an increase of ∼1.5 times of the hardness of samples with a fractional increase of infill of 5%. However, when grouping the samples on the basis of infill percentage (for any considered layer height level) a significant variability of breaking strength was observed. Moreover, a high variance was also observed among the replicates indicating as important variability reside in the sample. This could be caused by different microstructure properties caused by the shape, dimension, connectivity of pores produced during baking. Finally, a principal component analysis (PCA) was performed taking into account all attributes of baked samples with the aim to highlight a possible discrimination. The PC model accounted for the 93.6% of the total variance of the samples with 3 principal components (PC): PC1 of 69.0%, PC2 of 19.1% and PC3 of 5.5%. In general, all variables showed a power contribution in the definition of PC model higher than 0.88. However, among them the breaking strength was the most important followed by solid fraction, diameter, layer height and moisture content while the infill level, weight loss and the height of 3D printed samples were less important in explaining of sample variability (data not shown).

Figures 4.13a and 13b respectively show the plot of loading and the plot of score in the PC1-PC2 axes. According to the above discussion an excellent relationship was found for diameter of samples and the layer height which were practically overlapped on the right hand of PCa axis. Moreover, in the left hand of PC1 axis, solid fraction, moisture content and breaking strength of baked samples were close stating a good relationship among them. Of course, when the amount of solid matrix of the sample increased an increase of the hardness of samples was detected. When the infill percentage increased the solid fraction also increased, although they were not hardly related. This, as previously discussed, was likely caused by two main reasons: 1. the difference between the designed infill level and the real solid fraction obtained on the printed samples; 2. the effect of vapor produced during heating on the amount and the dimension of voids created on baked samples.

Furthermore, according to the results of Figure 4.6, the level of layer height used during printing and the height of samples were inversely related as a consequence of the irregularly deposition of the dough. When analysing the principal component projection of the scores of samples, a good discrimination between two series group was obtained. More specifically, the first classification (solid lines) may be obtained through the variable infill, solid fraction, breaking strength and moisture content. Considering both figs 13a and 13b, it was observed that the samples printed with infill levels of 20% and 15% fell in the same direction of the all above variables stating the highest values of these attributes. Contrarily, the samples printed at infill 10% were in the opposite directions showing the lowest values of the considered attributed. Moreover, the snacks printed with infill of 10% and layer height of 0.5 mm were close to the weight loss meaning that they were subjected to the greatest weight loss during baking. Similarly, the samples printed with infill of 20% and layer height of 0.3 mm were characterized from the highest moisture content, solid fraction and breaking strength.

Another interesting classification of samples was highlighted with the dot lines. Again, three main groups were observed particularly on the basis of diameter, layer height and, in opposite direction, the height of samples. Samples printed by using the layer height of 0.5 mm were classified for the highest diameter and layer height while the samples printed with 0.3 mm were grouped for the highest height of samples while the samples printed by using a layer height of 0.4 were in the middle of the two variables showing intermediate values of height and diameter. This is in accordance of the above discussion where we hypothesized a not efficient deposition of dough when the layer height increased, leading to a decrease in height of samples.

Figure 4.13. a) Principal component projection of the loading plot of the quality attributes of 3D printed snacks; b) Principal component projection of the score plot of the 3D samples printed with different infill and layer eight levels.

a

b
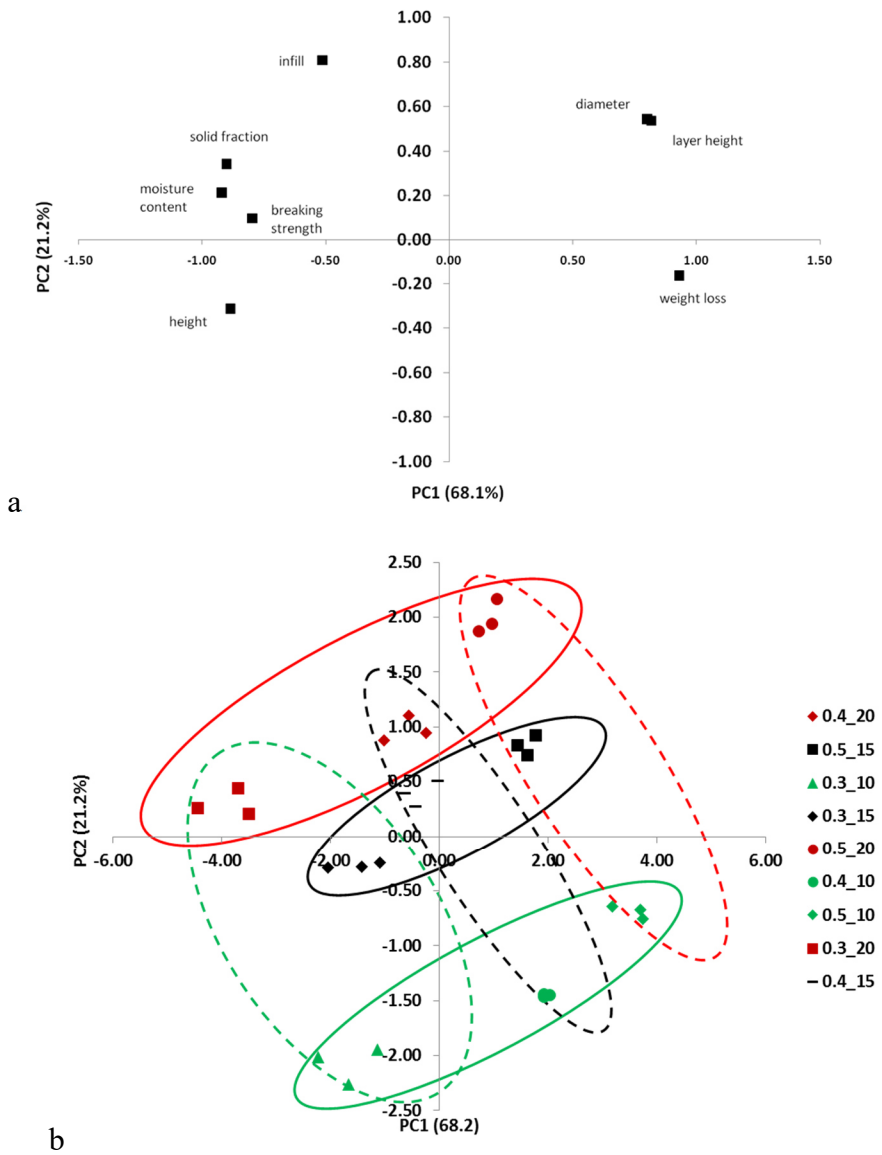
3.4.   Conclusion

3D printing successfully enabled to obtain 3D designed cereal-based snacks. For the first time, the effects of infill density and layer height levels on the printing performances of wheat dough were analysed. Results proved as the obtained snacks kept the main features of the designed structure both before and after baking, although some unexpected behaviours were observed. The diameter of samples was directly related with the layer height while their heights reduced with the increase of layer height. Probably this was because the 3D printers are still exclusively optimized for synthetic materials, such as PLA, and are unable to keep a good equilibrium between print speed and travel speed of the extruder when materials with different rheological properties are used. Taking into account the fraction of solid matrix and pores as well as the hardness of obtained 3D printed snacks, the infill level showed the highest contribution. A direct relationship between infill level and solid fraction of both raw and baked snacks as well as of their hardness was detected; however, a high variability in the breaking strength of samples was observed. This resides both in the effect of layer height used during printing and by the natural variability of voids (shape, dimension, connectivity) randomly produced during baking. The internal structure of the snacks generally maintained the designed one, except for samples printed with layer height of 0.3 mm, for which the irregular deposition of the dough led to random filling of the pre-existing void phase. For a practical application of 3D printing in the field of food, particularly for cereal-based product, a precise setting of all printing parameters should be performed as a function of mechanical properties of dough. Furthermore, the study of the rheological properties and their relationship with the printing variables will be of crucial importance to improve the quality of 3D food objects.

Chapter 5

—— On printability, quality and nutritional properties of 3D printed cereal based snacks enriched with edible insects ——

Abstract

3D printing technology was employed to obtain snacks with a designed cylindrical geometry from wheat flour doughs substituted with ground larvae of Yellow mealworms (*Tenebrio molitor*) as novel source of proteins. The main microstructural features, quality, and nutritional attributes were studied as a function of formulation, baking time and temperature. The substitution of ground insects up to 20 g/100 g (d.b.) decreased the dough stability as measured by farinographic test. This caused a higher dough deposition during printing that slightly increased the thickness of printed dough filaments. Baking did not modify the main designed features of snacks, but it increased snacks height due to water evaporation between consecutively deposited layers. Together with the increasing insect substitution, baking conditions modified some quality attributes of 3D printed snacks, altering their microstructure, mechanical properties and protein digestibility, inducing non-enzymatic browning reactions. Snacks with tailored quality attributes were obtained by optimizing baking conditions through a desirability function, and compared for their nutritional quality. The substitution of wheat flour with 0, 10 and 20% ground insects significantly increased the total essential amino acid (aa), respectively from 32.5 to 38.2 and 41.3 g/100 g protein. The protein digestibility corrected amino acid score increased from 41.6 to 65.2 from 0 to 20% insect enrichment, with lysine and methionine+cysteine being the respective limiting aa. Our results validate the rational promotion of insects based on nutritional arguments and indicate that together with wheat flour, they could be suitable ingredients to manufacture 3D printed foods without adverse impact on technological quality.

5.1   Introduction

Edible insects have been recognized as a sustainable source high-value animal proteins, bearing the potential to help satisfying the raising demand of meat products (van Huis, 2013). The protein content of insects ranges from 40 to 75 g/100 g on dry weight basis, mainly depending on the species and the stage of life cycle (Verkerk et al., 2007). Furthermore, thanks to their wide micronutrient variations, insects could also serve as equivalents of shellfish, nuts and pulses (Raubenheimer et al., 2014). Globally, around 2 billion people eat almost 1900 species of insects as part of their diet, particularly in Asia, Africa and South America (FAO, 2013). Contrariwise, in parts of the world where the consumption of insects in not traditional, such as Europe and North America, consumer negative perception is identified as a significant barrier to their widespread adoption (Deroy et al., 2015; Looy et al., 2014; Shelomi, 2015; Tan et al., 2015). To overcome the disgust of Western consumers, most of the existing research has focused on rational promotion through ethical and nutritional arguments (De Boer et al., 2013), identification of psychological individual traits (Schösler et al., 2012; Tan et al., 2016a; Verbeke, 2015), sensory appeal and appropriateness of developed food product (Caparros Megido et al., 2014; Tan et al., 2015). Recently, Tan et al., (2016) confirmed that presenting insects invisibly into familiar food carriers increases their acceptability. Not surprisingly, researches are being performed on the quality of dry forms of insects (Azzollini et al., 2016) and their extracts (Bußler et al., 2016; Yi et al., 2013; Zhao et al., 2016). At the same time, though, since familiarity arises sensory expectations, the combination of insects with a carrier perceived as inappropriate results in low consumption intentions. Therefore, alongside socially aware marketing campaigns and advances in processing practices, the design appropriate insect products with no sensory expectations is a critical factor. To this end, 3D printing has been recognized as an important tool at disposal of edible insect industries (Payne et al., 2016).

3D printing, better known as additive manufacturing (AM), is an innovative process of fabrication where a digitally-controlled robotic construction process can make three-dimensional objects based on a layer-by-layer deposition. AM refers to a group of three main technologies classified as selective binding, selective solidification and selective deposition. Engineering, manufacturing and medicine are key areas where AM is driving major innovations (Campbell et al., 2011). Besides, food is also regarded as an area with large potential for industrial and home applications of 3D printing (Lipton et al., 2015; Pallottino et al., 2016; Sun et al., 2015; Wegrzyn et al., 2012). Among numerous

applications, additive food manufacturing (AFM) is becoming popular thanks to the possibility to design foods with appealing forms, new textures and personalized nutritional values (Severini & Derossi, 2016; Yang et al., 2015). Perhaps thanks to its low cost and ease of use, in AFM, the selective deposition has become the most widely studied technology. With this technology, a soft-material formulated of edible ingredients is loaded into a cylinder and extruded in consecutive layers through a nozzle by force of a piston (Godoi et al., 2016). Aregawi et al. (2015) applied the selective deposition system to print cookies with a honeycomb structure, while Lipton et al. (2010) printed a cube with a deconstructed meat paste with the aid of transglutaminase enzyme. Severini et al. (2016) obtained snacks with different texture by printing a wheat dough with designed values of porosity. The European PERFORMANCE project employed the same technology to design 3D printed meals with proper consistency for older people who have difficulties with swallowing (Fp7, 2016). An example of 3D printing technology applied to edible insects is represented by Soares & Forkes (2014), who printed larvae of Yellow mealworms (*T. molitor*) in combination with fondant to produce icing for top cakes' decoration.

Larvae of Yellow mealworms have been commercially farmed for human consumption in many regions of the world (Kim et al., 2016). Furthermore, in countries such as USA, Canada, Mexico, Belgium and the Netherlands, dry powders of Yellow mealworm larvae or their derivatives can already be found in the market (Dossey et al. 2016). The design of 3D printed foods containing Yellow mealworm larvae may help to fully realize their potential and contribute to improve the nutritional value of familiar raw food matters.

In this Chapter, it is investigated the printability and technological characteristics of 3D printed snacks obtained with a wheat flour dough substituted with different amounts of Yellow mealworm powder. The effect of mealworm powder and baking conditions on some physical properties and microstructure of snacks was analyzed. Furthermore, the nutritional value, protein digestibility and amino acid profile was compared among snacks obtained at different levels of substitution.

5.2 Materials and methods

5.2.1 Dough preparation

Wheat flour of type 0 was provided by Molino Taramazzo (Pezzolo Valle Uzzone, Cuneo, Italy). Microwave-dried larvae of Yellow mealworms were supplied by HaoCheng Mealworm Inc. (Xiangtan, Hunan, China) and ground for 60 s at 6000 rpm in a knife mill (Grindomix GM 200, Retsch, Germany) to pass through 900 μm sieves. Three blends of wheat flour and mealworm powder were formulated in mass ratios of 100:0, 90:10 and 80:20 on a dry matter basis as indicated in Table 1. For each flour blend, a faringograph test was performed according to the standard AACC method 54-21 (Brabender, Duisburg, Germany) to determine dough properties, including the optimal mixing time and water absorption. For experiments, the doughs were mixed in the faringograph to reach the development time and left to rest for 10 min before use.

5.2.2 Experimental design

A Box-Behnken design of three independent variables, level of insect substitution (g/100 g flour blend, dry matter basis), baking time (min) and baking temperature (°C), and three level of variations were used for experiments. Before baking, 3D printed snacks from the three types substituted doughs were analyzed in triplicate for their dimension and microstructure to study their printability. Afterwards, snacks were baked as indicated in Table 5.1. A total number of 15 experiments were performed and the response surface methodology was used to investigate the effect of the three independent variables on the properties of the samples. A desirability profile reported in section 2.10 was employed to optimize the baking conditions and compare the amino acid profile of 3D printed snacks.

Table 5.1. The arrangement of Box-Behnken design

Experiments	Codes			Variables		
	(x_1)	(x_2)	(x_3)	Insect enrichment (%)	Baking time (min)	Baking temperature (°C)
1	-1	-1	0	0	14	200
2	1	-1	0	20	14	200
3	-1	1	0	0	22	200
4	1	1	0	20	22	200
5	-1	0	-1	0	18	180
6	1	0	-1	20	18	180
7	-1	0	1	0	18	220
8	1	0	1	20	18	220
9	0	-1	-1	10	14	180
10	0	1	-1	10	22	180
11	0	-1	1	10	14	220
12	0	1	1	10	22	220
13	0	0	0	10	18	200
14	0	0	0	10	18	200
15	0	0	0	10	18	200

5.2.3 Production of snacks by 3D printing

3D printing process was performed by using a 3D Printer mod. Delta 2040 (Wasp project, Italy) equipped with the Clay extruder kit 2.00 (Wasproject, Italy). The dough, inserted into a stainless-steel chamber, was pushed by a piston at 6 bar through a plastic tube to continuously flow on the head of extruder. For printing, a three-dimensional cylinder (Figure 5.1) was designed by using the software Thinkercad (Autodesc, Inc.), the model was saved in .stl extension and sliced by the software CURA 15.04.2 (Ultimaker B,V., The Netherlands). The other printing conditions were set as follows: print speed (30 mm/s), travel speed (50 mm/s) layer height 0.5 mm and nozzle size 0.84 mm. An infill value of 15% was chosen to obtain the same infill pattern as in Severini et al., (2016). The variable infill only refers to the filling of the inner part of the structure, without considering the external shell. Considering also the shell, the designed objects had a total solid fraction of 36%. Objects were printed on a stainless-steel screen (2 mm mesh) and frozen at -18 °C until being baked in a convection oven (Vitality CE116KT – SAMSUNG, South Korea) at conditions reported in Table 1. Before analyses, snacks were dried at 50 °C until constant weight. For analysis of color, *in vitro* protein digestibility, and analysis of amino acids, snacks were milled (Grindomix GM 200, Retsch, Germany) to pass through 90 μm sieves.

5.2.4 Proximate composition

Flour blends and larvae powder were analyzed for: lipid by method of Bligh & Dyer (1959) and ash by gravimetric method (AOAC, 1923). Protein content was analyzed by Dumas method of combustion (AOAC, 1996) using a Nitrogen/Protein analyzer (model FP-528, Leco St. Joseph, USA). EDTA was used as standard (Elemental Microanalysis Ltd, Okehampton, UK). Due to difference of the sample's protein origin, a nitrogen-protein conversion factor was calculated for each formulation. N-protein conversion factors of 5.71 and 6.25 were used respectively for wheat and insect proteins. For their blends, the N-conversion factors were computed as weight average between single N-factors and protein content.

5.2.5 Moisture loss

Analysis of macrostructure and microstructure

Moisture of baked samples was determined by drying three specimens at 105 °C until constant weight. Moisture loss (ML) was calculated as in Eq.1

$$ML\ (\%) = (moisture_{raw\ snacks} - moisture_{baked\ snacks}/moisture_{raw\ snacks}) \times 100 \qquad Eq.1$$

5.2.6 Analysis of macrostructure and microstructure

Macrostructure and microstructure of snacks were analyzed by X-ray microtomography. Three snacks from each treatment were placed on a sample holder and scanned by a micro-CT scan (SkyScan 1174, Brüker, Kontich, Belgium) with the following settings: voltage 50 kV, current 800 µA, sample rotation 360°, rotation step 0.6°, average frame 3, magnification 28.5 µm, exposure time 1600 ms. 2D analysis of snacks' diameter and height was performed on the entire objects as described in Severini et al. (2016). For 3D analysis, a number of 300 cross sectional greyscale images selected at the middle height of samples were reconstructed with the Skyscan NRecon software (version 1.6.2.0) converted to binary scale by Otsu's method and 3D analyzed with the software CTAn (version 1.12.0.0). The volume of interest was selected by the shrink-wrap function and eroded automatically to adjust to the surface of the sample. Given the nature of the samples, the structure thickness function was applied to measure the filament thickness of raw samples and the pore wall thickness of baked samples. Solid fraction was calculated as the ratio between the volume of solids and the total volume of interest.

5.2.7   Analysis of color

The color of baked snacks was determinate by measuring luminosity (L), red index (a*) and Yellow index (b*) according to the CIELab system definition by a chroma meter Konica Minolta CR-410 (Minolta, Osaka, Japan) calibrated with a white calibration plate CR-A44 (Minolta, Osaka, Japan). Results were reported as browning index (BI) as calculated by Pathare et al., (2013). All the analyses were performed in triplicate.

5.2.8   Analysis of mechanical properties of snacks

Mechanical properties of 3D printed snacks were measured with a texture analyzer (TA-XTplus) equipped with a 50.00 kg load cell and controlled by the software Exponent 6.1.4.0 (Stable Micro Systems, Surrey, UK). Samples were placed horizontally and compressed until 50% of their initial diameter by a circular 75 mm compression plate. Analysis was performed on three different specimens. From the force-displacement curves, the maximum compression force was extracted and considered as the hardness (N).

5.2.9   *In-vitro* protein digestibility

In-vitro protein digestibility was assayed using the pH drop method of Hsu et al. (1977) as modified by Tinus (2012). Samples, milled and sifted as in section 5.2.3, were weighed containing an equivalent of 62.5 g of protein and suspended in 10 mL of milli-Q water at 37 °C for 15 min. Successively, the pH was adjusted to about 8.0 with 0.1 mol/L HCl and/or NaOH. The day of use, 10 mL of multi-enzyme solution consisting of 16 mg of trypsin (T0303, trypsin from porcine pancreas, 13.000-20.000 BAFE units/mg protein, Sigma Aldrich), 13 mg protease (P5147, protease from *Streptomyces griseus* Type XIV, ⩾3.5 units/mg solids, Sigma Aldrich) and 31 mg of chymotrypsin (C4129, α-Chymotrypsin from bovine pancreas Type II, ⩾ 40 units/mg protein) was prepared in milli-Q water, kept at 37 °C and the pH was adjusted to 8.0. Upon rehydration of sample, 1 mL of multi-enzyme solution was added and the pH of the digesta measured after 10 min with continuous stirring. The drop in pH at 10 min of digestion from initial pH of about 8.0 (ΔpH_{10min}) gave the percent *in-vitro* protein digestibility (IVPD) following the Eq. 2

$$IVPD = 65.66 + 18.1 \times \Delta pH_{10min} \hspace{4cm} Eq.2$$

5.2.10   Analysis of amino acids

Analysis of amino acids (AA) was conducted on samples with optimized baking conditions (section 2.11) and ground insect flour according to the Agilent Technologies Protocol (Henderson et al., 2000). For hydrolysis, about 20 mg of milled samples (<90 μm) were weighed in Pyrex microcapillary tubes (Pierce Chemical Company, Rockford, IL) with 6 N HCl, and kept under vacuum for 24 hours at 110°C. After hydrolysis, samples were filtered using Spartan-HPLC 13-mm syringe filters (0.45 μm, 30 mm; Schleicher and Schuell, Dassel, Germany) and diluted with distilled water (1:20 vol/vol). Before injection, AA were derivatized and analyzed by HPLC. The HPLC system (1100 series, Agilent Technologies, Waldbronn, Germany) was equipped with a Zorbax Eclipse AAA column (Palo Alto, CA), a fluorescence detector (model G1321A), and a diode array detector (model G1315A). Standards were used to identify peaks (5061-3330/1/2/3/4 and 5062-2478) (Sigma-Aldrich, St. Louis, MO) and data were integrated using the software Agilent Chemstation ver. B.04.03 (Agilent Technologies, Santa Clara, USA) Analysis was performed on duplicate samples and results were reported as mg of amino acid per g of protein. Furthermore, to analyze protein quality, the amino acid profile was compared to reference pattern protein proposed by WHO/FAO/UNU Expert Consultation, (2007). Protein digestibility corrected amino acid score (PDCAAS) was calculated as in Eq. 3

PDCAAS = [(mg of the limiting AA in 1 g tested protein) / (mg of the same AA in 1g of reference protein)] x *in-vitro* protein digestibility (%) x 100

5.2.11 Statistical analysis

After baking, data from the experimental design were fitted with a polynomial model (Eq. 4) in order to study the effects of independent variables (x_i) on the measured attributes of snack (y).

$$y = B_0 + \sum B_i x_i + \sum B_{ii} x^2_{ii} + \sum B_{ij} x_{ij}$$
Eq. 4

where B_0 represents the initial value of the dependent variables, B_i, B_{ii}, B_{ij} indicate the coefficients, x_i is the linear effect of the independent variables, x^2_{ii} refers to the nonlinear (quadratic) effect of the independent variables and x_{ij} is the interactive effect of two independent variables. The significance of the equation coefficients for each response variable was obtained by multiple regression analysis using the F test with a $p < 0.05$. The goodness of fit was evaluated by coefficient of determination (R^2).

To optimize the baking conditions, a desirability function was applied (Derringer & Suich, 1980). This function simultaneously integrates the regression equations obtained for each quality parameter in a multi-response method (Derossi et al., 2015; Vera et al., 2014; Yu et al., 2013). In the present research, the desirability function was designed to optimize the baking conditions of 3D printed snacks (obtain a single optimal baking time and temperature) and allow a comparison of the amino acid profile of snacks differing only by their mealworm content. The objectives established included the maximization of moisture loss and minimal solid fraction to allow a uniform cooking (Severini et al., 2016), and the minimization of the maximum compression force. For this purpose, data from the design of experiment were fitted with Eq. 4 considering only the baking variables, and leaving the mealworm substitution as a confounding variable. For each dependent variable considered (moisture loss, solid fraction, average compression force), the polynomial equation considering two independent variables still described more than 70% of the data variability, yet providing a good estimation the mathematical coefficients.

Significant difference among properties of raw 3D printed snacks and amino acid content was evaluated by one-way analysis of variance (ANOVA) followed by Fisher LSD post-hoc test at the 0.05 significance level for between-group comparison. All analyses were carried out using the statistical software STATISTICA (version 12, Stat Soft, OK, USA).

5.3 Results and Discussions

5.3.1 Nutritional composition of 3D printed baked snacks

The nutritional composition of larvae powder and flour blends is provided in Table 5.2. The protein content of larvae powder was of 54.2 g/100 g d.b., similar to that reported in literature (FAO, 2013), and much higher than 11.7 g/100 g found in wheat flour. Therefore, enriching wheat flour with larvae powder at 10 and 20% increased the protein content respectively to 15.9 and 20.4 g/100g. Beside protein content, the quality of protein as defined by amino acid profile is discussed in section 5.3.6. Lipid content in blends increased from 1.1 to 3.4 and 5.6 g/100 g (dry basis) respectively at 0, 10 and 20% insect enrichment.

Figure 5.2. Nutritional composition of flour blends and ground larvae of *T. molitor*. Data are expressed as g/100g (dry basis).

Component	Insect enrichment			Larvae of *T. molitor*
	0%	10%	20%	
Protein	11.7[a]	15.9[b]	20.4[c]	54.2
Lipid	1.1[a]	3.4[b]	5.6[c]	28.3
Ash	0.7[a]	1.0[b]	1.3[c]	3.8
Other*	86.5	79.7	72.7	13.7

Means (n = 3) with different subscript within the same row are significantly different ($p < 0.05$)
*Includes fibre, carbohydrates, and vitamins.

5.3.2 Farinograph results

Results of farinograph tests are reported in Table 5.3. Water absorption capacity significantly decreased by increasing grounded insects. This effect could be due to either the presence of hydrophobic compounds such as fatty acids present in grounded mealworms (Pareyt et al., 2011), and to the dilution of starch and gluten, which have a high absorption capacity. Moreover, when dough moisture was expressed on wet basis, no significant differences were observed among different doughs, having an average moisture of 41.1 g H_2O/g f.w.

Figure 5.3. Farinograph characteristics of different flour blends.

| Insect enrichment (%)	Water absorption (%)	Development time (min)	Stability (min)
0	56.3[a]	7.1[a]	10.3[a]
10	53.6[b]	6.4[b]	9.3[b]
20	51.6[c]	6.2[b]	9.3[b]

Means (n = 3) with different subscript within the same column are significantly different ($p < 0.05$)

The substitution of wheat flour with grounded insects significantly reduced the development time from 7.1 to 6.2 min. This value is an indicator of hydration capacity of flour particles, and, yet, as reported by Aghamirzaei et al., (2015) the presence of hydrophobic component could be responsible of this observation. Furthermore, the addition of grounded insects reduced the stability time and weakened the dough. One reason for the weakening of dough resulting from insect addition could stem from the fact that the substitution of gluten proteins by the non-gluten-forming proteins causes a dilution effect and consequently weakens the dough. Secondly, as with soy (Ribotta et al., 2005), insects' protein may have interacted with gluten proteins by both covalent and non-covalent links with consequent deleterious effects on dough stability. Last but not least, fat content of insects may have acted as shortening agent, interfering with the gluten formation and causing a weakening effect (Pareyt et al., 2011).

5.3.3   Dimensional and microstructural properties of 3D printed snacks

Representative cross sectional and frontal X-ray images of 3D printed snacks are shown in Figure 5.1. Overall, objects were successfully printed in all dimensions, following the designed cylindrical structure. In transverse view, a clear distinction between the perimeter (shell) and the inner structure (infill) can be made. Standing outside, the shell gives the circular shape to the objects, while the infill provides support in a square-like pattern to avoid the structural collapse during manufacturing. In frontal view, snacks were parallelepiped-shaped showing a regular deposition between consecutive upper layers. Differences among samples are visible in both directions, and objects appear larger as the level of insects increases.

Figure 5.1. Three-dimensional designed structure, representative cross-sectional and frontal X-ray tomography images of 3D printed snacks.
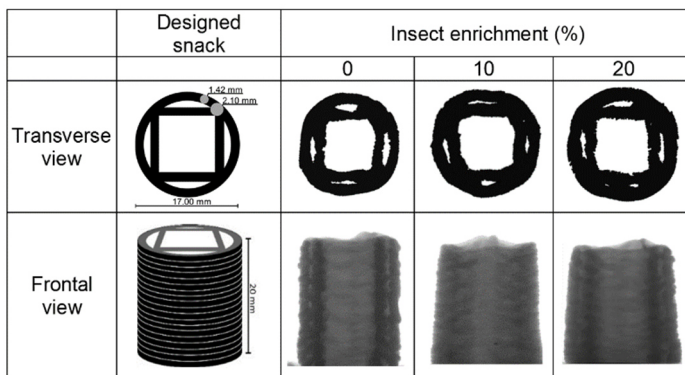
Measured physical characteristics of 3D printed snacks are reported in Table 5.4. Results show that the overall diameter and height of printed objects matched the designed dimensions, but differences occurred with the level of insect enrichment. More specifically, the diameter stayed around the designed 17 mm at 0% and 10% insects, but exceeded of almost 2 mm at 20% enrichment. Similarly, the height of printed snacks decreased to 19.2 mm and 18.9 mm at 10 and 20% insects, differing from the designed 20 mm. Consistently with the changes in dimensions, insect enrichment raised the amount of the deposited material as observed from the sample weight (Table 5.4). For instance, an average weight of 3.8, 4.0 and 4.4 g was measured for snacks printed at 0, 10 and 20% insects. Clearly, the formulation altered the printability of snacks, modifying their dimensional attributes. The filament of material of 3D printed snacks occupied about 68.6% of the object volume, which is much higher than the designed 33% (Table 5.4).

Table 5.4. Physical properties of 3D snacks printed with different formulations.

Insect enrichment (%)	Average weight (g)	Moisture (g H_2O/g fw)	Diameter (mm)	Height (mm)	Solid fraction (%)
designed	-	-	17.0	20.0	36.0
0	3.8[a]	41.1[a]	16.9[a]	19.6[a]	68.1[a]
10	4.0[b]	39.6[a]	17.4[b]	19.2[a,b]	68.9[a]
20	4.4[c]	41.1[a]	18.7[c]	18.9[b]	69.1[a]

Means (n = 3) with different subscript within the same column are significantly different (p<0.05)

Differences between the designed and measured solid fraction was also reported by in Chapter 4, were the mismatch was attributed to differences in flow behavior between wheat dough and synthetic materials such as PLA, ABS, nylon etc., for which software governing printers' movements are designed. A detailed analysis of the printed filament thickness distribution is essential to explain these outcomes. In 3D printing, the nozzle size determines the ideal diameter of the printed filament, and in this case a nozzle size 0.84 mm was used. When printed, however, the filament assumes an ellipsoidal shape with its radiuses mainly defined by the nozzle size and layer height. In our case, given the nozzle size area of 0.554 mm² and a layer height set at 0.5, we estimated the filament to deposit as an ellipses 1.42 mm width and 0.5 mm high. Furthermore, as reported in Figure 5.1, filaments of thickness around 2.00 mm would characterize conjunction zones between the shell and infill.

Figure 5.2 shows the distribution of filament thickness in 3D printed raw objects obtained with different formulations. As expected, all formulations showed a double bell curve characteristics of the designed structure, where the first peak represents the thickness of the single filament, and the second, thicker, corresponds to conjunction zones. In formulations at 0 and 10% insects, the thickness of single filaments ranged between 1.5 and 2.3 mm, staying close to expected, while at 20% enrichment, the single filament was much thicker than predicted, ranging between 1.5 to 2.7 mm. At the same time, the conjunction zones were almost twice as thick as the theoretically predicted, ranging between 3.0 and 4.3 mm. Since printing settings were equal to all formulations, differences in filament thickness can only be due to dough properties. As observed by farinograph analysis, the increase of insects' content reduced the formation of gluten and weakened the dough. Therefore, it is likely that the higher content of fat, especially at 20% insect enrichment, may have determined a higher deposition flow, causing differences in structural attributes. Besides, dimensional biases in conjunction zones could also be attributed to the deceleration of the printer movements occurring in proximity of direction changes.

Figure 5.2. Distribution of filament thickness vs percent volume of 3D printed raw snacks. Legend reports the different level of insect enrichment.
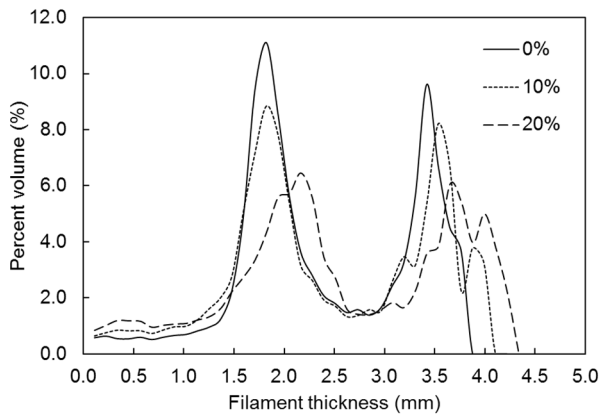
5.3.4 Effect of formulation and baking conditions on the structure of 3D printed snacks

The visual aspect of 3D printed baked snacks obtained with different formulations is reported in Figure 5.3. It can be observed that baking did not alter the structure of snacks, which maintained a hollow cylindrical shape provided with a square-like infill pattern.

Figure 5.3. 3D printed snacks with different formulations baked at 200°C for 22 min.

	Insect enrichment (%)		
	0	10	20
Transverse view			
Frontal view			
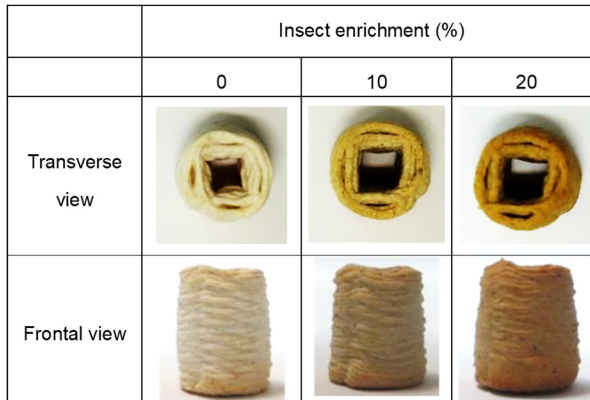
Interestingly, though, dimensional analysis revealed that instead of expanding due to an oven-spring effect, baking decreased snacks diameter. Snacks at 0 and 20% insect enrichment reached about 15 and 18 mm diameter respectively (Figure 5.4) (Severini et al., 2016)(C Severini et al., 2016). In Chapter 4, the reduction of diameter was linked to the removal of water during baking. In this experiment, the polynomial model of Eq. 4 also described the loss of moisture occurring during baking, showing a correlation coefficient of 0.98 (Table 5.5). In addition, it can be observed that samples shrunk differently depending on formulation (Figure 5.4). For instance, at a baking temperature of 180 °C (18 min), the reduction of diameter was of 13.5% for snacks formulated with wheat flour, and only of 4.8% for snacks formulated at 20% insects. This suggests that the radial tension causing the reduction of diameter is lower with the addition of insects, and it is probably related to the lower gluten development and low stability as measured by the farinograph test. Regardless the dimension of raw objects, snack diameter increased with baking temperature. The better evaporation of water at higher temperature as fit by Eq. 1 may explain this trend.

Figure 5.4. Three-dimensional plot describing the effects of insect enrichment and baking temperature on diameter of 3D printed snacks.
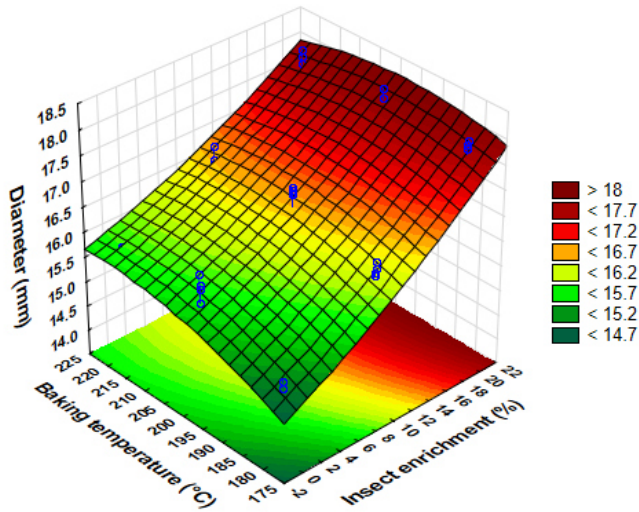

Table 5.5. Parameters estimate and correlation coefficient of polynomial equation of response variables as a function of insect enrichment (x1), baking time (x2) and baking temperature (x3).

Equation parameters estimates	Response variables						
	Microstructure				Quality		
	Diameter (mm)	Height (mm)	Moisture loss (%)	Solid fraction (%)	Browning index	Hardness (N)	Protein digestibility (%)
Intercept	16.546	19.559	77.523	47.917	48.286	39.332	82.136
x_1	2.225	0.219	**	-1.540	42.057	11.184	-3.364
x_1^2	**	**	6.393	**	**	-4.122	**
x_2	**	0.200	27.841	-4.334	16.429	9.862	**
x_2^2	**	**	4.621	**	**	-5.781	**
x_3	0.378	0.401	14.541	-5.216	12.214	**	-1.207
x_3^2	0.188	**	4.072	-1.263	**	-11.278	0.872
x_1*x_2	-0.438	**	**	-1.918	9.991	-8.239	**
x_1*x_3	-0.331	**	**	**	**	-4.023	**
x_2*x_3	**	**	-4.752	**	6.904	16.206	**
Global fit							
R^2	0.923	0.804	0.983	0.863	0.923	0.924	0.745

** Values holding stars did not significantly describe the response variable (p>0.05)

Furthermore, by looking at the internal geometry of snacks shown in Figure 5.7c, it can be observed that at higher baking temperature the infill filament is enlarged towards the internal empty space. This suggests that upon baking, a cavity of water vapor may form in the space between the infill and the shell, pushing both filaments in either directions. On the contrary to what observed for diameter, the height of snacks increased with baking (Figure 5.5). By fitting the height of baked samples, the polynomial model of Eq. 4 revealed that linear variables were all significant in describing this trend. Moreover, compared to raw snacks, the rise in height was only evident for those enriched with insects. For instance, where the raise was maximized (220°C and 22 min), at 0% insect enrichment the height increased of only 0.2 mm, while snacks at 20% insects reached a height of 20.1 mm, compared to 18.9 mm of the respective raw object. An explanation to this outcome can be found viewing at how snacks are originally obtained. The FDM technology deposits layers of material consecutively one upon the other to obtain the final printed object. Upon baking, water vapor escapes in all directions, including those in-between layers. Consequently, this may tend to lift consecutive filaments and cause a rise of the overall object height. Reasons why this effect could not be observed in snacks at 0% insect enrichment are still unknown, but it not far-fetched to link this behavior to the stronger-developed gluten.

Figure 5.5. Three-dimensional plot describing the effects of insect enrichment and baking temperature on height of 3D printed snacks.
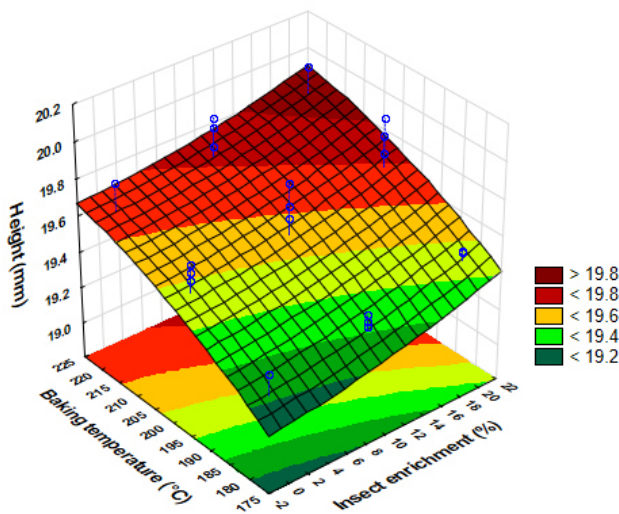
Figure 5.6 shows the solid fraction of baked snacks as a function of baking time and temperature. Overall, after baking, the solid fraction of snacks was significantly lower than raw objects, ranging between 44 and 55%. These variations are the resultant of changes of snack dimensions and the removal of water, which evaporating leaves room for newly formed pores with walls that constitute the new structure.

Figure 5.6. Three-dimensional plot describing the effects of baking time and temperature on solid fraction of 3D printed baked snacks.
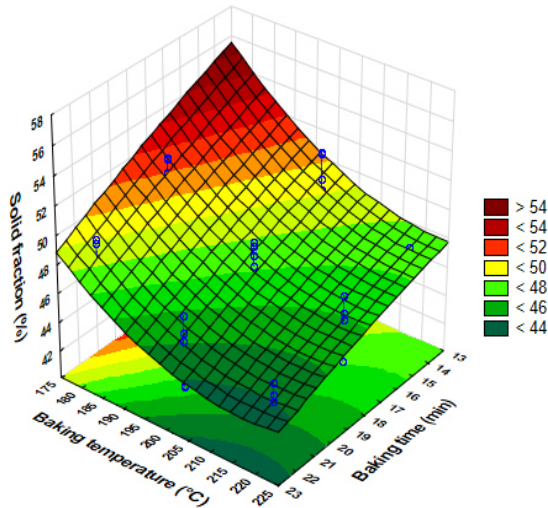

Figure 5.7 shows a more detailed analysis of the solid fraction comparing snacks at different at variable levels. All snacks were characterized by the five main designed pores and several small pores inside the printed filaments generated during baking. The structure thickness showed a double bell curve, which could be associated to specific zones. Low values of thickness seem to reflect the internal structure of the snack, where the filament is highly porous. This structure seems to change slightly with variables. For instance, snacks with 20% insect enrichment showed a thinner structure compared to that at 0% insects, probably due to a better water evaporation. Similarly, a higher baking time contributed to the formation of a thinner structure. A second area of thickness characterized the structure of all snacks in the range between 600 and 1000 μm. This zone seems to reflect the outer part of the shell (Van Dyck et al., 2014) and it is similar to the crust-like structure characteristics of bread. Furthermore, the presence of this external and compact zone may be one of the causes of the limited expansion of snacks.

Figure 5.7. Cross sectional X-ray images and structure thickness distribution of 3D printed baked snacks compared between two levels of variable. Numbers in each image and legend in the graph correspond to experiments as reported in Table 1.
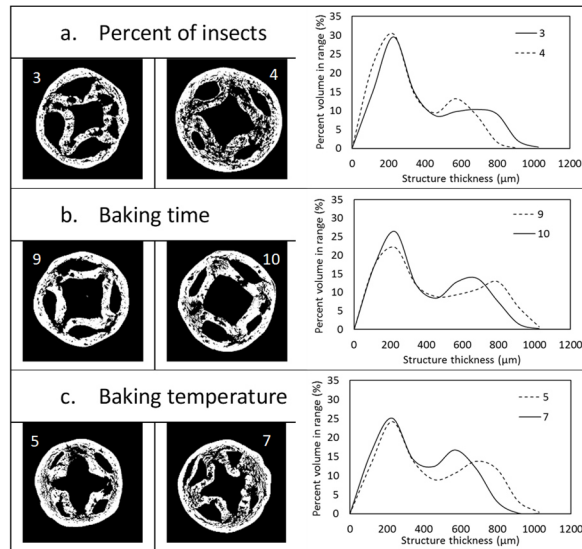
5.3.5 Effect of formulation and baking conditions on quality of 3D printed snacks

As reported in Table 5.5, polynomial model of Eq. 4 precisely described experimental changes of browning index (BI), showing a correlation coefficient of 0.923. More specifically, all experimental variables determined significant linear changes in the response variable. Figure 5.8 shows the three-dimensional plot describing the effects of baking time and insect enrichment on browning index. The level of insect enrichment was directly related to the browning index, displaying the greatest effect. Snacks baked at 22 min showed a BI of about 20 compared to a BI of about 60 for those obtained at 20% insect enrichment. This outcome was expected, as compared to wheat flour, insects have a more brown color which may easily darken light foods(Azzollini et al., 2016) (Chapter 1). The effect of insects on snack color can be visually observed in Figure 5.3. Similarly, baking time and temperature showed a positive relationship with BI of samples, exhibiting an estimated effect of 16.429 and 12.214. This behavior could be explained considering the effect of non-enzymatic browning reactions such as Maillard reactions and sugar caramelization. While Maillard reactions are associated with degradation and polymerization reactions between reducing sugars and amino acids, sugar caramelization occurs due to carbohydrate degradation reactions.

In bakery products, both reactions take place when the dough is subjected to high temperature in a continuous time (Purlis, 2010). Furthermore, the polynomial equation revealed a strong interaction between insect enrichment and baking time. Such effect, observed with the greater slope at 20% insect enrichment (Figure 5.8), clearly indicates a synergic effect of baking time and insect enrichment on Maillard reactions, due to the increase in protein content.

Figure 5.8. Three-dimensional plot describing the effects of baking time and level of insect enrichment on browning index of 3D printed baked snacks.
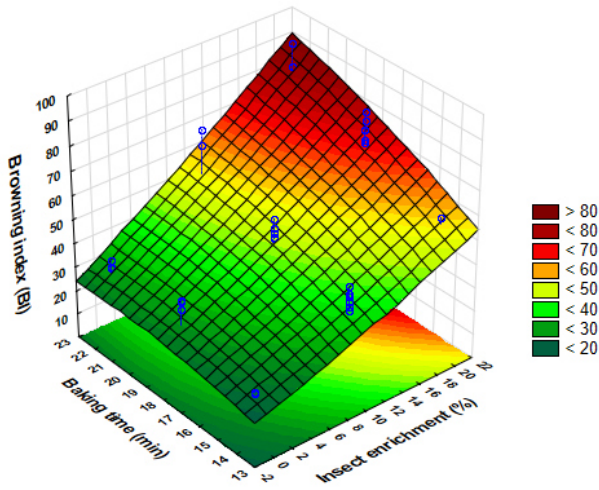
In this experiment, hardness corresponded to the maximum force recorded during the compression of snacks in the axial direction. The polynomial equation well fitted the trend of hardness, describing 92% of experimental variability (Table 5.5). As shown in Figure 5.9, hardness increased with the level of insect enrichment.

Figure 5.9. Three-dimensional plot describing the effects of baking temperature and level of insect enrichment on hardness of 3D printed baked snacks.
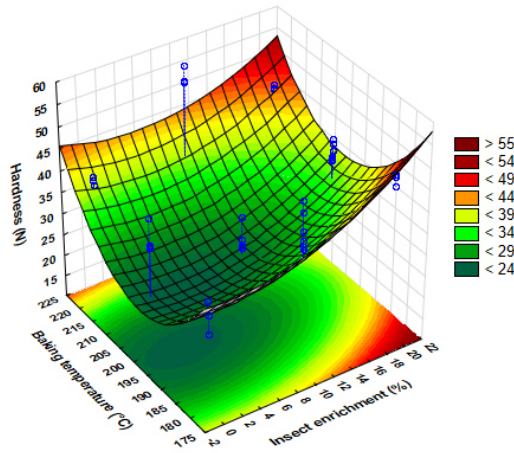
For instance, at 220 °C, snacks at 0% level of insect enrichment had a hardness of about 35 N, compared to about 52 N for those at 20% insect enrichment. Given the complexity of the structure, not clear conclusions can be drawn. In general, since printing, snacks with higher level of insects showed a higher weight, diameter, and structure thickness. Therefore, it is likely that these properties have contributed to the hardness of samples. Furthermore, baking temperature showed a strong quadratic effect on hardness. Probably, the higher hardness at low temperature is the result of a limited expansion occurring at low temperature that preserved the snack solidity. Yet, the higher hardness measured at high baking temperature may be due to a harder external crust. No linear correlation was found between the hardness of snacks and their mean wall thickness, probably because the mean of wall thickness does not well describe the microstructure of snacks. Furthermore, hardness may also depend on starch pasting properties and protein coagulation. However, this is a subject which goes beyond the scope of this study and therefore would require targeted investigations.

Protein digestibility decreased as insect increased and baking temperature decreased (Figure 5.10). The effect of time on protein digestibility was negligible as appears in Table 5.5. In this case, the descriptive abilities of the polynomial equation (Eq. 4) were moderate, represented by a r^2 of 0.745. The lower protein digestibility for formulation containing insects confirmed the expectations.
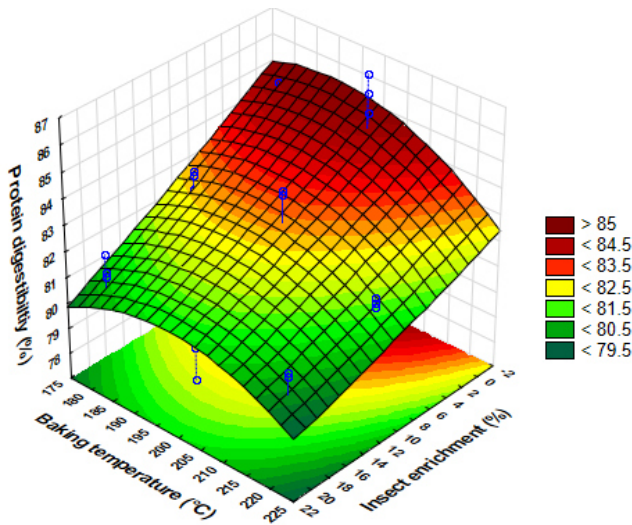
Figure 5.10. Three-dimensional plot describing the effects of baking temperature and level of insect enrichment on protein digestibility of 3D printed baked snacks.

In fact, as Finke (2007) found out, in insects, a significant amount of amino acids (from 9.3 to 32.7%) are either highly sclerotized or bound to chitin, and may therefore be difficult to digest. Since insect proteins accounted for about 32% and 54% of total proteins respectively at 10 and 20% enrichment, a low protein digestibility was expected. For confirmation, grounded Yellow mealworm larvae (microwave dried) were analyzed for their protein digestibility, and the analysis revealed that 78.8% of mealworm proteins were digestible. Despite being apparently low, our values were higher than those of Marono et al., (2015) and Yi et al., (2016), who identified a level of protein digestibility of native Yellow mealworm proteins of 66 and 54%, respectively. Differences are likely due to drying process of insects used this research and performed by the provider, which may have denatured proteins and increased their digestibility.

5.3.6 Optimization of baking conditions and comparison of amino acid profile of 3D printed snacks.

Desirability function was used to optimize baking conditions and compare the amino acid profile of 3D printed baked snacks only differing by their mealworm content. Figure 5.11 reports the desirability profile of samples as a function of each independent variable (baking time and temperature) at the optimum conditions. The function enabled to obtain a maximum desirability of 0.693 when snacks were baked for 22 min at 200 °C. Under these conditions, snacks had a hardness of 38.3 N, a solid fraction of 44.9 and a moisture loss of 92.8%.

Figure 5.11. Supplementary material. Profile of desirability of 3D printed snacks as function of baking time and temperature.
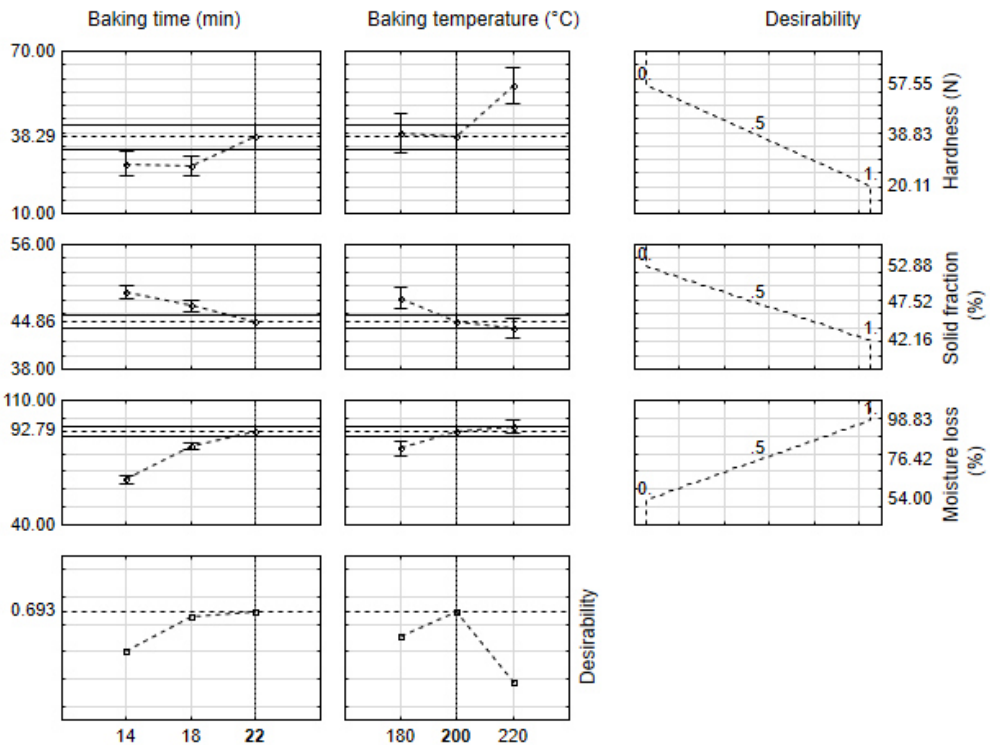
The amino acid profile of snacks obtained with different formulation and Yellow mealworm larvae is shown in Table 5.6. Total sum of essential amino acid content increased with level of insect enrichment from 32.5% to 38.2% and 41.3% respectively at 0, 10 and 20% insects, while dry larvae contained about 49% of essential amino acids.

Table 5.6. Amino acid profile of different snacks obtained with different formulation and baked for 22 min at 200 °C and recommendation for adult. Values are reported as mg of amino acid in 1 g of protein. Values in brackets correspond to mg amino acid in 1 g of snack or larvae.

	Level of insect enrichment				Reference protein* adult
Amino acids	0%	10%	20%	Larvae of *T. molitor*	
Essential					
Ile	54.15[a] (6.1)	51.89[a] (7.9)	54.15[a] (10.7)	48.87 (24.7)	30
His	45.09[a] (5.1)	60.30[b] (9.1)	62.44[c] (12.4)	76.47 (38.7)	15
Leu	86.36[a] (9.7)	85.57[a] (12.3)	85.33[a] (16.9)	81.79 (41.4)	59
Lys	22.22[a] (2.5)	34.15[b] (5.2)	47.63[c] (9.4)	67.66 (34.2)	45
Met + Cys	11.57[a] (1.3)	14.18[b] (2.2)	17.85[c] (3.5)	20.60 (10.4)	22
Phe + Tyr	42.27[a] (4.7)	44.59[a] (6.8)	47.69[a] (9.4)	64.13 (32.5)	38
Thr	15.29[a] (1.7)	35.67[b] (5.4)	39.39[b] (7.8)	58.10 (29.4)	23
Trp	8.03[a] (0.9)	8.78[a] (1.3)	10.84[b] (2.1)	12.35 (6.3)	6
Val	40.08[a] (4.5)	47.24[b] (7.2)	51.28[c] (10.1)	59.16 (29.9)	39
Non-essential					
Ala	2.45[a] (0.3)	3.32[a] (0.5)	9.11[b] (1.8)	26.27 (13.3)	
Arg	57.95[a] (6.5)	103.78[b] (15.7)	119.38[b] (23.6)	158.07 (80.0)	
Asp	41.50[a] (4.6)	60.33[b] (9.1)	70.36[c] (13.9)	92.13 (46.6)	
Gly	24.51[a] (2.7)	30.90[b] (4.7)	32.27[b] (6.4)	30.77 (15.6)	
Glu	477.01[a] (53.4)	352.59[b] (53.4)	288.00[c] (57.0)	144.49 (73.1)	
Gln	6.68[a] (0.7)	6.55[a] (1.0)	8.25[b] (1.6)	10.76 (5.4)	
Pro	14.81[a] (1.7)	12.50[a] (1.9)	12.56[a] (2.5)	5.05 (2.6)	
Ser	50.22[a] (5.6)	47.43[b] (7.2)	46.89[b] (9.3)	43.42 (22.0)	
EA	325.06	382.37	413.30	489.12	
NEA	675.13	617.40	586.84	510.96	
% EA/tot AA	32.5	38.2	41.3	48.9	
Limiting amino acid	Lys	Met+Cys	Met+Cys	Met+Cys	
PDCAAS (%)	41.6	53.1	65.2	73.7	

Different letters among columns indicate significant difference ($p<0.05$)
*(WHO/FAO/UNU Expert Consultation, 2007)

Compared to the WHO/FAO/UNU Expert Consultation (2007) amino acid requirement for adults, snacks obtained with only wheat flour had the lowest level of lysine, resulting the most limiting amino acid, followed by methionine + cysteine and tyrosine. The high lysine content of Yellow mealworm larvae (67.7 mg/g protein) can help offset this deficiency. In fact, lysine increased from 22.2 to 34.2 and 47.6 mg/g protein at 0, 10 and 20% insect enrichment respectively, reaching the required amino acid content of reference protein. Similarly, Aguilar-Miranda, et al. (2002) increased the content of lysine from 29 to 44 mg/g protein by substituting maize flour with about 7% (w/w) of Yellow mealworm powder in tortilla preparation. In our experiments, threonine also increased from 15.3 to 35.7 and 39.4 mg/g protein respectively at 0, 10 and 20% insect enrichment, reaching the amino acid content of reference protein set at 23 mg/g protein. At the same time, though, despite increasing by 54% (11.6 to 17.9 mg/g protein respectively at 0 and 20% insect enrichment), the content of sulphur amino acids (methionine + cysteine) was yet lower than required amino acid of reference protein (22 mg/g protein). Of course, this is due to the lower content of methionine + cysteine in larvae of Yellow mealworms compared to the recommended level for humans. The content of methionine + cysteine of Yellow mealworm powder in our study was similar to that of 21.3 mg/g protein found by Zhao et al., (2016), which confirmed the limitation.

True protein digestibility of snacks was 84.2, 82.2 and 80.3% respectively at 0, 10 an 20% insect enrichment, and 78.7% for ground larvae of Yellow mealworm. Therefore, the protein digestibility corrected amino acid score (PDCAAS) for 3D printed snacks with 20% insects was of 65.2%, much higher than 41.6% at 0% insects, confirming respectively sulphur amino acids and lysine as limiting amino acids.

5.4   Conclusions

3D printing technology was applied to create snacks with a designed geometry and made of different formulations of wheat flour containing edible insects as novel source of proteins. Enriching wheat flour with different levels of ground larvae of Yellow mealworms modified the printability of snacks, changing their dimensions but still maintaining the main structural features. Together with formulation, baking conditions modified attributes of 3D printed snacks, modifying their microstructure, inducing non-enzymatic browning reactions, altering mechanical properties and protein digestibility. Snacks with tailored quality attributes were obtained by optimizing baking conditions through a desirability function and compared for their nutritional quality. A significant improvement of the amino acid profile of wheat flour was observed when snacks were enriched with different levels of ground insects, validating the rational promotion of insects based on nutritional arguments. Therefore, our results indicate that together with wheat flour, ground Yellow mealworm could be suitable ingredients to manufacture 3D printed foods with specific designs and improved nutritional quality without adverse impact on technological quality. Further studies on the sensory properties and attitudes towards the consumption of 3D printed snack containing edible insects would be warranty to confirm the demonstrated efficacy of Yellow mealworms as a novel ingredient in 3D food printing.

Chapter 6

—— General discussion ——

6.1   Introduction

Protein intake is fundamental to human health. Animal proteins are considered as high quality proteins as they provide sufficient amount of essential amino acids. However, the way they are currently produced is placing a heavy strain on global resources. In the face of changing food consumption patterns, a rising global population and increasingly scarce resources, a shift towards more sustainable source of animal proteins is needed. Insects hold a high potential for food protein security. However, despite being nourishment for over 2 billion people, insect consumption is a new concept in many parts of the world, especially in industrialized countries. An emerging body of research is evidencing that the disgust towards insects as food, which is typical of Western populations, can be overcome when they are offered in an unrecognizable form into familiar food carriers. To date, very little information is available about nutritional improvements and technological attitudes of insects' powder in food preparation. Supplementation of maize flour tortillas with 6.7% of Yellow mealworm (*Tenebrio molitor*) powder was reported to significantly improve the amino acid profile, with a 2% increase in total protein (Aguilar-Miranda et al., 2002). In addition, 5% enrichment of wheat buns with edible termites powder showed a significant increase in protein, retinol, riboflavin, iron and zinc contents without affecting the product thickness and sensorial attributes (Kinyury et al., 2009). By replacing 10% of lean pork in emulsion sausages with whole and defatted ground Yellow mealworms, Kim et al., (2016) noticed an increase in protein content from 22.6% to 26 and 31% respectively and good technological performance.

At the start of this research project, little information was available on processing edible insects into grounded powder, suitable for mass market. Therefore, the effect of processing conditions (blanching and drying) on the quality of larvae of Yellow mealworms was selected as the first topic to be investigated in this thesis (Chapter 2).

Afterwards, the increasing trend of snack consumption combined with consumers' demand of healthy foods, empowered for investigation of the effective use of an insect powder into extruded foods, which are typically made of raw materials high in starch. Fillers, which is the word for supplementary ingredients added in extrusion-cooking, are usually included to improve nutritional and sensory quality of snacks, but are known to impair their technological properties, such as expansion and texture. For this reason, the technological aspects addressing the inclusion of Yellow mealworm powder in extrusion cooking was selected as the second topic to be investigated in this thesis (Chapter 3).

Additive manufacturing, also known as 3D printing, is considered a disruptive technology projected to revolutionize manufacturing. Applications in the food sector would allow to realize goods with complex geometries and tailored sensory and nutritional properties out of edible materials. This view inspired the third topic of this thesis. Here, it was studied the application of 3D printing in: i) implementing some variables governing the technology and, ii) understanding links between internal designed geometries and mechanical properties of new manufactured foods (Chapter 4).

Successively, the 3D printing was adopted to develop a computer controlled cereal snack with a specific design and enriched with grounded larvae of Yellow mealworms (Chapter 5). In this study, the effects of formulation and processing conditions on microstructure, nutritional profile and quality attributes of snacks were investigated. Table 6.1 provides an overview of outline of this thesis. The progress made towards the accomplishment of the proposed aims will be discussed in this chapter.

Table 6.1. Overview of subjects studied in this thesis.

Subject	Principal investigation	Target variables
- From live insects to dry powder	- Blanching - Drying treatments	- Nutritional composition - Drying kinetics - Sorption isotherms - Colour development
- Extrusion-cooking with edible insects	- Formulation - Processing	- Extrusion performance - Nutritional composition - Mechanical properties - Microstructure - Digestibility
- 3D printing for food constructs	- Design - Processing	- Printing performance - Microstructure - Baking performance - Mechanical properties
- 3D printing of doughs with edible insects	- Formulation - Processing - Optimisation	- Printing performance - Nutritional composition - Microstructure - Baking performance - Mechanical properties - Colour development - Digestibility

6.2   Main findings

In Chapter 2, the blanching of larvae allowed to obtain a semi-finished product stable in colour and suitable for drying. During blanching, larvae exoskeleton played a containment effect of nutrients, avoiding their leakage in the blanching liquid. The Page model well described the drying kinetic of larvae at each temperature considered. Larvae of Yellow mealworms presented a type II sorption isotherm, typical of hygroscopic foods high protein food, and the blanching treatment reduced larvae hygroscopicity. These findings suggest that the Page model can be used to predict drying behaviour of larvae with a high accuracy and allow to obtain a stable product at 5% moisture (d.b.), as given by the monolayer moisture content.

In Chapter 3, the substitution of wheat flour with 20% dry and ground larvae impaired the physical properties of extruded snacks, and this was related to the high content of lipids in larvae. However, at 10% level of substitution, the adoption of high barrel temperature and screw speed improved their microstructure, in terms of expansion, porosity and pore characteristics. At this percentage, protein content increased by 35%, and provided more than 16% energy of the formulation, enough to claim the snack as "source of protein" according to European food law. In addition, shear forces in extrusion cooking increased the digestibility of Yellow mealworm protein, which was expected to be low due to the schlerotisation in larval exoskeleton. A strong relationship between the physical features of pores and the nutrients digestibility (starch and protein) was identified, and high shear forces in extrusion cooking improved the digestibility of larvae protein. Furthermore, the observed mechanical properties were shown to depend on the microstructure of snacks, so the dimension of pores and their wall thickness described the magnitude of compression forces. These results confirm the pivotal role of microstructure in governing the nutritional and mechanical proprieties of food. Findings indicate that the microstructural features of extruded snacks can be modulated in such a way that texture is optimized and nutrient digestibility is maximized.

In Chapter 4, 3D printing has proven to be a successful technology in obtaining computer controlled cereal snacks with specific designed geometries. Cylindrical objects of 25 mm height, 20 mm diameter and 10, 15 and 20% porosity were obtained. Fused deposition modelling showed high accuracy in reproducing external aspects and internal morphological features of printed snacks. However, numerically-quantified two-dimensionality of microstructure revealed that values of porosity did not match the set

values. In this regard, the printing variable layer height was proven as critical in correct material deposition, leading to under-extrusion and over-extrusion respectively at low and high set values. Different internal patterns of snacks led to distinctive quantitative evaporation of water during baking, most likely due to diverse convective and conductive mechanisms of heat, respectively through voids and solid material. For the first time, the mechanical properties of 3D printed snacks were correlated with their internal structure, supporting the use of this technology for producing foods with tailored mechanical properties.

In Chapter 5, the use of 3D printing technology was shown to be a feasible strategy to design and realize cereal snacks formulated with edible insects. Objects were successfully printed in all dimensions, following the designed cylindrical shape with a distinct inner structure. In line with Chapter 3, the presence of lipids was considered the main limiting agent against an extensive substitution of wheat flour with ground larvae of Yellow mealworms. The interference of lipids with gluten formation and, the dilution of the latter with non-gluten proteins, caused a weakening effect on the dough mixing stability. Consequently, this resulted in a higher net rate of material deposition, leading to differences in structural quality of final objects. Nutritionally speaking, the substitution of wheat flour with larvae of Yellow mealworms resulted in a substantial improvement of the protein content and amino acid profile of snacks. However, respect to findings of Chapter 3, a no increase in protein digestibility was observed for Yellow mealworm protein, probably due to the absence of shear forces occurring in extrusion-cooking. These results validate the rational promotion of edible insects based on nutritional arguments and indicate their suitability to be considered valuable food ingredients in 3D printing technology, without substantial impact on technological quality.

6.3   Methodological considerations and implications for future research

6.3.1   From live larvae to a dry ingredient

A blanching treatment followed by hot-air drying was shown to be an effective process to obtain dry larvae of Yellow mealworms suitable for food industries. The main reason for drying larvae lays on the easier storage, cheaper transportation and easy handling of dry products compared to their fresh counterpart. As alternative drying method, lyophilisation preserved the colour of fresh larva the most, but yet, if no blanching was applied, degradative browning reactions were observed when larvae were kept at high moisture. As for crustaceans, the formation of brown pigments is a common problem that occurs due

to biochemical oxidation of phenols by polyphenol oxidases (PPO) and further polymerization into dark pigments called melanin. Despite having no harm for consumers, browning of insects would decrease their quality, shelf life, and subsequently, their commercial value. Therefore, methods for prevention of browning reactions need to be adopted to avoid, for instance, recovery of enzymatic discolouration reactions or even proteolytic activities when dry larvae are added to high moisture foods. In this instance, a blanching was chosen as treatment to prevent browning reactions. Alongside inactivation of browning enzymes, blanching has proven to be an effective method to reduce microbial load of Yellow mealworm larvae and extend their shelf life (Klunder et al., 2012; Vandeweyer et al., 2017). This, of course, would be a matter of concern if seeking to exploit the techno-functional properties of Yellow mealworm proteins. In fact, it is likely that properties like emulsion capacity, gel forming capacity, foaming potential etc., may be impaired by heat treatments. In that case, in order to preserve techno-functional properties while processing insects into a dry product, different processing solutions need to be investigated. For instance, hot air drying (<50°C) can still be a valuable solution if applied to larvae blended to a paste and in presence of anti-browning agents, such as sodium disulfite or ascorbic acid (Yi et al., 2016). This would increase the heat exposed surface and accelerate the drying process, while preventing browning reactions and maintaining the energy input lower than lyophilisation. Importance should also be given to oxidative reactions caused by drying treatment and occurring throughout the product shelf life. Besides, the fractionation of insects into their constituents like protein, lipids and chitin may be a feasible strategy to pursue the adoption of insects as food and at the same time use their constituents at full potential, i.e. protein may be used for their functional properties, lipids as fat replacers and chitin as fibre. On the other hand, this arises questions on environmental sustainability of solvent-based fractionation but bodes well when considering aqueous or dry fractionation technologies. One of the reasons for avoiding extractions in this thesis is based on the prompt use of outcomes. In fact, since the consumption of larvae of Yellow mealworms is already allowed in few European countries, including the Netherlands, Belgium and United Kingdom, results of this thesis could immediately be exploited by food industries to tackle the introduction of insects in the market. From a nutritional point of view, Yellow mealworm have shown to have a high content of proteins and be a good source of important amino acids, confirming their potential in being valid alternative of current meat products, or ingredients in complex formulations.

6.3.2 Yellow mealworms as ingredient in extrusion cooking

The dry powder of Yellow mealworm was successfully incorporated in extruded snacks. Ready-to-eat expanded snacks are very popular among Western consumers principally due to their convenience, attractive appearance and unique texture attributes. In fact, the consumption of expanded products have increased dramatically in recent years and their global market is projected to reach 31 billion dollars by 2019 (marketsandmarkets, 2014). Besides, this type of food is highly valued by consumers for being seasoned with different flavours, from cheese to chilli, crustaceans, tomato, lemon, onion, herbs and other spices. For this reason, outcomes of this research place the adoption of extrusion-cooking process as a valid strategy for inclusion of a powder of Yellow mealworm in puffed snacks. If seeking for the highest protein fortification of snacks with Yellow mealworms, in this thesis, the presence of lipids is surely a limitation. In fact, the substitution of wheat flour with 20% Yellow mealworm powder caused an increase in lipid content of 500%, from 0.9 to 5.4% on dry basis, and resulted in a strong reduction of expansion, which impaired textural properties. In future research, either the use of protein extract or emulsifying agent would be advisable. From a nutritional point of view, the lipid concentration of 5.4% should still be considered much lower than those found in many extruded commercial products, in which lipid content may reach 35% of total weight due to addition of seasonings after extrusion (Ilo et al., 2000). In this study, snacks obtained with a substitution with 10% Yellow mealworm powder showed an increase in protein content of 35%, from 11.8 to 15.9%. Moreover, the nutritional improvement would be much higher if Yellow mealworms were incorporated in low protein snacks, such as rice, potato or tapioca. Yet, additional value to this improvement should be given considering protein composition. In fact, although no detailed information are available, it is reasonable to believe that similarly to 3D printed snacks, the presence of insects in may also have improved their amino acid profile. Improvements were not only observed in protein content, but also in their digestibility. In fact, a significant amount of insects amino acids (from 9.3 to 32.7%) are either highly sclerotized or bound to chitin, and are therefore difficult to digest (Finke, 2007). After extrusion, values of protein digestibility were significantly higher than those found in literature, suggesting that shear forces during processing may have mechanically enhanced their digestibility. Furthermore, the role of microstructure of puffed snacks in governing both their mechanical and nutritional properties was confirmed, paving the way for designing of innovative food microstructures with tailored texture and digestibility characteristics.

6.3.3   3D printing and the potential of insects as food

3D printing has proven to be a powerful technology in the food sector. In this thesis, snacks of wheat dough and Yellow mealworms were successfully printed with the aid of a "fused deposition modelling" printer and cylinders with a specific design were realized. The printing variable, layer height, and the inclusion of Yellow mealworms altered the deposition of material. In all cases, the porosity of printed snacks was significantly lower than the designed value due to over-extrusion. However, this should not be considered as a limitation for the technology, but rather an added value. In fact, thanks to its flexibility, numerous printing parameters like printing speed, travel speed, nozzle size, retraction etc. can be adapted case by case to print foods with different consistencies and rheological properties. Furthermore, this thesis aimed at evaluating the influence of one printing variable and the dough formulation taken singularly, rather than finding the best printing conditions that would optimise the accuracy of the final objects. Given the high degree of freedom of the technology, future studies in 3D printing of edible insects could also be performed by deposition of viscous aqueous suspensions of insect proteins. In this case, heat-induced gelifying properties of Yellow mealworm proteins recently reported by Zhao et al., (2016) could be exploited to build 3D foods out of 100% insects, without the need of supporting material, like wheat dough in this thesis. Finally, three arguments can be elaborated that would help exploring the full potential of the technology. At first, a comprehensive study linking the rheological properties of food with their deposition behaviour is needed. Furthermore, the development of 3D printers for food applications must also seek for optimization of software interfaces, which are currently available only for synthetic materials such as PLA, ABS, nylon, PET etc. Last but not least, in order for studies to be comparable, a standardisation of hardware settings is needed.

6.4 Recommendations

In the future, insects will likely occupy a significant position in the global protein nutrition picture. However, where insects are now a substantial source of nutrients, ecological implications on vegetation, fauna and the ecosystem itself are increasing concerns. Anthropogenic factors like overexploitation of resources and uncontrolled harvesting from the wild have imposed further threats to food security. Therefore, creating multifaceted solutions to address this issue, and developing a solid supply chain is paramount to ensure access and availability of insects, not only in low income countries. To fully realize the potential insects hold in terms of food protein security, a range of multidisciplinary actors should all be part of a cooperative global model, and create a sustainable and reliable insect supply chain with a consistent quality by addressing the following points:

- development of shared guidelines and hygienic standards for industrial rearing of high quality insects for food consumption;

- optimization of harvesting practices to reduce losses and inefficiencies;

- understanding and co-design key processing technologies for development of new products;

- comparison of environmental impact of insect rearing with alternative sources proteins (soy, algae, rapeseeds, etc.);

- advancement of consumer awareness towards the concept of insect as food and feed by means of local/national actions;

- assessment of risks factors associated to long-term exposure and ingestion of insects;

- development of a clear and comprehensive legal framework at the international level that would lead towards the full deployment of insects from the household scale to the industrial scale from production to consumption.

References

Abbasi, T., Abbasi, T., & Abbasi, S. A. (2015). Reducing the global environmental impact of livestock production: the minilivestock option. *Journal of Cleaner Production*. 112(2) 1754-1766.

Agbisit, R., Alavi, S., Cheng, E., Herald, T., & Trater, A. (2007). Relationship between microstructure and Mechanical Properties of Cellular Cornstarch Extrudates. *Journal of Texture Studies*, *38*, 199–219.

Aghamirzaei, M., Peighambardoust, S. H., Azadmard-Damirchi, S., & Majzoobi, M. (2015). Effects of grape seed powder as a functional ingredient on flour physicochemical characteristics and dough rheological properties. *Journal of Agricultural Science and Technology*, *17*(2), 365–373.

Aguilar-Miranda, E. D., Lopez, M. G., Escamilla-Santana, C., & Barba de la Rosa, a. P. (2002). Characteristics of maize flour tortilla supplemented with ground Tenebrio molitor larvae. *Journal of Agricultural and Food Chemistry*, *50*(1), 192–195.

Altan, A., McCarthy, K. L., & Maskan, M. (2008). Evaluation of snack foods from barley-tomato pomace blends by extrusion processing. *Journal of Food Engineering*, *84*(2), 231–242.

Altan, A., McCarthy, K. L., & Maskan, M. (2009). Effect of extrusion cooking on functional properties and in vitro starch digestibility of barley-based extrudates from fruit and vegetable by-products. *Journal of Food Science*, *74*(2).

Anakware, P., Feninf, K., Osekre, E., & Obeng-Ofori, D. (2015). Insects as food and feed : A review. *International Journal of Agricultural Research and Review*, *3*(1), 143–151.

AOAC. (1920). Fat (crude) or ether extract in animal feed; method 920.39. *Official Methods for Analysis of the Association of Official Analyricsl Chemists*.

AOAC. (1923). Ash of flour; method 923.03. *Official Methods for Analysis of the Association of Official Analyricsl Chemists*.

AOAC. (1995). Official methods of analysis. *Association of Official Analytical Chemists*.

AOAC. (1996). Nitrogen (total) in fertilizers; method 993.13. *Official Methods for Analysis of the Association of Official Analyricsl Chemists*.

AOAC. (1999). Loss on drying (Moisture) for feeds; method 930.15. *Official Methods for Analysis of the Association of Official Analyricsl Chemists*.

AACC (2000). Approved methods of the AACC. Method 10-10B (10th ed.,). *Analysis of the Association of Official Analyricsl Chemists*.

AOAC. (2005). Starch (total) in cereal products; method 996.11. *Official Methods for Analysis of the Association of Official Analyricsl Chemists*.

Aregawi W., Verbonen, P, Vancauwenberghe, V., Bongaers, E., van den Eijnden, E., van Bommel, K., Diaz, J., & Nicolai, B. (2015a). Structural-mechanical analysis of cookies produced by conventional and 3D printing techniques. In *Proceedings of the 29th EFFoSt International Conference. Vol 1* (pp 415-419).

Aregawi, W., Verbonen, P., Vancauwenberghe, V., Bongaers, E., van den Eijden, E., van Bommel, K., Nicolai, B. (2015). Structure design of 3D printed cookies in relation to texture. In *Proceedings of the 29th EFFoSt International Conference. Vol 1* (pp. 420–425).

ASTM. Standard Terminology for Additive Manufacturing Technologies (2015). ASTM International, West Conshohocken, PA, 2012.

Azzollini, D., Derossi, A., & Severini, C. (2016). Understanding the drying kinetic and hygroscopic behaviour of larvae of yellow mealworm (Tenebrio molitor) and the effects on their quality. *Journal of Insects as Food and Feed*, *2*(4), 233–243.

Berman, B. (2012). 3-D Printing: The new industrial revolution. *Business Horizons*, 55, 155-162.

Bhattacharya, S. (1997). Twin-screw extrusion of rice-green gram blend: Extrusion and extrudate characteristics. *Journal of Food Engineering*, *32*(1), 83–99.

Bligh, E., & Dyer, W. (1959). A rapid method of total lipid extraction and purification. *Canadian Journal of Biochemistry and Physiology*, *37*(8), 911–917.

Box, G.E.P., Hunter, W.G., & Hunter, J.S. (1978). Statistics for experimenters. Wiley, New York.

Bose, S., Vahabzadeh, S., & Bandyopadhyay, A. (2013). Bone tissue engineering using 3D printing. *Materials Today*, 16, 496-504.

Brennan, M. A., Derbyshire, E., Tiwari, B. K., & Brennan, C. S. (2013). Ready-to-eat snack products: The role of extrusion technology in developing consumer acceptable and nutritious snacks. *International Journal of Food Science and Technology*, *48*(5), 893–902.

Bußler, S., Rumpold, B. A., Fröhling, A., Jander, E., Rawel, H. M., & Schlüter, O. K. (2016). Cold atmospheric pressure plasma processing of insect flour from Tenebrio molitor: Impact on microbial load and quality attributes in comparison to dry heat treatment. *Innovative Food Science & Emerging Technologies*, *In press*.

Caivano, J. L., & del Pilar Buera, M. (2012). *Color in Food.* (J. L. Caivano & M. del Pilar Buera, Eds.). Boca Raton, Florida: CRC Press.

Campbell, Thomas Williams, Christopher Ivanova, Olga Garrett, B. (2012). *Could 3D Printing Change the World? Technologies, Potential, and Implications of Additive Manufacturing.* Strategic foresight initiative. Report

Caparros Megido, R., Gierts, C., Blecker, C., Brostaux, Y., Haubruge, E., Alabi, T., & Francis, F. (2016). Consumer acceptance of insect-based alternative meat products in Western countries. *Appetite*, *52*, 237–243.

Caparros Megido, R., Sablon, L., Geuens, M., Brostaux, Y., Alabi, T., Blecker, C., Francis, F. (2014). Edible Insects Acceptance by Belgian Consumers: Promising Attitude for Entomophagy Development. *Journal of Sensory Studies*, *29*(1), 14–20.

Causer, C. (2009). They've got a golden ticket. *Potentials*, IEEE, 28, 42-44.

Chanvrier, H., Appelqvist, A., Bird, A. R., Gilbert, E., Htoon, A., Li, Z., Topping, D. (2007). Processing of novel elevated amylose wheats: functional properties of starch digestibility of extruded products. *Journal of Agricultural and Food Chemistry*, *55*, 10248–10257.

Chanvrier, H., Desbois, F., Perotti, F., Salzmann, C., Chassagne, S., Gumy, J.-C., & Blank, I. (2013). Starch-based extruded cereals enriched in fibers: A behavior of composite solid foams. *Carbohydrate Polymers*, *98*(1), 842–853.

Chanvrier, H., Jakubczyk, E., Gondek, E., & Gumy, J. C. (2013). Insights into the texture of extruded cereals: Structure and acoustic properties. *Innovative Food Science & Emerging Technologies*, *24*(April), 9–12.

Chanvrier, H., Valle, G. Della, & Lourdin, D. (2006). Mechanical behaviour of corn flour and starch–zein based materials in the glassy state: A matrix–particle interpretation. *Carbohydrate Polymers*, *65*(3), 346–356.

Cranck. (1975). *The mathematics of diffusion.* London: Oxford University Press.

Day, L., & Swanson, B. G. (2013). Functionality of protein-fortified extrudates. *Comprehensive Reviews in Food Science and Food Safety*, *12*(5), 546–564.

De Boer, J., Schösler, H., & Boersema, J. J. (2013). Motivational differences in food orientation and the choice of snacks made from lentils, locusts, seaweed or "hybrid" meat. *Food Quality and Preference*, *28*(1), 32–35.

De Pilli, T., Carbone, B. F., Derossi, A., Fiore, A. G., & Severini, C. (2008). Effects of operating conditions on oil loss and structure of almond snacks. *International Journal of Food Science & Technology*, *43*(3), 430–439.

DeFoliart, G. R. (1999). Insects as food: why the western attitude is important. *Annual Review of Entomology*, *44*(80), 21–50.

Derossi, A, Severini, C., Mastro A, De Pilli, T. (2015). Study and optimization of osmotic dehydration of cherry tomatoes in complex solution by response surface methodology and desirability approach. *LWT - Food Science and Technology*, *60*(2), 641–648.

Deroy, O., Reade, B., & Spence, C. (2015). The insectivore's dilemma, and how to take the West out of it. *Food Quality and PreferenceFood Quality and Preference*, *44*, 44–55.

Derringer, G., & Suich, R. (1980). Simultaneous Optimization of Several Response Variables. *Journal of Quality Technology*, *12*(4), 214–219.

Diaz, J., van Bommel, K., Noort, M., & Vallons, K. (2015). Successfully developing food products using 3D printing technologies: Challenges, opportunities and future outlook. In *Proceedings of the 29th EFFoSt International*, 10-12 November, Athens, vol. 1, pp 428-431.

Dossey, A. T., Morales-Ramos, J. A., & Rojas, M. G. (2016). *Insects as sustainable food ingredients: production, processing and food applications.* (A. T. Dossey, J. A. Morales-Ramos, & M. G. Rojas, Eds.). Elsevier Inc.

Erbay, Z., & Icier, F. (2010). A review of thin layer drying of foods: theory, modeling, and experimental results. *Critical Reviews in Food Science and Nutrition*, *50*(5), 441–464.

Erdogdu, F., Balaban, M. O., Otwell, W. S., & Garrido, L. (2004). Cook-related yield loss for pacific white (Penaeus vannamei) shrimp previously treated with phosphates: effects of shrimp size and internal temperature distribution. *Journal of Food Engineering*, *64*(3), 297–300.

FAO. (2006). *Livestock's long shadow - environmental issues and options. Food and Agriculture Organization of the United Nations* (Vol. 3).

FAO. (2009). *How to Feed the World in 2050. Food and Agriculture Organization of the United Nations, Rome. Insights from an expert meeting at FAO.*

FAO. (2012). World agriculture towards 2030 / 2050. The 2012 Revision. *Food and Agriculture Organization of the United Nations. ESA Working Paper*, *12*(3), 1–154.

FAO. (2013). *Edible insects. Future prospects for food and feed security. Food and Agriculture Organization of the United Nations* (Vol. 171).

Finke, M. D. (2007). Estimate of chitin in raw whole insects. *Zoo Biology*, *26*, 105–115.

Foley, J. A., Ramankutty, N., Brauman, K. A., Cassidy, E. S., Gerber, J. S., Johnston, M., … Zaks, D. P. M. (2011). Solutions for a cultivated planet. *Nature*, *478*(7369), 337–42.

Food and Nutrition Board. (2002). *Dietary Reference Intakes for Energy, Carbohydrate, Fiber, Fat, Fatty Acids, Cholesterol, Protein, and Amino Acids.* Washington D.C.: The National Academies Press.

Fp7. (2016). PERFORMANCE. Retrieved December 1, 2016, from http://www.performance-fp7.eu/

Gausemeier, J., Echterhoff, N., & Wall, M. (2011). Thinking ahead the Future of Additive Manufacturing- Analysis of Promisin Industries. *Gausemeier, Jürgen Echterhoff, Niklas Kokoschaka, Martin Wall, Marina*, 103. Retrieved from https://dmrc.uni-paderborn.de/fileadmin/dmrc/06_Downloads/01_Studies/DMRC_Study_Part_1.pdf

Gburek, U., Vorndran, E., Muller, F.A., & Barralet, J.E. (2007). Low temperature direct 3D printed bioceramics and biocomposites as drug release matrices. *Journal of Controlled Release*, 122, 173-180.

Ghaly, A., & Alkoaik, F. (2009). The yellow mealworm as a novel source of protein. *American Journal of Agricultural and Biological Sciences*, *4*(4), 319–331.

Gibson, L. J., & Ashby, M. F. (1997). *Cellular solids: Structure and Properties* (2nd editio). Cambridge University Press.

Godoi, F. C., Prakash, S., & Bhandari, B. R. (2016). 3d printing technologies applied for food design: Status and prospects. *Journal of Food Engineering*, *179*, 44–54.

Gonçalves, A. A., & de Oliveira, A. R. M. (2016). Melanosis in crustaceans: A review. *LWT - Food Science and Technology*, *65*, 791–799.

Goyanes, A., Buanz, A.B.M., Basit, A.W., & Gaisford, S. (2014). Fused-filament 3D printing (3DP) for fabrication of tablets. *International Journal of Pharmaceutics*, 476, 88-92.

Gracia-Julia, A., Hurtado-Pnol, S., Leung, A., & Capellas, M. (2015). Extrusion behavior of food materials in a 3D Food Printer. Pectin based bio-ink formulations for 3-D printing of porous foods. *In Proceedings of the 29th EFFoSt International, 10-12 November*, Athens, vol 2, pp 1740-1741.

Gray, N. (2010). Looking to the future: Creating novel foods using 3D printing. Retrieved November 30, 2016, from http://www.foodnavigator.com/Science/Looking-to-the-future-Creating-novel-foods-using-3D-printing

Guha, M., Ali, S. Z., & Bhattacharya, S. (1998). Effect of barrel temperature and screw speed on rapid viscoanalyser pasting behaviour of rice extrudate. *International Journal of Food Science & Technology*, *33*, 259–266.

Gustavo, G. V, Fontana, A. J., Schmidt, S. J., & Labuza, T. P. (2008). *Water Activity in Foods: Fundamentals and Applications*. (G. V Gustavo, A. J. Fontana, S. J. Schmidt, & T. P. Labuza, Eds.). Ames, Iowa, USA: Blackwell Publishing Ltd.

Guy, R. (2001). *Extrusion cooking. Technologies and applications*. Cambridge: Woodhead Pubblishing Limited.

Harris, M. (1985). *Good to eat. Riddles of food and culture*. New York: Simon and Schuster.

Hartmann, C., & Siegrist, M. (2016). Becoming an insectivore: Results of an experiment. *Food Quality and Preference*, *51*, 118–122.

Hao, L., Mellor, S., Seaman, O., Henderson, J., Sewell, N., & Sloan, M. (2010). Material characterization and process development for chocolate additive layer manufacturing. *Vitrtual and Physical Prototyping*, 5, 57-64.

Henderson, J., Ricker, R., Bidlingmeyer, B. a., & Woodward, C. (2000). Rapid, accurate, sensitive, and reproducible HPLC analysis of amino acids.

Hosseinpour, S., Rafiee, S., Mohtasebi, S. S., & Aghbashlo, M. (2013). Application of computer vision technique for on-line monitoring of shrimp color changes during drying. *Journal of Food Engineering*, *115*(1), 99–114.

Hsu, H. W., Vavak, D. L., Satterlee, L. D., & Miller, G. A. (1977). A multienzyme technique for estimating protein digestibility. *Journal of Food Science*, *42*(5), 1269–1273.

Huang, W., Zheng, Q., Sun, W., Xu, H., & Yang, X. (2007). Levofloxacin implants with predefined microstructure fabricated by three-dimensional printing technique. *International Journal of Pharmaceutics*, 339,33-38.

Ilo, S., Schoenlechner, R., & Berghofe, E. (2000). Role of lipids in the extrusion cooking processes. *Grasas Y Aceites*, *51*(1–2), 97–110.

Incropera, F. P., & DeWitt, D. B. (1996). *Fondamentals of heat and mass transfer* (4th editio). New York, NY: John Wiley & Sons.

Italian Food Regulation. Decreto del Presidente della Repubblica 9 Febbraio 2001, n. 187. https://www.politicheagricole.it/flex/files/2/f/6/D.34ca305e98ded6c87bfc/DPR _187_2001.pdf (December 2015).

Jain, D., & Pathare, P. B. (2007). Study the drying kinetics of open sun drying of fish. *Journal of Food Engineering*, *78*(4), 1315–1319.

Jalabert-Malbos, M. L., Mishellany-Dutour, A., Woda, A., & Peyron, M. A. (2007). Particle size distribution in the food bolus after mastication of natural foods. *Food Quality and Preference*, *18*(5), 803–812.

Jongema, Y. (2012). World list of edible insects, (April), 1–70. Retrieved from http://www.wageningenur.nl/en/Expertise-Services/Chair-groups/Plant-Sciences/Laboratory-of-Entomology/Edible-insects/Worldwide-species-list.htm

Joshi, S. M. R., Bera, M. B., & Panesar, P. S. (2014). Extrusion cooking of maize/spirulina mixture: factors affecting expanded product characteristics and sensory quality. *Journal of Food Processing and Preservation*, *38*(2), 655–664.

Karkle, E. L., Keller, L., Dogan, H., & Alavi, S. (2012). Matrix transformation in fiber-added extruded products: Impact of different hydration regimens on texture, microstructure and digestibility. *Journal of Food Engineering*, *108*(1), 171–182.

Kim, H.-W., Setyabrata, D., Lee, Y. J., Jones, O. G., & Kim, Y. H. B. (2016). Pre-treated mealworm larvae and silkworm pupae as a novel protein ingredient in emulsion sausages. *Innovative Food Science & Emerging Technologies*, *38*, 116–123.

Kinyuru, J. (2009). Process development, nutrition and sensory qualities of wheat buns enriched with edible termites (Macrotermes subhylanus) from lake victoria region, Kenya. *African Journal of Food Agriculture Nutrition and Development*, *21*(8), 2–3.

Kinyury, J., Kenih, G., & Njoroge, M. (2009). Process development, nutrition and sensory qualities of wheat buns enriched with edible termites (Macrotermes subhylanus) from Lake Victoria Region, Kenya. *African Journal of Food Agriculture Nutrition and Development*, *9*(8), 1739–1750.

Klunder, H. C., Wolkers-Rooijackers, J., Korpela, J. M., & Nout, M. J. R. (2012). Microbiological aspects of processing and storage of edible insects. *Food Control*, *26*(2), 628–631.

Lazou, A. E., Michailidis, P. A., Thymi, S., Krokida, M. K., & Bisharat, G. I. (2007). Structural properties of corn-legume based extrudates as a function of processing conditions and raw material characteristics. *International Journal of Food Properties*, *10*(4), 721–738.

Le Goff, G., & Delarue, J. (2015). Non-verbal evaluation of acceptance of insect-based products using a simple and holistic analysis of facial expressions. *Food Quality and Preference*, *In press*, 1–9. http://doi.org/10.1016/j.foodqual.2016.01.008

Li, L., Zhao, Z., & Liu, H. (2013). Feasibility of feeding yellow mealworm (Tenebrio molitor L.) in bioregenerative life support systems as a source of animal protein for humans. *Acta Astronautica*, *92*(1), 103–109.

Li, S., Zhang, H. Q., Tony Jin, Z., & Hsieh, F. (2005). Textural modification of soya bean/corn extrudates as affected by moisture content, screw speed and soya bean concentration. *International Journal of Food Science & Technology*, *40*(7), 731–741.

Lin, S., Hsieh, F., & Huff, H. . (1998). Effects of Lipids and Processing Conditions on Degree of Starch Gelatinization of Extruded Dry Pet Food. *Animal Feed Science and Technology*, *71*(3–4), 283–294.

Lipton, J., Arnold, D., Nigh, F., Lopez, N., Cohen, D., Norén, N., & Lipson, H. (2010). Multi-Material Food Printing With Complex Internal Structure Suitable for Conventional Post-Processing. In *21st Solid Freeform Fabrication Symposium (SFF'10)* (pp. 809–815).

Lipton, J. I., Cutler, M., Nigl, F., Cohen, D., & Lipson, H. (2015). Additive Manufacturing for the Food Industry - A review. *Trends in Food Science & Technology*, *43*(1), 114–123.

Looy, H., Dunkel, F. V., & Wood, J. R. (2014). How then shall we eat? Insect-eating attitudes and sustainable foodways. *Agriculture and Human Values*, *31*(1), 131–141.

Klomp, D., Hoppenbrouwers, M., de Kruif, B., van den Eijnden, E., Berkhout, M., Jolanda, H., & van Bommel, K. (2015). Process control in 3D food printing. *In Proceedings of the 29th EFFoSt International*, 10-12 November, Athens, vol 1, pp 427.

marketsandmarkets. (2014). Extruded Snacks Market by Type (Potato, Corn, Rice, Tapioca, Mixed Grain, and Others) & by Geography. *Global Trends and Forecasts to 2019*, *FB 2542*, 1–212.

Marono, S., Piccolo, G., Loponte, R., Di Meo, C., Attia, Y. a., Nizza, A., & Bovera, F. (2015). In vitro crude protein digestibility of Tenebrio molitor and Hermetia illucens insect meals and its correlation with chemical composition traits. *Italian Journal of Animal Science*, *14*(3889).

Martins, M. G., Martins, D. E. G., & Pena, R. D. S. (2015). Drying kinetics and hygroscopic behavior of pirarucu (Arapaima gigas) fillet with different salt contents. *LWT - Food Science and Technology*, *62*(1), 144–151.

McGrew, W. C. (2014). The "other faunivory" revisited: Insectivory in human and non-human primates and the evolution of human diet. *Journal of Human Evolution*, *71*, 4–11.

Miglietta, P. P., De Leo, F., Ruberti, M., & Massari, S. (2015). Mealworms for food: A water footprint perspective. *Water*, *7*(11), 6190–6203.

Minekus, M., Alminger, M., Alvito, P., Ballance, S., Bohn, T., Bourlieu, C., … Brodkorb, A. (2014). A standardised static in vitro digestion method suitable for food – an international consensus. *Food Funct. Food Funct*, *5*(5), 1113–1124.

Mironov, V., Trusk, T., Kasyanov, V, Little, S, Swaja, R., & Markwald, R.R. (2009). Biofabrication: a 21st century manufacturing paradigm. *Biofabrication*, 1.

Moraru, C. I., & Kokini, J. L. (2003). Nucleation and Expansion During Extrusion and Microwave Heating of Cereal Foods. *Comprehensive Reviews in Food Science and Food Safety*, *2*(4), 147–165.

Moscicki, L. (2011). *Extrusion-Cooking Techniques. Applications, Theory and Sustainability.* (L. Moscicki, Ed.). Weinheim, Germany: Wiley-VCH Verlag & Co. KGaA.

Murphy, S.V., & Atala, A. (2014). 3D bioprinting of tissues and organs. *Nature biotechnology*, 32, (8), 773-785.

Netherlands Organisation for Applied Scientific Research (2015). 3D Food Printing. https://www.tno.nl/media/2217/3d_food_printing. dowloaded 30/09/2015.

Niamnuy, C., Devahastin, S., & Soponronnarit, S. (2008). Changes in protein compositions and their effects on physical changes of shrimp during boiling in salt solution. *Food Chemistry*, *108*(1), 165–175.

Nielsen, P. m., Petersen, D., & Dambmann, C. (2001). Improved method for Determining Food Protein Degree of Hydrolysis. *Journal of Food Science*, *66*(5), 642–646.

Nowak, V., Persijin, D., Rittenschober, D., & Charrondiere, U. R. (2014). Review of food composition data on edible insects. *Food Chemistry*, *193*, 39–46.

Onwulata, C. I., Konstance, R. P., Smith, P. W., & Holsinger, V. H. (2001). Co-extrusion of Dietary Fiber and Milk Proteins in Expanded Corn Products. *LWT - Food Science and Technology*, *34*, 424–429.

Onwulata, C. I., Smith, P. W., Konstance, R. P., & Holsinger, V. H. (2001). Incorporation of whey products in extruded corn , potato or rice. *Food Research International*, *34*, 679–687.

Oonincx, D. G. A. B., & de Boer, I. J. M. (2012). Environmental Impact of the Production of Mealworms as a Protein Source for Humans – A Life Cycle Assessment. *PLoS ONE*, *7*(12), 1–5.

Oonincx, D. G. a B., van Itterbeeck, J., Heetkamp, M. J. W., van den Brand, H., van Loon, J. J. a, & van Huis, A. (2010). An exploration on greenhouse gas and ammonia production by insect species suitable for animal or human consumption. *PLoS ONE*, *5*(12), 1–7.

Ortiz, J., Lemus-Mondaca, R., Vega-Gálvez, A., Ah-Hen, K., Puente-Diaz, L., Zura-Bravo, L., & Aubourg, S. (2013). Influence of air-drying temperature on drying kinetics, colour, firmness and biochemical characteristics of Atlantic salmon (Salmo salar L.) fillets. *Food Chemistry*, *139*(1–4), 162–169.

Pallottino, F., Hakola, L., Costa, C., Antonucci, F., Figorilli, S., Seisto, A., & Menesatti, P. (2016). Printing on Food or Food Printing: a Review. *Food and Bioprocess Technology*, *9*, 725–733.

Pareyt, B., Finnie, S. M., Putseys, J. A., & Delcour, J. A. (2011). Lipids in bread making: Sources, interactions, and impact on bread quality. *Journal of Cereal Science*, *54*(3), 266–279.

Pathare, P. B., Opara, U. L., & Al-Said, F. A. J. (2013). Colour Measurement and Analysis in Fresh and Processed Foods: A Review. *Food and Bioprocess Technology*, *6*(1), 36–60.

Payne, C. L. R., Dobermann, D., Forkes, A., House, J., Josephs, J., McBride, A., Soares, S. (2016). Insects as food and feed: European perspectives on recent research and future priorities. *Journal of Insects as Food and Feed*, *2*(4), 269–276.

Payne, C. L. R., Scarborough, P., Rayner, M., & Nonaka, K. (2016). A systematic review of nutrient composition data available for twelve commercially available edible insects, and comparison with reference values. *Trends in Food Science & Technology*. (47) 69-77.

Pelletier, N., & Tyedmers, P. (2010). Forecasting potential global environmental costs of livestock production 2000-2050. *Proceedings of the National Academy of Sciences*, *107*(43), 18371–18374.

Pinkerton, A. J. (2016). Lasers in additive manufacturing. *Optics and Laser Technology*, *78*, 25–32.

Purlis, E. (2010). Browning development in bakery products – A review. *Journal of Food Engineering*, *99*(3), 239–249.

Ramos-Elorduy, J., Gonzales, A. E., Hernandez, A. V., & Pino, J. M. (2002). Ramos-Elorduy, González_Use of Tenebrio molitor (Coleoptera Tenebrionidae) to recycle organic wastes and as feed for broiler chickens_20.pdf. *Veterinary Entomology*, *95*(1), 214–220.

Ramos-Elorduy, J., & González, E. (2002). Use of Tenebrio molitor (Coleoptera: Tenebrionidae) to recycle organic wastes and as feed for broiler chickens. *Journal of Economic Entomology*, *95*(1), 214–220.

Ramos-Elorduy, J., Pino-M, J. M., & Cuevas-Correa, S. (1998). Insectos comestibles del estado de México y determinación de su valor nutritivo. *Anales Del Instituto de Biología Universidad Autónoma de México, Serie Zoología.* Retrieved from http://www.ejournal.unam.mx/zoo/069-01/ZOO69106.pdf

Ramos Diaz, J. M., Suuronen, J.-P., Deegan, K. C., Serimaa, R., Tuorila, H., & Jouppila, K. (2015). Physical and sensory characteristics of corn-based extruded snacks containing amaranth, quinoa and kañiwa flour. *LWT - Food Science and Technology*, *64*(2), 1047–1056.

Raubenheimer, D., & Rothman, J. M. (2011). Nutritional Ecology of Entomophagy in Humans and Other Primates. *Annual Review of Entomology*, *58*(1).

Raubenheimer, D., Rothman, J. M., Pontzer, H., & Simpson, S. J. (2014). Macronutrient contributions of insects to the diets of hunter–gatherers: A geometric analysis. *Journal of Human Evolution*, *71*, 70–76.

Ribotta, P. D., León, A. E., Pérez, G. T., & Añón, M. C. (2005). Electrophoresis studies for determining wheat-soy protein interactions in dough and bread. *European Food Research and Technology*, *221*(1–2), 48–53.

Robin, F., Dubois, C., Pineau, N., Labat, E., Théoduloz, C., & Curti, D. (2012). Process, structure and texture of extruded whole wheat. *Journal of Cereal Science*, *56*(2), 358–366.

Robin, F., Dubois, C., Pineau, N., Schuchmann, H. P., & Palzer, S. (2011). Expansion mechanism of extruded foams supplemented with wheat bran. *Journal of Food Engineering*, *107*(1), 80–89.

Rumpold, B. A., Fröhling, A., Reineke, K., Knorr, D., Boguslawski, S., Ehlbeck, J., & Schlüter, O. (2014). Comparison of volumetric and surface decontamination techniques for innovative processing of mealworm larvae (Tenebrio molitor). *Innovative Food Science & Emerging Technologies*, *26*, 232–214.

Rumpold, B. a., & Schlüter, O. K. (2013). Potential and challenges of insects as an innovative source for food and feed production. *Innovative Food Science & Emerging Technologies*, *17*, 1–11.

Rumpold, B. A., & Schlüter, O. K. (2013). Nutritional composition and safety aspects of edible insects. *Molecular Nutrition and Food Research*, *57*(5), 802–823.

Rumpold, B., & Schlüter, O. (2013). Nutritional composition and safety aspects of edible insects. *Molecular Nutrition & Food Research*, *57*(5), 802–823.

Sachs, E., Cima, M., Williams, P., Brancazio, D., & Cornie, J. (1992). Three dimensional printing: rapid tooling and prototypes directly from a CAD model. *Journal of Manufacturing Science and Engineering*, 114(4), 481–488.

Salwin, H. (1963). Moisture levels required for stability in dehydrated foods. *Food Technology*, *17*, 1114–1121.

Schösler, H., de Boer, J., & Boersema, J. J. (2012). Can we cut out the meat of the dish? Constructing consumer-oriented pathways towards meat substitution. *Appetite*, *58*(1), 39–47.

Severini, C., & Derossi, A. (2016). Could the 3D Printing Technology be a Useful Strategy to Obtain Customized Nutrition? *Journal of Clinical Gastroenterology*, *50*(December), S175–S178.

Severini, C., Derossi, A., & Azzollini, D. (2016). Variables affecting the printability of foods: Preliminary tests on cereal-based products. *Innovative Food Science & Emerging Technologies*, *38*, 281–291.

Sharma, G. ., & Prasad, S. (2004). Effective moisture diffusivity of garlic cloves undergoing microwave-convective drying. *Journal of Food Engineering*, *65*(4), 609–617.

Shelomi, M. (2015). Why we still don't eat insects: Assessing entomophagy promotion through a diffusion of innovations framework. *Trends in Food Science & Technology*, *45*(2), 311–318.

Siemianowska, E., Kosewska, A., Aljewicz, M., Skibniewska, K. a., Polak-Juszczak, L., Jarocki, A., & Jędras, M. (2013). Larvae of mealworm (Tenebrio molitor L.) as European novel food. *Agricultural Sciences*, *4*(6), 287–291.

Singh, R. R. B., Rao, K. H., Anjaneyulu, A. S. R., & Patil, G. R. (2001). Moisture sorption properties of smoked chicken sausages from spent hen meat. *Food Research International*, *34*(2–3), 143–148.

Singh, S., Gamlath, S., & Wakeling, L. (2007). Nutritional aspects of food extrusion: a review. *International Journal of Food Science & Technology*, *42*(8), 916–929.

Smil, V. (2002). Worldwide transformation of diets, burdens of meat production and opportunities for novel food proteins. *Enzyme and Microbial Technology*, *30*(3), 305–311.

Soares, S., & Forkes, A. (2014). Insects au gratin - an investigation into the experiences of developing a 3d printer that uses insect protein based flour as a building medium for the production of sustainable food. *International Conference of Engineering and Product Design Education*, (4 & 5 September).

Sobral, J., Caridade, S.G., Sousa, R.A., Amno, J.F., & Reis, R. (2011). Three-dimensional plotted scaffolds with controlled pore size gradients: Effect of scaffold geometry on mechanical performance and cell seeding efficiency. *Acta Biomaterialia*, 7, 1009-1018.

Southerland, D., Walters, P., & Huson, D. (2011). Edible 3D Printing. In *Digital Fabrication 2011 Conference, NIP 27, 27th International Conference on Digital Printing Technologies* (pp. 819–822). Retrieved from http://www.imaging.org/ist/publications/reporter/articles/REP26_5_6_NIP27D F11_SOUTHERLAND_PG819.pdf

Souza, T. De, Souza, H. De, & Pena, R. (2013). A rapid method to obtaining moisture sorption isotherms of a starchy product. *Starch-Stärke*, (65), 433–436.

Spiess, W., & Wolf, W. (1983). *The results of the COST 90 project on water activity*. (Jowitt et al., Ed.). London: Applied Science Publisher.

Srikiatden, J., & Roberts, J. S. (2007). Moisture Transfer in Solid Food Materials: A Review of Mechanisms, Models, and Measurements. *International Journal of Food Properties*, *10*(4), 739–777.

Stuknytė, M., Cattaneo, S., Pagani, M. A., Marti, A., Micard, V., Hogenboom, J., & De Noni, I. (2014). Spaghetti from durum wheat: effect of drying conditions on heat damage, ultrastructure and in vitro digestibility. *Food Chemistry*, *149*, 40–6.

Sumargo, F., Gulati, P., Weier, S. A., Clarke, J., & Rose, D. J. (2016). Effects of processing moisture on the physical properties and in vitro digestibility of starch and protein in extruded brown rice and pinto bean composite flours. *Food Chemistry*, *211*, 726–733.

Sun, J., Zhou, W., Huang, D., Fuh, J. Y. H., & Hong, G. S. (2015). An Overview of 3D Printing Technologies for Food Fabrication. *Food and Bioprocess Technology*, *8*(8), 1605–1615.

Tan, H. S. G., Fischer, A. R. H., Tinchan, P., Stieger, M., Steenbekkers, L. P. a., & van Trijp, H. C. M. (2015). Insects as food: Exploring cultural exposure and individual experience as determinants of acceptance. *Food Quality and Preference*, *42*, 78–89.

Tan, H. S. G., van den Berg, E., & Stieger, M. (2016a). The influence of product preparation, familiarity and individual traits on the consumer acceptance of insects as food. *Food Quality and Preference*, *52*, 222–231.

Tan, H. S. G., van den Berg, E., & Stieger, M. (2016b). The influence of product preparation, familiarity and individual traits on the consumer acceptance of insects as food. *Food Quality and Preference.*

Tessmar, J., Bradl, F., & Gopferich, A. (2009). Hydrogels for tissue engineering. In U. Meyer, T. Meyer, J. Handschel, & H. Wiesmann (Eds.). *Fundamentals of tissue engineering and regenerative medicine*, pp 495-517. Berlin, F.R.G: Springer.

The-CandyFab-Project (2008). CandyFab. Retrieved from http://wiki.candyfab.org/. 29Sept2015

Tinus, T., Damour, M., Van Riel, V., & Sopade, P. a. (2012). Particle size-starch-protein digestibility relationships in cowpea (Vigna unguiculata). *Journal of Food Engineering*, *113*(2), 254–264.

Trujillo, F. J., Yeow, P. C., & Pham, Q. T. (2003). Moisture sorption isotherm of fresh lean beef and external beef fat. *Journal of Food Engineering*, *60*(4), 357–366.

Tzompa-Sosa, D. A., Yi, L., van Valenberg, H. J. F., van Boekel, M. A. J. S., & Lakemond, C. M. M. (2014). Insect lipid profile: aqueous versus organic solvent-based extraction methods. *Food Research International*, *62*, 1087–1094.

Urs, K. C. D., & Hopkins, T. L. (1973). Effect of moisture on growth rate and development of two strains of Tenebrio molitor L. (Coleoptera, Tenebrionidae). *Journal of Stored Products Research*, *8*(4), 291–297.

Utela, B., Storti, D., Anderson, R., & Ganter, M. (2008). *Journal of Manufacturing Processes*, 10, 96-104

Vallons, K.J.R., Diaz, J., van Bommel, K., & Noort, M. (2015). The role of gelation dynamics in food printing. *In Proceedings of the 29th EFFoSt International, Athens, vol 1,* pp 426.

Vancauwenberghe, V., Mbong V.B.M., Kokalj, T., Wang, Z., Verbonen, P., Lammertyn, J. & Nicolai, B. (2015). Pectin based bio-ink formulations for 3-D printing of porous foods. In *Proceedings of the 29th EFFoSt International*, 10-12 November, Athens.

van Broekhoven, S., Oonincx, D. G. a B., van Huis, A., & van Loon, J. J. a. (2015). Growth performance and feed conversion efficiency of three edible mealworm species (Coleoptera: Tenebrionidae) on diets composed of organic by-products. *Journal of Insect Physiology*, (January).

Van der Spiegel, M., Noordam, M. Y., & van der Fels-Klerx, H. J. (2013). Safety of Novel Protein Sources (Insects, Microalgae, Seaweed, Duckweed, and Rapeseed) and Legislative Aspects for Their Application in Food and Feed Production. *Comprehensive Reviews in Food Science and Food Safety*, *12*(6), 662–678.

Van Dyck, T., Verboven, P., Herremans, E., Defraeye, T., Van Campenhout, L., Wevers, M., … Nicolaï, B. (2014). Characterisation of structural patterns in bread as evaluated by X-ray computer tomography. *Journal of Food Engineering*, *123*, 67–77.

van Huis, A. (2013). Potential of Insects as Food and Feed in Assuring Food Security. *Annual Review of Entomology*, *58*, 563–583.

Vandeweyer, D., Lenaerts, S., Callens, A., & Van Campenhout, L. (2017). Effect of blanching followed by refrigerated storage or industrial microwave drying on the microbial load of yellow mealworm larvae (Tenebrio molitor). *Food Control*, *71*, 311–314.

Veldkamp, T., Duinkerken, G. Van, Huis, A. Van, M, C. M., Ottevanger, E., Bosch, G., & Boekel, M. A. J. S. Van. (2012). Insects as a sustainable feed ingredient in pig and poultry diets - a feasibility study. *Wageningen UR Livestock Research*, *Report 638*, 62.

Vera Candioti, L., De Zan, M. M., Cámara, M. S., & Goicoechea, H. C. (2014). Experimental design and multiple response optimization. Using the desirability function in analytical methods development. *Talanta*, *124*(JUNE), 123–138.

Verbeke, W. (2015). Profiling consumers who are ready to adopt insects as a meat substitute in a Western society. *Food Quality and Preference*, *39*, 147–155.

Verkerk, M. C., Tramper, J., van Trijp, J. C. M., & Martens, D. E. (2007). Insect cells for human food. *Biotechnology Advances*, *25*(2), 198–202.

Warren, F. J., Zhang, B., Waltzer, G., Gidley, M. J., & Dhital, S. (2015). The interplay of α-amylase and amyloglucosidase activities on the digestion of starch in in vitro enzymic systems. *Carbohydrate Polymers*, *117*, 192–200.

Wegrzyn, T. F., Golding, M., & Archer, R. H. (2012). Food Layered Manufacture: A new process for constructing solid foods. *Trends in Food Science and Technology*, *27*(2), 66–72.

WHO/FAO/UNU Expert Consultation. (2007). *Protein and amino acid requirements in human nutrition. World Health Organization technical report series.*

Wohlers, T. (2015). *3D Printing and Additive Manufacturing State of the Industry: Wohlers Associates Inc.*

Woolnough, J. W., Bird, A. R., Monro, J. A., & Brennan, C. S. (2010). The effect of a brief Salivary α-Amylase exposure during chewing on subsequent in vitro starch digestion curve profiles. *International Journal of Molecular Sciences*, *11*(8), 2780–2790.

Xie, X., Wang, J., Li, X., Jia, W., & Zhang, C. (2015). Mathematical Modeling on Combined Mid-infrared and Hot Air Drying of Beef Meat. *Advance Journal of Food Science and Technology*, *8*(4), 283–290.

Yang, F., Zhang, M., & Bhandari, B. (2015). Recent Development in 3D Food Printing. *Critical Reviews in Food Science and Nutrition* (Vol. 8398).

Yen, A. L. (2009). Edible insects: Traditional knowledge or western phobia? *Entomological Research*, *39*(5), 289–298.

Yi, L., Lakemond, C. M. M., Sagis, L. M. C., Eisner-Schadler, V., van Huis, A., & van Boekel, M. A. J. S. (2013). Extraction and characterisation of protein fractions from five insect species. *Food Chemistry*, *141*(4), 3341–8.

Yi, L., Van Boekel, M. A. J. S., Boeren, S., & Lakemond, C. M. M. (2016). Protein identification and in vitro digestion of fractions from Tenebrio molitor. *European Food Research and Technology*. DOI 10.1007/s00217-015-2632-6

Yi, L., Van Boekel, M. A. J. S., & Lakemond, C. M. M. (2016). Extracting *Tenebrio molitor* protein while preventing browning: effect of pH and NaCl on protein yield. *Journal of Insects as Food and Feed*, *1*(1), 1–12.

Yu, L., Ramaswamy, H. S., & Boye, J. (2013). Protein rich extruded products prepared from soy protein isolate-corn flour blends. *LWT - Food Science and Technology*, *50*(1), 279–289.

Zhao, X., Vázquez-Gutiérrez, J. L., Johansson, D. P., Landberg, R., & Langton, M. (2016). Yellow mealworm protein for food purposes - Extraction and functional properties. *PLoS ONE*, *11*(2), 1–17.
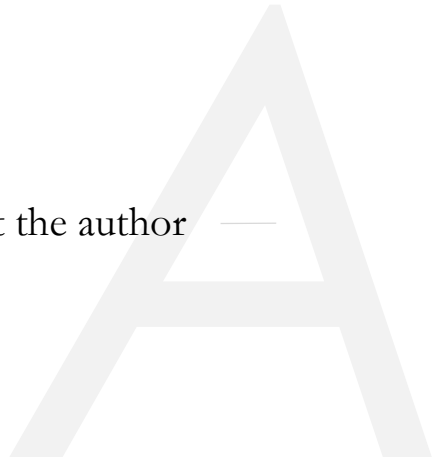
Acknowledgments
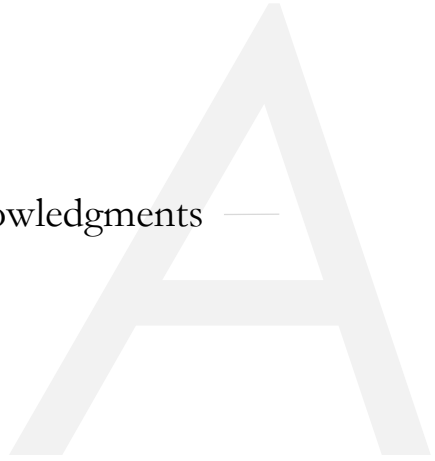
Thanks to all who enriched me.

My parents, for strength, my tutor, for guidance, my colleagues, for sharing, my friends, for encouragement.

About the author

Domenico Azzollini was born the 13th of August 1985 in Bisceglie, Italy. He obtained his high school diploma at the Institute for Professional Education in Enogastronomy and Hotel Accommodation Services in Molfetta, in 2004. In the same year, he started his Bachelor in Food Science and Technology at University of Foggia, which was finished with the project 'Use of humectants for stabilisation of vegetable creams'. In 2008, he started his Master in Food Science and Technology at University of Foggia. He finalised his study, *with Honours*, with a graduation project on recovery and valorisation of by-products from the brewing industry, at Department of Food and Environmental Science of University of Helsinki, Finland. This was followed by an internship at laboratory of technological quality of cereal flours, at Casillo group, Corato, Italy. Afterwards, he started a PhD research project within the Laboratory of Emerging Technologies and Food Formulation, at University of Foggia. He conducted part of his PhD research within the group of Food Quality and Design, at Department of Agrotechnology and Food Sciences, Wageningen University, the Netherlands. Outcomes of this PhD project were presented in this thesis, entitled 'The use of edible insects in conventional and innovative foods. Applications in extruded and 3D printed snacks'.

List of publications

o Severini C., Azzollini D., Jouppila K., Loponen J., Derossi A., De Pilli T. (2015). **Effect of enzymatic and technological treatments on solubilisation of arabinoxylans from brewer's spent grain**. *Journal of Cereal Science*. Vol. 65, pp. 162-166.

o Tomberlin J.K., van Huis A., Benhow M.E., Azzollini D., and co-authors (2015). **Protecting the environment through insect farming as a means to produce protein for use as livestock, poultry, and aquaculture**. *Journal of Insects as Food and Feed*. Vol. 1(4), pp. 307-309.

o Azzollini D., Derossi A., Severini C. (2016). **Understanding the drying kinetic and hygroscopic behaviour of larvae of yellow mealworm (*Tenebrio molitor*) and the effects on their quality**. *Journal of Insects as Food and Feed*. Vol 2(4), pp. 233-243.

o Severini C., Derossi A., Azzollini D. (2016). **Variables affecting the printability of foods: Preliminary tests on cereal-based products**. *Journal of Innovative Food Science and Emerging Technologies*. Vol. 38, pp 281-291.

o Azzollini D., Derossi A., Fogliano V., Lakemond C.M.M., Severini C**. Insect-enriched extruded snacks: mapping structure, texture and digestibility as a function of formulation and process conditions**. Submitted for publication.

o Azzollini D., Derossi A., Albenzio M., Severini C. **On printability, quality and nutritional properties of 3D printed cereal-based snacks enriched with edible insects**. Manuscript in submission.

o Derossi A., Caporizzi R., Azzollini D., Severini C. **Application of 3D Food Printing for customized food. A case on the development of fruit-based snacks for children**. Submitted for publication.

Overview of completed training activities

Courses	Institute	Year
Discipline specific activities		
Statistics	Unifg	2014
Food, nutrition and health	Unifg	2014
Metabolomics	Unifg	2014
Proteomic analysis	Unifg	2014
Biomedical applications in dietary/nutritional interventions	Unifg	2014
ENT 21306 Insects as food and feed	WUR	2016
General courses		
English	Unifg	2014
Epistemology and research philosophy	Unifg	2014
Marketing of functional food products	Unifg	2014
Food law	Unifg	2014
Project management		2014
Analysis of bioelectrical signals	Unifg	2014
Teaching		
Functional food processing technology	Unifg	2014/2015/2016
ENT- Insects as Food and Feed	WUR	2016
General activities		
EXPO school	EXPO Milan	2014
Summer school: eating walking thinking	Milano-Bicocca	2015

Unifg (University of Foggia)

WUR (Wageningen University and Research)

Conferences

o Attendance: *Insects to feed the world* (2014). Wageningen University & Food and Agriculture Organization of the United Nations. Wageningen, NL.

o Poster: **Azzollini D**., Halloran A. (2014). *Barilla Forum on Food and Nutrition*. Bocconi University, Milan, IT.

o Poster: **Azzollini D**., Derossi A., Severini C. (2015). Dehydration kinetics, hygroscopic behaviour and colour changes of Yellow mealworms (*Tenebrio molitor*) as affected from different processing conditions. EFFoST 29th International Conference. *Food Science Research and Innovation: Delivering sustainable solutions to the global economy and society*. Athens (Greece).

o Oral presentation: **Severini C**., Derossi A., Azzollini D. (2015). Novel food formula suitable for 3D printing. *8th probiotics, prebiotics & new foods*. Università Urbaniana, Rome, Italy.

o Oral presentation: **Severini C**., Derossi A., Azzollini D. (2015). Food formulation for 3D printing. *VBFoodNet*, Nha Trang, Vietnam.